Supporting Information

Pyridyl-Benzimidazole Derivatives Decorated with Phenylazo Substituents and their Low-Spin Iron(II) Complexes: Synthesis, Structural and Photoisomerization Study

Jakub Orvoš,[a] Róbert Fischer,[a]* Barbora Brachňaková,[b,d] Ján Pavlik,[b] Ján Moncoľ,[b] Alexandra Šagátová,[b] Marek Fronc,[c] Jozef Kožíšek,[c] Lucie Routaboul,[d] Azzedine Bousseksou [d] and Ivan Šalitroš[b,e,f]*

a) Department of Organic Chemistry, Faculty of Chemical and Food Technology, Slovak University of Technology in Bratislava, Bratislava SK-81237, Slovakia,
b) Department of Inorganic Chemistry, Faculty of Chemical and Food Technology, Slovak University of Technology in Bratislava, Bratislava SK-81237, Slovakia, **e-mail:* ivan.salitros@stuba.sk
c) Department of Physical Chemistry, Faculty of Chemical and Food Technology, Slovak University of Technology in Bratislava, Bratislava SK-81237, Slovakia
d) LCC, CNRS & Université de Toulouse, 205 route de Narbonne, 31077 Toulouse, France
e) Department of Inorganic Chemistry, Regional Centre of Advanced Technologies and Materials, Faculty of Science, Palacký University, 17. listopadu 12, 771 46 Olomouc, Czech Republic
f) Central European Institute of Technology, Brno University of Technology, Purkyňova 123, 61200 Brno, Czech Republic

Contents

SI 1.Experimental section

1.1 Materials and experimental techniques

Materials: All starting compounds, solvents, and ferrous compounds were used as received without any further purification. Dimethyl 4-azidopyridine-2,6-dicarboxylate (**1b**) was prepared using already published procedure.[1] Amino-substituted picolinic acids **2a**, **3a**, **4a** and **5a** were commercially available.

Flash column chromatography was carried out with a Büchi system (Pump Manager C-615 and Fraction Collector C-660) using Normasil 60 silica gel (0.040–0.063 mm; VWR). Thin Layer Chromatography (TLC) analysis was carried out using TLC silica gel 60 F_{254} (aluminium sheets, Merck), and plates were visualized with UV light or by treatment with permanganate solution followed by heating.

Melting points were obtained using a Melting Point B-540 (Büchi) instrument.

Infrared spectra were recorded as neat samples with a Nicolet 5700 FTIR spectrometer with an ATR Smart Orbit Diamond adapter (Thermo Electron Corporation).

NMR spectra were recorded with a Varian INOVA-300 spectrometer (^{1}H, 299.95 MHz, and ^{13}C, 75.42 MHz), a Bruker Avance NEO (^{1}H, 400 MHz) and a Varian VNMRS-600 instrument (^{1}H, 599.75 MHz, and ^{13}C, 150.81 MHz) in DMSO-d_6 and $CDCl_3$ using tetramethylsilane as the internal standard. Data are presented as follows: chemical shift (in ppm), multiplicity, coupling constants (*J*/Hz) and integration. The pyridine ring protons are designated as follows: 3-H, 4-H, 5-H and 6-H. Evans method of determination of magnetic susceptibility of **C1** and **C2** has been carried out on Bruker Avance NEO (^{1}H, 400 MHz) using the ^{t}BuOH as standard.

Photoisomerization experiments of ligands **L1-L5** were carried out with Brucker NMR (600 MHz) in DMSO-d_6 (for **L1**) and CD_3OD (for **L2-L5**). The NMR tubes were irradiated by UV light (filter: FGUV11-UV, 25 mm;150 W halogen light source, LOT-Quantum Design) outside of the spectrometer and immediately after 5 minutes of light exposition, the spectra were collected.

HRMS analysis was carried out with an Orbitrap Velos Pro spectrometer (Thermo Fisher Scientific) or with electrospray ionization time of flight (ESI ToF) mass spectrometer Bruker microTOF QII.

UV-VIS absorption spectroscopy was employed for the detection of reversible photoisomerization of organic ligands **L1-L5** and complexes **C1-C2**. Spectra were carried out on a Cary 60 spectrophotometer in the range 200 - 800 nm and 150 W halogen light source (250 – 1700 nm, LOT-Quantum Design) has been employed for the UV or VIS irradiation of solutions. UV filter (FGUV11-UV, 25 mm) and 450 nm band pass VIS filter (FWHM-10 nm, 25.0 mm) along with the IR filter (elimination of the heat) were used for the selection of desired wavelengths. The solutions in the quartz cuvette were stirred within the photochemical experiments at room temperature and time dependent UV-VIS spectra were collected every 15 seconds.

Next, the thermal stability of *Z* isomers in dark was carried out on Specord 250+ spectrophotometer in region 200 – 1100 nm. The ethanolic solution compounds **L2-L5** in the quartz cuvette were irradiated by 365 nm LED source (10 x 5 W) for 5 minutes until the

photostationary phase was reached. After irradiation, the solution was placed in the spectrophotometer and the back *Z*→*E* isomerization was monitored for 21 hours. Spectra were collected every 15 minutes in dark. The blue laser light irradiation (405 nm) of **L1** solution afforded intense *E*-to-*Z* photoconversion comparing to UV LED light, therefore the blue laser light with 405 nm has been used for the formation of photostationary state and for the kinetic studies. Spectra of **L1** were collected every 5 minutes for 3 hours in dark.

Last set of photoexperiments of the compounds **C1** and **C2** were performed in ethanol in the quartz cuvette and at room temperature. The solutions were irradiated by 405 nm laser (*E* to *Z*) and 460 nm LED light (*Z* to *E*) and spectra were collected every 5 minutes for 1 hour.

Single crystal X-ray diffraction. Data collection and cell refinement of **L1**, **L4**, **L5**, **C1**, **C2** and **C4** at 100 K were made using a Stoe StadiVari diffractometer. The diffractometer was equipped with an HPAD detector (Pilatus3R 300K) and a microfocused X-ray source (Xenocs Genix3D Cu HF). Data collection and cell refinement of **C3** at 110 K were made using Bruker Kappa APEX2 diffractometer. The programs ShelXT, ShelXL (ver. 2018/3), OLEX2 and MERCURY have been used for structure determination, refinement, finalization and drawing.[2]

Magnetic experiments. Magnetic property measurements were performed using PPMS VersaLab instrument (Quantum Design). Magnetization was recorded under an external magnetic field of 0.1 T at sweeping rates of ±1 K min^{-1}.

1.2 Computational details

The potential energy surface (PES) scan calculations for rotation around the azo double-bond were carried out with the program ORCA 4.2.0[3] in two steps. In the first one, thirty nine –CNNC– dihedral angles spanning from 180° to 46° were set fixed and the rest of molecule was optimized by state-averaged active space self-consistent field method (SA-CAS[4,3]SCF).[4] To increase the stability of calculation, only two lowest roots with weights 0.8 and 0.2 were taken into account. In the second step, SA-CAS[4,3]SCF with all six equally-weighted roots was used on geometries obtained from the first step and complemented by strongly-contracted *N*-electron valence perturbation theory of second-order (NEVPT2).[5] The resolution of identity approximation for Coulomb and exchange integrals (RI-JK)[6] was set on. For all atoms the basis set def2-SVP[7] was used with auxiliary basis set def2/J.[8] Increased integration grid was used in these calculations (level 6 in ORCA convention).

The finite-temperature conformer search in solution was performed with the method GFN2-xTB[9] using the programs XTB 6.4.1[10] and CREST 2.11.1.[11] For conformer search the improved metadynamic sampling (iMTD)[12] and genetic Z-matrix crossing (GC)[14] were employed. The DFT energetic sorting of found conformers was performed with the code CENSO 1.1.2[14] and the NMR spectra were enumerated with the code ANMR.[14] Both of these programs delegated portions of calculation to ORCA 5.0.1. The effect of solvent was simulated using the CPCM approach[15] Since the ethanol solvent used experimentally is not supported, the solvent parameters of methanol were set as the most similar substitute. The conformers were optimized and sorted in several consecutive steps using b97-3c[16]/def2-SV(P), r2scan-3c[17]/def2-mTZVPP[17] and pw6b95-d4[18]/def2-TZVPD methods. Corresponding free energies were calculated at 363 K with the entropic contribution obtained by rigid-rotor-harmonic-oscillator (RRHO) approximation.[19] The chemical shielding constants and spin-spin coupling constants

were calculated using the dispersion-corrected meta-GGA functional TPSS-D4[20,21] and basis set pcsSeg-2[22] for the former case and pcJ-2[23] for the latter one.
The electronic spectra of both geometric isomers were obtained by the state-of-the-art method STEOM-DLPNO-CCSD[24] within ORCA 5.0.2 using the geometries optimized at the B3LYP-D3[25,26]/def2-TZVP[6] level in methanol solution. The basis set def2-TZVP was also used for calculation of the electronic spectra. The calculations were performed with the TCutPNOsingles keyword set to 1.0×10^{-12} and the active space selection keywords "Othresh" and "Vthresh" set to 5.0×10^{-3}. In all calculations, eight roots were searched for and the effect of solvent was simulated by the experimental implementation of CPCM approximation, again with parameters for methanol. The spectra were drawn using the gaussian line shape with halfwidth of 20 nm.

1.3 Synthesis of reported compounds

The synthesis of **L1** is visualized on the Scheme S1, synthesis of ligands **L2**-**L4** on the Scheme S2 and synthesis of **L5** on Scheme S3.

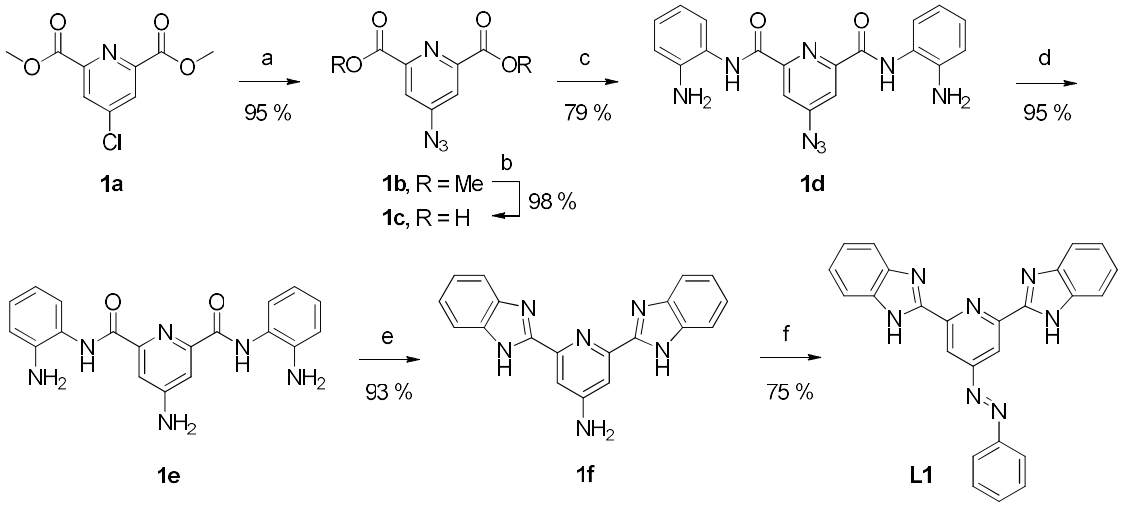

Scheme S1. Synthesis of ligand **L1**. Reaction conditions: (a) NaN_3, DMF, 50 °C, 24 h; (b) $LiOH \cdot H_2O$, THF/H_2O (1:1), r.t., 20 min; (c) *o*-phenylenediamine, TBTU, DIPEA, DMF, r.t., 20 h; (d) H_2 (4 bar), Pd/C (10 wt%), MeOH, r.t., 2 h; (e) AcOH, 100 °C, 1 h; (f) nitrosobenzene, 50 % aq. NaOH, TBAB, pyridine, 50 °C, 3.5 h.

4-Azidopyridine-2,6-dicarboxylic acid (1c)
To a stirred suspension of diester **1b** (3.17 g, 13.42 mmol) in THF (70 mL) was added a solution of $LiOH \cdot H_2O$ (2.82 g; 67.20 mmol) in H_2O (70 mL), and the mixture was vigorously stirred at r.t. for 20 min. When TLC showed that the substrate had disappeared (EtOAc), most of the solvent was removed under reduced pressure, and the aqueous residue was acidified to a pH 2 with aqueous hydrochloric acid (15 %, w/w). The precipitate was collected by filtration, washed with minimal water (2 × 10 mL) and dried in vacuum desiccator for 24 h to give dicarboxylic acid **1c** (2.75 g; 13.21 mmol; 98 %) as a pale brown powder of sufficient purity to be used in next reaction without further purification; m.p. >185 °C; decomposition
IR (ATR, cm^{-1}): 3502, 3089, 2124, 1726, 1672, 1587, 1302, 1172, 997, 898, 789, 680.
^1H NMR (300 MHz, DMSO-d_6): δ(ppm) 7.82 (s, 2 H, 3-H, 5-H).
^{13}C NMR (75 MHz, DMSO-d_6): δ(ppm) 165.1, 151.2, 149.9, 117.6.

HRMS (ESI): calcd. for $C_7H_5N_4O_4$ $[M+H]^+$ 209.0306; found 181.0244, the azido group was cleaved into elemental nitrogen and the corresponding fragment ion during the measurement.

N^2,N^6-Bis(2-aminophenyl)-4-azidopyridine-2,6-dicarboxamide (1d)

To a stirred solution of dicarboxylic acid **1c** (2.35 g,11.29 mmol) in anhydrous DMF (225 mL) at r.t. were sequentially added DIPEA (7.88 ml, 45.24 mmol) and *o*-phenylenediamine (3.67 g, 33.94 mmol). The resulting solution was cooled down to 0 °C, and TBTU (7.62 g, 23.73 mmol) was added. After stirring for 10 min, the cooling bath was removed, and stirring was continued at r.t. for 20 h. After this time, the reaction mixture was diluted with CH_2Cl_2 (700 mL) and sequentially washed with sat. aq. $NaHCO_3$ solution (700 mL), aqueous formic acid (700 mL, 0.5 %, v/v) and water (700 mL). After phase separation, the organic layer was dried over $MgSO_4$ and concentrated *in vacuo*. The residue was purified by FCC (CH_2Cl_2/MeOH, 97:3) to give dicarboxamide **1d** (3.47 g, 8.93 mmol, 79 %) as a yellowish crystalline powder, which decomposed slowly by the action of daylight; R_f = 0.29 (cyclohexane/EtOAc, 5:2); m.p. 187–188 °C, decomposition.

IR (ATR, cm^{-1}): 3406, 3327, 3263, 2120, 1660, 1589, 1519, 1458, 1150, 865, 747.

^{1}H NMR (300 MHz, DMSO-d_6): δ(ppm) 10.71 (bs, 2 H, CO-NH), 7.91 (s, 2 H, 3-H, 5-H), 7.16 (dd, *J* = 1.4, 7.8 Hz, 2 H, H-Ph), 7.04 (ddd, *J* = 1.5, 7.3, 8.0 Hz, 2 H, H-Ph), 6.82 (dd, *J* = 1.4, 8.0 Hz, 2 H, H-Ph), 6.64 (ddd, *J* = 1.4, 7.3, 7.8 Hz, 2 H, H-Ph), 4.98 (s, 4 H, 2 × Ph-NH_2).

^{13}C NMR (75 MHz, DMSO-d_6): δ(ppm) 161.4, 151.7, 150.7, 144.0, 127.5, 127.3, 122.0, 116.2, 115.9, 114.7.

HRMS (ESI): calcd. for $C_{19}H_{17}N_8O_2$ $[M+H]^+$ 389.1469; found 389.1472.

4-Amino-N^2,N^6-bis(2-aminophenyl)pyridine-2,6-dicarboxamide (1e)

A suspension of dicarboxamide **1d** (4.04 g, 10.40 mmol) and Pd/C (10 wt% Pd, 2.34 g, 2.2 mmol) in MeOH (170 mL) was vigorously stirred under H_2 atmosphere (4 bar) at r.t. for 2 h. After this time, the catalyst was removed by filtration through a pad of Celite and washed with MeOH. The filtrate was concentrated under reduced pressure to give amino derivative **1e** (3.60 g, 9.93 mmol, 95 %) as a pale brown powder of sufficient purity to be used in the next reaction without further purification; R_f = 0.25 (EtOAc); m.p. 222–224 °C, decomposition.

IR (ATR, cm^{-1}): 3462, 3342, 3311, 3227, 1677, 1597, 1514, 1457, 1272, 1139, 1001, 870, 734.

^{1}H NMR (600 MHz, DMSO-d_6): δ(ppm) 10.52 (s, 2 H, 2 × CO-NH), 7.46 (s, 2 H, 3-H, 5-H), 7.18 (dd, *J* = 1.5, 7.9 Hz, 2 H, 2 × H-Ph), 7.01 (td, *J* = 1.5, 7.9 Hz, 2 H, 2 × H-Ph), 6.81 (dd, *J* = 1.4, 8.0 Hz, 2 H, 2 × H-Ph), 6.72 (bs, 2 H, py-NH_2), 6.63 (td, *J* = 1.4, 7.5 Hz, 2 H, 2 × H-Ph), 4.90 (bs, 4 H, 2 × Ph-NH_2).

^{13}C NMR (150 MHz, DMSO-d_6): δ(ppm) 162.7, 156.9, 149.3, 143.6, 127.1, 126.8, 122.8, 116.3, 116.0, 108.7.

HRMS (ESI): calcd. for $C_{19}H_{19}N_6O_2$ $[M+H]^+$ 363.1564; found 363.1565.

2,6-Bis(1*H*-benzo[*d*]imidazol-2-yl)pyridin-4-amine (1f)

Dicarboxamide **1e** (3.60 g, 9.93 mmol) was dissolved in acetic acid (180 mL), and the resulting solution was heated at 100 °C for 1 h. After this time, the solvent was evaporated in vacuo. The solid residue was triturated with 26 % aqueous ammonia (170 mL), filtered, washed with water (2 × 20 mL) and dried in vacuum desiccator for 24 h to give bis(bisbenzimidazole)pyridine **1f**

(3.02 g, 9.25 mmol, 93 %) as an off-white powder of sufficient purity to be used in the next reaction without further purification; R_f = 0.50 (EtOAc/MeOH/NH_4OH, 85:13.5:1.5); m.p. >405 °C, decomposition.
IR (ATR, cm^{-1}): 3446, 3292, 3130, 1609, 1563, 1446, 1273, 1203, 985, 848, 727, 542.
^1H NMR (300 MHz, DMSO-d_6): δ(ppm) 12.77 (bs, 2 H, 2 × bzim-N*H*), 7.77–7.65 (m, 4 H, 4 × H-bzim), 7.54 (s, 2 H, 3-H, 5-H), 7.36–7.20 (m, 4 H, 4 × H-bzim), 6.65 (bs, 2 H, py-NH_2).
^{13}C NMR (75 MHz, DMSO-d_6): δ(ppm) 156.3, 151.5, 147.8, 144.1, 134.1, 123.2, 121.8, 119.4, 111.5, 105.9.
HRMS (ESI): calcd. for $C_{19}H_{15}N_6$ $[M+H]^+$ 327.1353; found 327.1352.

(*E*)-2,2'-[4-(Phenyldiazenyl)pyridine-2,6-diyl]bis(1*H*-benzo[*d*]imidazole) (L1)
To a well-stirred suspension of bis(benzimidazole)pyridine **1f** (1.5 g, 4.60 mmol) in pyridine (30 mL) at 50 °C were sequentially added TBAB (0.30 g, 0.93 mmol) and aqueous NaOH solution (2.45 mL, 45.9 mmol, 50 % w/w). After stirring at 50 °C for 10 min, solid nitrosobenzene (0.99 g, 9.24 mmol) was added, and the resulting mixture was stirred at 50 °C for 2 h. After this time, a second portion of nitrosobenzene (0.49 g, 4.57 mmol) was added, and stirring was continued at the same temperature for additional 1.5 h. Then, the reaction mixture was cooled down to r.t., diluted with CH_2Cl_2 (300 mL) and sequentially washed with water (2 × 500 mL) and brine (500 mL). After phase separation, the organic layer was dried over $MgSO_4$, and the solvent was evaporated in vacuo. The residue was purified by FCC (hexanes/acetone/NH_4OH, 2:1:0.02) to give phenylazo derivative **L1** (1.44 g, 3.47 mmol, 75 %) as bright orange powder; R_f = 0.35 (cyclohexane/acetone/NH_4OH, 2:1:0.02); m.p. 359–362 °C, decomposition.
IR (ATR, cm^{-1}): 3226, 3059, 1600, 1568, 1429, 1141, 897, 766, 733, 677.
^1H NMR (600 MHz, DMSO-d_6): δ(ppm) 13.09 (bs, 2 H, 2 × bzim-NH), 8.61 (s, 2 H, 3-H, 5-H), 8.12–8.09 (m, 2 H, 2 × H-Ph), 7.83–7.80 (m, 2 H, 2 × H-bzim), 7.77–7.75 (m, 2 H, 2 × H-bzim), 7.73–7.69 (m, 3 H, 3 × H-Ph), 7.38 (ddd, *J* = 1.1, 7.1, 8.0 Hz, 2 H, 2 × H-bzim), 7.31 (ddd, *J* = 1.1, 7.1, 8.0 Hz, 2 H, 2 × H-bzim).
^{13}C NMR (150 MHz, DMSO-d_6): δ(ppm) 158.8, 151.8, 150.0, 149.8, 144.1, 134.4, 133.4, 129.8, 124.0, 123.5, 122.4, 119.9, 113.3, 111.9.
HRMS (ESI): calcd. for $C_{25}H_{18}N_7$ $[M+H]^+$ 416.1619; found 416.1618.

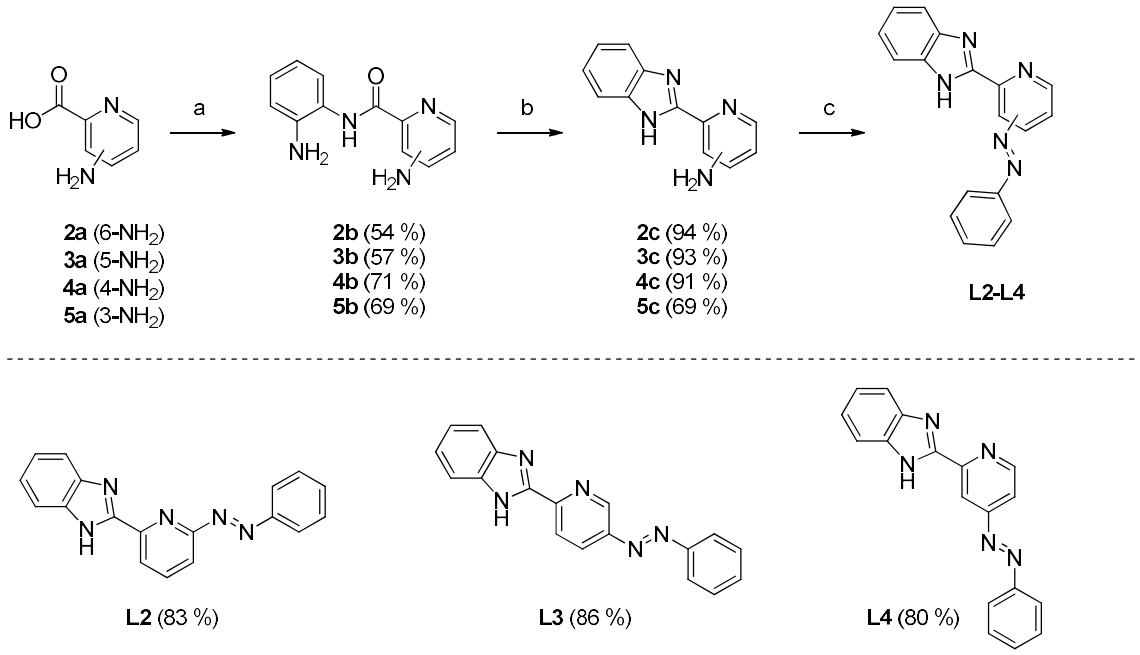

Scheme S2 Synthesis of ligands **L2**, **L3**, and **L4**. Reaction conditions: (a) *o*-phenylenediamine, TBTU, DIPEA, DMF, r.t., 20–25 h; (b) AcOH, 100 °C, 1 h; (c) nitrosobenzene, 50 % aq. NaOH, TBAB, pyridine, 50 °C, 3.5–5 h.

6-Amino-*N*-(2-aminophenyl)picolinamide (2b)

To a stirred suspension of 6-aminopicolinic acid (**2a**, 1.00 g,7.24 mmol) in anhydrous DMF (120 mL) at r.t. were sequentially added DIPEA (2.52 mL,14.48 mmol) and *o*-phenylenediamine (1.17 g,10.86 mmol). The resulting mixture was cooled down to 0 °C, and TBTU (2.56 g,7.96 mmol) was added. After stirring for 10 min, the cooling bath was removed, and stirring was continued at r.t. for 25 h. After this time, the reaction mixture was concentrated under reduced pressure, the residue was dissolved in CH_2Cl_2 (100 mL), and the solution was sequentially washed with sat.aq. $NaHCO_3$ (100 mL) and aqueous acetic acid (100 mL, 0.5% v/v). The organic layer was dried over $MgSO_4$, and the solvent was evaporated under reduced pressure. The residue was purified by FCC (CH_2Cl_2/EtOAc, 1:1) to give amide **2b** (0.9 g, 3.94 mmol, 54 %) as a yellowish solid; R_f = 0.24 (CH_2Cl_2/EtOAc, 1:1); m.p. 139–141 °C.

IR (ATR, cm^{-1}): 3373, 3353, 3308, 3167, 1669, 1633, 1590, 1519, 1452, 1431, 1358, 1274, 988, 815, 740.

^{1}H NMR (300 MHz, DMSO-d_6): δ(ppm) 9.74 (bs, 1 H, CO-NH), 7.59 (dd, *J* = 7.2, 8.3 Hz, 1 H, 4-H), 7.60–7.55 (m, 1 H, H-Ph), 7.27 (dd, *J* = 0.9, 7.3 Hz, 1 H, 3-H), 6.94 (ddd, *J* = 1.5, 7.2, 7.9 Hz, 1 H, H-Ph), 6.83 (dd, *J* = 1.5, 8.0 Hz, 1 H, H-Ph), 6.69 (dd, *J* = 0.9, 8.3 Hz, 1 H, 5-H), 6.65 (ddd, *J* = 1.5, 7.2, 7.9 Hz, 1 H, H-Ph), 6.26 (bs, 2 H, py-N*H*$_2$), 4.87 (bs, 2 H, Ph-N*H*$_2$).

^{13}C NMR (75 MHz, DMSO-d_6): δ(ppm) 162.5, 158.5, 147.9, 141.0, 138.3, 125.5, 124.1, 123.4, 117.1, 116.7, 111.6, 110.1.

HRMS (ESI): calcd. for $C_{12}H_{13}N_4O$ $[M+H]^+$ 229.1084; found 229.1082.

6-(1*H*-Benzo[*d*]imidazol-2-yl)pyridin-2-amine (2c)

Amide **2b** (0.82 g, 3.59 mmol) was dissolved in acetic acid (20 mL), and the resulting solution was heated at 100 °C for 1 h. After this time, the solvent was evaporated in vacuo, and the residue was co-evaporated with *n*-heptane (2 × 20 mL). The product was purified by FCC

(CH_2Cl_2/MeOH/NH_3, 19:1:0.1) to give benzimidazole **2c** (0.71 g, 3.38 mmol, 94 %) as a yellowish solid; R_f = 0.28 (CH_2Cl_2/MeOH/NH_3, 50:1:0.1); m.p.231–233 °C, decomposition.
IR (ATR, cm^{-1}): 3469, 3306, 1609, 1570, 1468, 1402, 1308, 1276, 985, 803, 742.
^{1}H NMR (300 MHz, DMSO-d_6): δ(ppm) 12.57 (bs, 1 H, bzim-N*H*), 7.69–7.62 (m, 1 H, H-bzim), 7.59–7.52 (m, 2 H, 4-H, H-bzim), 7.49 (dd, *J* = 1.0, 7.3 Hz, 1 H, 5-H), 7.22–7.14 (m, 2 H, 2 × H-bzim), 6.60 (dd, *J* = 1.0, 8.0 Hz, 1 H, 3-H), 5.99 (bs, 2 H, py-NH_2).
^{13}C NMR (75 MHz, DMSO-d_6): δ(ppm) 159.4, 151.4, 146.6, 143.9, 138.0, 134.7, 122.5, 121.6, 119.0, 112.0, 110.0, 109.3.
HRMS (ESI): calcd. for $C_{12}H_{11}N_4$ $[M+H]^+$ 211.0979; found 211.0980.

(*E*)-2-[6-(Phenyldiazenyl)pyridin-2-yl]-1*H*-benzo[*d*]imidazole (L2)
To a well-stirred solution of benzimidazole **2c** (0.7 g, 3.33 mmol) in pyridine (17 mL) at 50 °C were sequentially added TBAB (0.22 g,0.67 mmol) and aqueous NaOH solution (1.78 mL; 33.3 mmol, 50 % w/w). After stirring at 50 °C for 10 min, solid nitrosobenzene (0.71 g, 6.66 mmol) was added, and the resulting mixture was stirred at 50 °C for 1.5 h. After this time, a second portion of nitrosobenzene (0.36 g; 3.33 mmol) was added, and stirring was continued at the same temperature for additional 2 h. Then, the reaction mixture was cooled down to r.t., diluted with CH_2Cl_2 (100 mL) and washed with water (2 × 100 mL) and brine (100 mL). After phase separation, the organic layer was dried over $MgSO_4$, and the solvent was evaporated in vacuo. After co-evaporation with toluene (2 × 20 mL), the solid residue was triturated with hexanes (2 × 30 mL) and purified by FCC (CH_2Cl_2/acetone, 92:8) to give phenylazo derivative **L2** (0.84 g, 2.81 mmol, 83 %) as a brick-coloured powder; R_f = 0.19 (CH_2Cl_2/acetone, 94:6); m.p. 187–189 °C.
IR (ATR, cm^{-1}): 3053, 1591, 1565, 1414, 1387, 1313, 1275, 1151, 991, 813, 738, 687, 526.
^{1}H NMR (600 MHz, DMSO-d_6) δ(ppm): 13.23 (bs, 1 H, bzim-N*H*), 8.51 (dd, *J* = 0.8, 7.7 Hz, 1 H, 3-H), 8.23 (pseudo t, *J* = 7.8, 7.9 Hz, 1 H, 4-H), 8.03–7.99 (m, 2 H, H-Ph), 7.78 (dd, *J* = 0.8, 7.9 Hz, 1 H, 5-H), 7.76–7.73 (m, 1 H, H-bzim), 7.70–7.66 (m, 3 H, H-Ph), 7.62–7.59 (m, 1 H, H-bzim), 7.29–7.26 (m, 1 H, H-bzim), 7.25–7.23 (m, 1 H, H-bzim).
^{13}C NMR (150 MHz, DMSO-d_6) δ(ppm): 162.8, 151.8, 149.9, 148.5, 143.8, 140.3, 135.1, 132.8, 129.7, 123.4, 123.2, 123.1, 122.1, 119.4, 112.9, 112.4.
HRMS (ESI): calcd. for $C_{18}H_{14}N_5$ $[M+H]^+$ 300.1244; found 300.1254.

5-Amino-*N*-(2-aminophenyl)picolinamide (3b)
To a stirred solution of 5-aminopicolinic acid (**3a**, 1.00 g,7.24 mmol) in anhydrous DMF (120 mL) at r.t. were sequentially added DIPEA (2.52 ml,14.48 mmol) and *o*-phenylenediamine (1.17 g,10.86 mmol). The resulting mixture was cooled down to 0 °C, and TBTU (2.56 g,7.96 mmol) was added. After stirring for 10 min, the cooling bath was removed, and stirring was continued at r.t. for 22 h. After this time, the reaction mixture was concentrated under reduced pressure, the residue was dissolved in CH_2Cl_2 (100 mL), and the solution was sequentially washed with sat. aq. $NaHCO_3$ (100 mL) and aqueous acetic acid (100 mL, 0.5% v/v). The organic layer was dried over $MgSO_4$, and the solvent was evaporated under reduced pressure. The residue was purified by FCC (CH_2Cl_2/MeOH, 97:3) to give amide **3b** (0.95 g, 4.16 mmol, 57 %) as a yellowish solid; R_f = 0.26 (CH_2Cl_2/MeOH, 98:2); m.p. 168–170 °C.

IR (ATR, cm^{-1}): 3438, 3404, 3303, 3192, 1652, 1614, 1574, 1510, 1471, 1234, 1130, 1013, 857, 748.
^{1}H NMR (300 MHz, DMSO-d_6) δ(ppm): 9.70 (bs, 1 H, CO-NH), 8.00 (d, *J* = 2.7 Hz, 1 H, 6-H), 7.83 (d, *J* = 8.6 Hz, 1 H, 3-H), 7.54 (dd, *J* = 1.4, 7.9 Hz, 1 H, H-Ph), 7.03 (dd, *J* = 2.7, 8.6 Hz, 1 H, 4-H), 6.94–6.88 (m, 1 H, H-Ph), 6.82 (dd, *J* = 1.5, 7.9 Hz, 1 H, H-Ph), 6.67–6.61 (m, 1 H, H-Ph), 6.05 (bs, 2 H, py-NH_2), 4.81 (bs, 2 H, Ph-NH_2).
^{13}C NMR (75 MHz, DMSO-d_6) δ(ppm): 162.7, 147.7, 141.1, 137.3, 134.3, 125.1, 125.0, 123.7, 123.3, 119.3, 117.2, 116.9.
HRMS (ESI): calcd. for $C_{12}H_{13}N_4O$ $[M+H]^+$ 229.1084; found 229.1083.

6-(1*H*-Benzo[*d*]imidazol-2-yl)pyridin-3-amine (3c)
Amide **3b** (0.94 g, 4.12 mmol) was dissolved in acetic acid (20 mL), and the resulting solution was heated at 100 °C for 1 h. After this time, the solvent was evaporated *in vacuo*, and the residue was co-evaporated with *n*-heptane (2 × 20 mL). The product was purified by FCC (CH_2Cl_2/MeOH/NH_3, 14:1:0.1) to give benzimidazole **3c** (0.81 g, 3.83 mmol, 93 %) as a yellowish foam; R_f = 0.20 (CH_2Cl_2/MeOH/NH_3, 14:1:0.1); m.p. 210–216 °C.
IR (ATR, cm^{-1}): 3424, 3325, 3191, 1648, 1588, 1421, 1402, 1272, 968, 829, 739, 545.
^{1}H NMR (600 MHz, DMSO-d_6) δ(ppm): 12.61 (bs, 1 H, bzim-N*H*), 8.05 (d, *J* = 2.7 Hz, 1 H, 2-H), 7.99 (d, *J* = 8.5 Hz, 1 H, 5-H), 7.60–7.55 (m, 1 H, H-bzim), 7.47–7.42 (m, 1 H, H-bzim), 7.16–7.09 (m, 2 H, H-bzim), 7.06 (dd, *J* = 2.7, 8.5 Hz, 1 H, 4-H), 5.84 (bs, 2 H, py-NH_2).
^{13}C NMR (150 MHz, DMSO-d_6) δ(ppm): 152.0, 146.1, 136.2, 143.7, 135.3, 135.2, 122.3, 121.5 (× 2), 120.1, 117.8, 111.9.
HRMS (ESI): calcd. for $C_{12}H_{11}N_4$ $[M+H]^+$ 211.0979; found 211.0979.

(*E*)-2-[5-(Phenyldiazenyl)pyridin-2-yl]-1*H*-benzo[*d*]imidazole (L3)
To a well-stirred solution of benzimidazole **3c** (0.80 g, 3.81 mmol) in pyridine (18 mL) at 50 °C were sequentially added TBAB (0.25 g, 0.76 mmol) and aqueous NaOH solution (2.03 mL, 38.1 mmol, 50 % w/w). After stirring at 50 °C for 10 min, solid nitrosobenzene (0.82 g,7.62 mmol) was added, and the resulting mixture was stirred at 50 °C for 3 h. After this time, a second portion of nitrosobenzene (0.41 g,3.82 mmol) was added, and stirring was continued at the same temperature for additional 2 h. Then, the reaction mixture was cooled down to r.t., diluted with CH_2Cl_2 (100 mL) and washed with water (2 × 100 mL) and brine (100 mL). The organic layer was dried over $MgSO_4$, and the solvent was evaporated in vacuo. After co-evaporation with toluene (2 × 20 mL), the solid residue was triturated with hexanes (2 × 30 mL) and crystallized from *n*-butyl acetate to give phenylazo derivative **L3** (0.98 g, 3.27 mmol, 86 %) as an orange crystalline powder; R_f = 0.38 (CH_2Cl_2/CH_3CN/NH_3, 32:1:0.1); m.p. 239–253 °C.
IR (ATR, cm^{-1}): 3055, 1591, 1437, 1422, 1316, 1267, 1147, 1109, 854, 737, 681, 550, 444.
^{1}H NMR (300 MHz, DMSO-d_6) δ(ppm): 13.32 (s, 1 H, bzim-N*H*), 9.28 (dd, *J* = 0.8, 2.3 Hz, 1 H, 6-H), 8.54 (dd, *J* = 0.8, 8.5 Hz, 1 H, 3-H), 8.36 (dd, *J* = 2.3, 8.5 Hz, 1 H, 4-H), 7.95–8.01 (m, 2 H, H-Ph), 7.76–7.56 (m, 5 H, 2 × H-bzim, 3 × H-Ph), 7.32–7.22 (m, 2 H, H-bzim).
^{13}C NMR (75 MHz, DMSO-d_6) δ(ppm): 152.0, 150.4, 149.9, 147.4, 146.9, 144.0, 135.2, 132.4, 129.6, 127.8, 123.7, 122.9, 122.3, 122.2, 119.5, 112.2.
HRMS (ESI): calcd. for $C_{18}H_{14}N_5$ $[M+H]^+$ 300.1244; found 300.1243.

4-amino-*N*-(2-aminophenyl)picolinamide (4b)

To a well-stirred solution of 4-aminopicolinic acid hydrochloride (**4a**, 2.56 g, 14.66 mmol) in anhydrous DMF (150 mL) at r.t. were sequentially added DIPEA (7.7 mL, 44.2 mmol) and *o*-phenylenediamine (2.38 g, 22.0 mmol). The resulting mixture was cooled down to 0 °C, and TBTU (5.65 g, 17.6 mmol) was added. After stirring for 10 min, the cooling bath was removed, and stirring was continued at r.t. for 20 h. After this time, the reaction mixture was concentrated under reduced pressure, sat. aq. $NaHCO_3$ (290 mL) and Et_2O (290 mL) were added, and the resulting suspension was vigorously stirred for 10 min. Then, the solid precipitate was filtered, washed with water (10 mL), Et_2O (10 mL) and dried in vacuum desiccator for 24 h to give amide **4b** (2.37 g, 10.38 mmol, 71 %) as a pale yellow microcrystalline powder of sufficient purity to be used in the next reaction; R_f = 0.22 (CH_2Cl_2/MeOH, 93:7); m.p. 179–181 °C.

IR (ATR, cm^{-1}): 3450, 3322, 3208, 1676, 1633, 1589, 1516, 1482, 1359, 1282, 988, 824, 750.

^{1}H NMR (300 MHz, DMSO-d_6) δ(ppm): 9.99 (s, 1 H, CO-NH), 8.10 (d, *J* = 5.6 Hz, 1 H, 6-H), 7.58 (dd, *J* = 1.4, 8.0 Hz, 1 H, H-Ph), 7.33 (d, *J* = 2.4 Hz, 1 H, 3-H), 6.93 (ddd, *J* = 1.5, 7.2, 7.9 Hz, 1 H, H-Ph), 6.83 (dd, *J* = 1.5, 7.9 Hz, 1 H, H-Ph), 6.65 (dd, *J* = 2.4, 5.6 Hz, 1 H, 5-H), 6.68–6.63 (m, 1 H, H-Ph); 6.40 (bs, 2 H, py-NH_2); 4.83 (bs, 2 H, Ph-NH_2).

^{13}C NMR (75 MHz, DMSO-d_6) δ(ppm): 162.7, 155.7, 150.2, 148.3, 141.1, 125.4, 124.6, 123.6, 117.3, 116.9, 110.5, 107.1.

HRMS (ESI): calcd. for $C_{12}H_{13}N_4O$ $[M+H]^+$ 229.1084; found 229.1084.

2-(1*H*-Benzo[*d*]imidazol-2-yl)pyridin-4-amine (4c)

Amide **4b** (2.37 g, 10.38 mmol) was dissolved in acetic acid (25 mL), and the resulting solution was heated at 100 °C for 1 h. After this time, the solvent was evaporated *in vacuo*, and the residue was co-evaporated with *n*-heptane (2 × 20 mL). The product was purified by FCC (CH_2Cl_2/MeOH/NH_3, 10:1:0.1) to give benzimidazole **4c** (1.99 g, 9.45 mmol, 91 %) as a white solid; R_f = 0.26 (CH_2Cl_2/MeOH/NH_3, 9:1:0.1); m.p. 282–284 °C.

IR (ATR, cm^{-1}): 3469, 3120, 1634, 1604, 1492, 1446, 1268, 1195, 985, 900, 832, 738, 600, 460.

^{1}H NMR (600 MHz, DMSO-d_6) δ(ppm): 12.82 (bs, 1 H, bzim-N*H*), 8.14 (d, *J* = 5.6 Hz, 1 H, 6-H), 7.68–7.60 (m, 1 H, H-bzim), 7.54 (d, *J* = 2.3 Hz, 1 H, 3-H), 7.52–7.46 (m, 1 H, H-bzim), 7.23–7.14 (m, 2 H, H-bzim), 6.58 (dd, *J* = 2.4, 5.6 Hz, 1 H, 5-H), 6.30 (bs, 2 H, py-NH_2).

^{13}C NMR (150 MHz, DMSO-d_6) δ(ppm): 155.1, 151.7, 149.2, 148.6, 143.8, 134.7, 122.5, 121.5, 119.0, 111.8, 109.5, 106.1.

HRMS (ESI): calcd. for $C_{12}H_{11}N_4$ $[M+H]^+$ 211.0979; found 211.0979.

(*E*)-2-[4-(Phenyldiazenyl)pyridin-2-yl]-1*H*-benzo[*d*]imidazole (L4)

To a well-stirred solution of benzimidazole **4c** (1.99 g, 9.45 mmol) in pyridine (40 mL) at 50 °C were sequentially added TBAB (0.61 g, 1.89 mmol) and aqueous NaOH solution (5.05 mL, 94.7mmol, 50 % w/w). After stirring at 50 °C for 10 min, solid nitrosobenzene (2.03 g, 18.93 mmol) was added, and the resulting mixture was stirred at 50 °C for 1.5 h. After this time, a second portion of nitrosobenzene (1.02 g,9.46 mmol) was added, and stirring was continued at the same temperature for additional 3 h. Then, the reaction mixture was cooled down to r.t., diluted with CH_2Cl_2 (300 mL) and washed with water (2 × 300 mL) and brine (300 mL). The organic layer was dried over $MgSO_4$, and the solvent was evaporated in vacuo. After co-evaporation with toluene (2 × 50 mL), the solid residue was triturated with hexanes (100 mL).

The crude product was subsequently dissolved in CH_2Cl_2/EtOAc (1:1 v/v), the resulting solution was filtered through silica pad, and concentrated under reduced pressure. Crystallization of the solid residue (*n*-butyl acetate) gave phenylazo derivative **L4** (2.27 g, 7.57 mmol, 80 %) as an orange crystalline powder; R_f = 0.55 (CH_2Cl_2/MeOH/NH_3, 50:1:0.1); m.p. 197–199 °C.

IR (ATR, cm^{-1}): 3055, 1597, 1558, 1430, 1352, 1145, 846, 739, 683, 608, 456.

^{1}H NMR (300 MHz, DMSO-d_6) δ(ppm): 13.26 (bs, 1 H, bzim-N*H*), 8.96 (dd, *J* = 0.7, 5.2 Hz, 1 H, 6-H), 8.60 (dd, *J* = 0.7, 1.9 Hz, 1 H, 3-H), 8.06–8.00 (m, 2 H, 2 × H-Ph), 7.91 (dd, *J* = 1.9, 5.2 Hz, 1 H, 5-H), 7.78–7.72 (m, 1 H, 1 × H-bzim), 7.71–7.65 (m, 3 H, 3 × H-Ph), 7.61–7.55 (m, 1 H, 1 × H-bzim), 7.32–7.20 (m, 2 H, 2 × H-bzim).

^{13}C NMR (75 MHz, DMSO-d_6) δ(ppm): 157.5, 151.8, 151.5, 150.4, 150.2, 143.8, 135.0, 133.1, 129.7, 123.4, 123.3, 122.1, 119.4, 117.8, 112.3, 112.2.

HRMS (ESI): calcd. for $C_{18}H_{14}N_5$ $[M+H]^+$ 300.1244; found 300.1244.

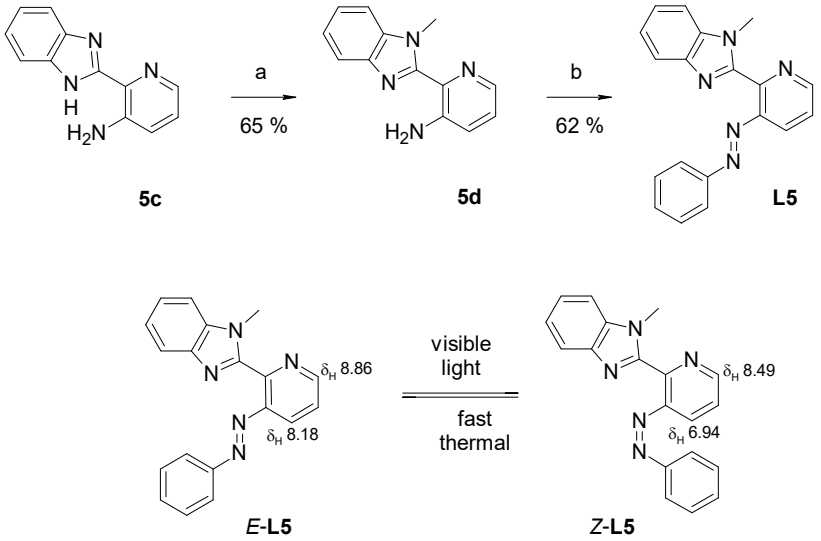

Scheme S3. Synthesis of ligand **L5**. Reaction conditions: (a) MeI, K_2CO_3, DMF, r.t., 15 h.; (b) nitrosobenzene, 50 % aq. NaOH, TBAB, pyridine, 50 °C, 5 h.

3-Amino-*N*-(2-aminophenyl)picolinamide (5b)

To a stirred suspension of 3-aminopicolinic acid (**5a**, 2.50 g, 18.10 mmol) in anhydrous DMF (260 mL) at r.t. were sequentially added DIPEA (6.3 mL, 36.2 mmol) and *o*-phenylenediamine (2.93 g, 27.10 mmol). The resulting mixture was cooled down to 0 °C, and TBTU (6.68 g, 20.80 mmol) was added. After stirring for 10 min, the cooling bath was removed, and stirring was continued at r.t. for 20 h. After this time, the reaction mixture was concentrated under reduced pressure, the residue was dissolved in CH_2Cl_2 (200 mL), and the solution was sequentially washed with sat. aq. $NaHCO_3$ (200 mL) and aqueous formic acid (200 mL, 0.5% v/v). The organic layer was dried over $MgSO_4$, and the solvent was evaporated under reduced pressure. The residue was purified by FCC (EtOAc) to give amide **5b** (2.84 g, 12.44 mmol, 69 %) as a yellow powder; R_f = 0.58 (EtOAc); m.p. 115–117 °C.

IR (ATR, cm^{-1}): 3421, 3344, 3307, 1640, 1608, 1502, 1455, 1225, 1146, 801, 744, 701, 665, 537.

^{1}H NMR (300 MHz, DMSO-d$_6$) δ(ppm): 9.94 (bs, 1 H, CO-NH), 7.88 (dd, *J* = 1.5, 4.1 Hz, 1 H, 6-H), 7.52 (dd, *J* = 1.4, 7.9 Hz, 1 H, H-Ph), 7.30 (dd, *J* = 4.1, 8.4 Hz, 1 H, 5-H), 7.22 (dd, *J* = 1.5, 8.4 Hz, 1 H, 4-H), 6.96–6.90 (m, 1 H, H-Ph), 6.89 (bs, 2 H, py-N*H*$_2$), 6.82 (dd, *J* = 1.5, 7.9 Hz, 1 H, H-Ph), 6.65 (ddd, *J* = 1.5, 7.2, 7.9 Hz, 1 H, H-Ph), 4.83 (bs, 2 H, Ph-N*H*$_2$).
^{13}C NMR (75 MHz, DMSO-d$_6$) δ(ppm): 165.7, 146.7, 141.4, 135.6, 128.5, 127.6, 125.3, 124.8, 124.4, 123.9, 117.1, 116.7.
HRMS (ESI): calcd. for $C_{12}H_{13}N_4O$ $[M+H]^+$ 229.1084; 229.1083.

2-(1*H*-Benzo[*d*]imidazol-2-yl)pyridin-3-amine (5c)
Amide **5b** (2.84 g, 12.44 mmol) was dissolved in acetic acid (40 mL), and the resulting solution was heated at 100 °C for 1 h. After this time, the solvent was evaporated in vacuo. After co-evaporation with *n*-heptane (2 × 20 mL), the solid residue was triturated with toluene (2 × 10 mL) and dried in vacuum desiccator for 48 h to give benzimidazole **5c** (1.84 g, 8.75 mmol, 69 %) as a pale brown powder of sufficient purity to be used in the next reaction without further purification; R_f = 0.26 (CH_2Cl_2/acetone, 95:5); m.p. 185–187 °C.
IR (ATR, cm^{-1}): 3354, 3164, 3052, 1601, 1469, 1406, 1312, 1224, 962, 794, 727, 646.
^{1}H NMR (300 MHz, DMSO-d$_6$) δ(ppm): 12.84 (bs, 1 H, bzim-N*H*), 7.96 (dd, *J* = 1.6, 4.2 Hz, 1 H, 6-H), 7.72–7.67 (m, 1 H, H-bzim), 7.56–7.51 (m, 1 H, H-bzim), 7.29 (bs, 2 H, py-N*H*$_2$), 7.28–7.15 (m, 4 H, 2 × H-bzim, 4-H, 5-H).
^{13}C NMR (75 MHz, DMSO-d$_6$) δ(ppm): 152.6, 144.3, 143.2, 136.4, 133.5, 128.7, 125.2, 122.9, 122.8, 121.5, 118.6, 111.5.
HRMS (ESI): calcd. for $C_{12}H_{11}N_4$ $[M+H]^+$ 211.0979; found 211.0978.

2-(1-Methyl-1*H*-benzo[*d*]imidazol-2-yl)pyridin-3-amine (5d)
Benzoimidazole **5c** (1.84 g, 8.75 mmol) was dissolved in dry DMF (20 mL), dried K_2CO_3 (2.42 g, 17.5 mmol) was added, and the resulting suspension was stirred at r.t. for 30 min. Then, methyl iodide (0.71 mL, 11.40 mmol) was added dropwise over 10 min. After stirring at r.t. for 15 h, the solvent was evaporated under reduced pressure, the residue was dissolved in EtOAc (100 mL), and the solution was washed with water (2 × 100 mL). The organic layer was dried over $MgSO_4$ and concentrated in vacuo. The product was purified by recrystallization (toluene) to give benzimidazole **5d** (1.27 g, 5.66 mmol, 65 %) as brown needles; R_f = 0.23 (CH_2Cl_2/MeOH, 97:3); m.p. 153–157 °C.
IR (ATR, cm^{-1}): 3407, 3294, 3053, 2937, 1599, 1455, 1266, 1064, 796, 736, 666.
^{1}H NMR (300 MHz, DMSO-d$_6$) δ(ppm): 7.98 (dd, *J* = 1.6, 4.2 Hz, 1 H, 6-H), 7.73–7.70 (m, 1 H, H-bzim), 7.60–7.63 (m, 1 H, H-bzim), 7.35–7.24 (m, 3 H, 2 × H-bzim, 4-H), 7.20 (dd, *J* = 4.2, 8.4 Hz, 1 H, 5-H), 7.15 (bs, 2 H, py-N*H*$_2$), 4.21 (s, 3 H, *N*-Me).
^{13}C NMR (75 MHz, DMSO-d$_6$) δ(ppm): 150.3, 145.3, 141.1, 135.9, 135.8, 130.4, 124.7, 123.0, 122.8, 122.1, 118.7, 110.2, 33.3.
HRMS (ESI): calcd. for $C_{13}H_{13}N_4$ $[M+H]^+$ 225.1135; found 225.1135.

(*E*)-1-Methyl-2-[3-(phenyldiazenyl)pyridin-2-yl]-1*H*-benzo[*d*]imidazole (L5)
To a well-stirred solution of benzimidazole **5d** (1.17 g, 5.22 mmol) in pyridine (15 mL) at r.t. were sequentially added TBAB (0.34 g, 1.05 mmol) and aqueous NaOH solution (2.8 mL, 52.3 mmol, 50 % w/w). After stirring at 50 °C for 10 min, solid nitrosobenzene (1.12 g,

10.46 mmol) was added, and the resulting mixture was stirred at 50 °C for 3 h. After this time, a second portion of nitrosobenzene (0.56 g, 5.22 mmol) was added, and stirring was continued at the same temperature for additional 2 h. Then, the reaction mixture was cooled down to r.t., diluted with CH_2Cl_2 (200 mL) and washed with water (2 × 200 mL) and brine (200 mL). The organic layer was dried over $MgSO_4$, and the solvent was evaporated in vacuo. After co-evaporation with toluene (2 × 20 mL), the solid residue was triturated with hexanes (100 mL). The crude product was subsequently dissolved in EtOAc, the solution was filtered through silica pad, and concentrated under reduced pressure. Crystallization (*o*-xylene) gave phenylazo derivative **L5** (1.01 g, 3.22 mmol, 62 %) as bright orange crystals; R_f = 0.15 (CH_2Cl_2/MeOH, 97:3); m.p. 155–159 °C.

IR (ATR, cm^{-1}): 3073, 3045, 2983, 1575, 1442, 1411, 1330, 1057, 751, 688, 435.

^{1}H NMR (600 MHz, $CDCl_3$) δ(ppm): 8.86 (dd, *J* = 1.5, 4.6 Hz,1 H, 6-H), 8.18 (dd, *J* = 1.5, 8.2 Hz, 1 H, 4-H), 7.88 (d, *J* = 7.9 Hz, 1 H, H-Ph), 7.79–7.75 (m, 2 H, H-bzim), 7.55 (dd, *J* = 4.6, 8.2 Hz, 1 H, 5-H), 7.45–7.41 (m, 4 H, H-Ph), 7.38–7.36 (m, 1 H, H-bzim), 7.34– 7.32 (m, 1 H, H-bzim), 3.83 (s, 3 H, *N*-Me).

^{13}C NMR (150 MHz, $CDCl_3$) δ(ppm): 152.6, 151.2, 150.2, 148.3, 147.8, 143.3, 136.1, 131.9, 129.1, 125.0, 124.5, 123.4, 123.2, 122.3, 120.5, 109.7, 31.4.

HRMS (ESI): calcd. for $C_{19}H_{16}N_5$ $[M+H]^+$ 314.1401; found 314.1401.

Gram-scale synthesis of (*E*)-2,2'-[4-(phenyldiazenyl)pyridine-2,6-diyl]bis(1*H*-benzo[*d*]imidazole) (L1)

Dimethyl 4-azidopyridine-2,6-dicarboxylate (**1b**) was synthesized using slightly modified literature procedure.[1] Sodium azide (14.13 g; 0.22 mol) was added to a solution of commercially available dimethyl 4-chloropyridine-2,6-dicarboxylate (**1a**, 4.99 g, 21.73 mmol) in DMF (65 mL), and the resulting suspension was stirred at 50 °C for 24 h. After this time, warm reaction mixture was filtered, the solid matter was washed with DMF, and the filtrate was evaporated *in vacuo*. The yellow solid residue was dissolved in CH_2Cl_2 (300 mL), and the resulting solution was sequentially washed with water (200 mL) and brine (100 mL). After phase separation, the organic layer was dried over $MgSO_4$ and concentrated under reduced pressure to give 4-azidopyridine-2,6-dicarboxylate (**1b**, 4.88 g; 20.66 mmol; 95 %) as yellowish microcrystaline powder; R_f = 0.35 (cyclohexane/EtOAc, 1:1); m.p. 160–161 °C (ref. m.p. 160 °C);^{1}H NMR (300 MHz, $CDCl_3$): δ 4.03 (s, 6 H, 2 × CO_2Me), 7.93 (s, 2 H, 3-H, 5-H).

To a stirred suspension of dimethyl 4-azidopyridine-2,6-dicarboxylate (**1b**, 4.86 g, 20.58 mmol) in THF (105 mL) was added a solution of $LiOH·H_2O$ (4.32 g; 0.103 mol) in H_2O (105 mL), and the mixture was vigorously stirred at r.t. When TLC (EtOAc) showed that the substrate had disappeared (20 min), most of THF was removed under reduced pressure, and the aqueous residue was acidified to a pH 2 with aqueous hydrochloric acid (15 %, w/w). The precipitate was collected by filtration, washed with minimal water (2 × 15 mL) and dried in vacuum desiccator for 24 h to give 4-azidopyridine-2,6-dicarboxylic acid (**1c**, 4.20 g; 20.17 mmol; 98 %) as a pale brown powder of sufficient purity to be used in next reaction without further purification.

To a stirred solution of 4-azidopyridine-2,6-dicarboxylic acid (**1c**, 4.18 g, 20.08 mmol) in anhydrous DMF (400 mL) at r.t. were sequentially added DIPEA (14.00 mL, 80.34 mmol) and *o*-phenylenediamine (6.52 g, 60.25 mmol). The resulting solution was cooled down to 0 °C,

and TBTU (13.54 g, 42.18 mmol) was added. After stirring for 10 min, the cooling bath was removed, and stirring was continued at r.t. for 20 h. After this time, the reaction mixture was diluted with CH_2Cl_2 (1 L) and sequentially washed with sat. aq. $NaHCO_3$ solution (1 L), aqueous formic acid (1 L, 0.5 %, v/v) and water (500 mL). After phase separation, the organic layer was dried over $MgSO_4$ and concentrated under reduced pressure. The solid residue was triturated with CH_2Cl_2 (2 × 8 mL) and dried *in vacuo* to give N^2,N^6-bis(2-aminophenyl)-4-azidopyridine-2,6-dicarboxamide (**1d**, 5.46 g, 14.06 mmol, 70 %) as a yellowish crystalline powder that decomposed slowly by the action of daylight, and therefore, it should be stored only for a limited time.

A suspension of N^2,N^6-bis(2-aminophenyl)-4-azidopyridine-2,6-dicarboxamide (**1d**, 5.44 g, 14.01 mmol) and Pd/C (10 wt% Pd, 1.49 g, 1.40 mmol) in MeOH (230 mL) was vigorously stirred under H_2 atmosphere (4 bar) at r.t. for 2 h. After this time, the catalyst was removed by filtration through a pad of Celite and washed with MeOH. The filtrate was concentrated under reduced pressure to give 4-amino-N^2,N^6-bis(2-aminophenyl)pyridine-2,6-dicarboxamide (**1e**, 4.82 g, 13.31 mmol, 95 %) as a pale brown powder of sufficient purity to be used in the next reaction without further purification.

4-Amino-N^2,N^6-bis(2-aminophenyl)pyridine-2,6-dicarboxamide (**1e**, 4.80 g, 13.25 mmol) was dissolved in acetic acid (200 mL), and the resulting solution was heated at 100 °C for 1 h. After this time, the solvent was evaporated *in vacuo*. The solid residue was triturated with 26 % aqueous ammonia (200 mL), filtered, washed with water (2 × 25 mL) and dried in vacuum desiccator for 24 h to give 2,6-bis(1*H*-benzo[*d*]imidazol-2-yl)pyridin-4-amine (**1f**, 4.02 g, 12.32 mmol, 93 %) as an off-white powder.

To a well-stirred suspension of 2,6-bis(1*H*-benzo[*d*]imidazol-2-yl)pyridin-4-amine (**1f**, 4.00 g, 12.26 mmol) in pyridine (80 mL) at 50 °C were sequentially added TBAB (0.79 g, 2.45 mmol) and aqueous NaOH solution (6.54 mL, 123 mmol, 50 % w/w). After stirring at 50 °C for 10 min, solid nitrosobenzene (2.63 g, 24.51 mmol) was added, and the resulting mixture was stirred at 50 °C for 2 h. After this time, a second portion of nitrosobenzene (1.31 g, 12.26 mmol) was added, and stirring was continued at the same temperature for additional 1.5 h. Then, the reaction mixture was cooled down to r.t., diluted with CH_2Cl_2 (800 mL) and sequentially washed with water (2 × 1 L) and brine (500 mL). After phase separation, the organic layer was dried over $MgSO_4$, and the solvent was evaporated *in vacuo*. The red solid residue was co-evaporated with toluene (2 × 50 mL), triturated with hexanes/toluene (3:1, v/v, 2 × 100 mL) and crystallized from *n*-butanol. The resulting crystals were collected by filtration, washed with ice-cold *n*-butanol (10 mL) and dried in vacuum oven at 120 °C for 5 h to give(*E*)-2,2'-[4-(phenyldiazenyl)pyridine-2,6-diyl]bis(1*H*-benzo[*d*]imidazole) (**L1**, 3.51 g, 8.46 mmol, 69 %) as a bright orange powder.

Synthesis of coordination compounds C1-C4

Compound **C1**

L1 (50 mg, 0.120 mmol, 2.0 eq) was dissolved in the solvent mixture acetonitrile-ethanol (5:1, 60 cm^3) and stirred under N_2 at room temperature for 30 minutes. The corresponding $Fe(BF_4)_2.6H_2O$ (20.3 mg, 0.006 mmol, 1.0 eq) salt was dissolved in of the same solvent mixture (5 cm^3) and promptly added into the ligand solution which caused color change to dark turquoise color. The reaction mixture was stirred for 2 hours, filtered and retained for the slow

evaporation at RT. The single-crystals were obtained in 27 % after three weeks. Elemental analysis for $[Fe(L1)_2](BF_4)_2 \cdot H_2O$ ($C_{50}H_{36}FeN_{14}B_2F_8O$; M_w= 1078.40 g.mol^{-1}) found % (expected %): C 55.79 (56.64); N 17.83 (18.49); H 3.09 (3.23). ESI ToF MS: $[Fe(L1)_2](BF_4)^+$ m/z = 973.2604 ($C_{50}H_{34}N_{14}FeBF_4^+$ requires m/z = 1035.1956); $[Fe(L1)_2]^{2+}$ m/z = 443.1322 ($C_{50}H_{34}N_{14}Fe^{2+}$ requires m/z = 443.1215). FT−IR (ATR, $\tilde{\nu}_{max}$/cm^{-1}): 3275 (O-H), 3062 (w, C-H_{ar}), 1608,1591, 1531 (m, C-C_{ar} and C_{ar}-N), 1487, 1460, 1433 (m, C_{ar}-NN and/or C-C_{ar}). UV – VIS (ethanol, λ/nm, 10^{-5} mol.L^{-1}): 330, 664. ^{1}H NMR (400 MHz, DMSO-d_6): δ(ppm) 13.14; 9.93; 9.07; 8.66; 8.40; 8.15; 7.94; 7.83; 7.75; 7.39; 6.96; 6.65; 6.57

Compound **C2**

The compound **C2** was prepared by reaction of **L1** (50 mg, 0.120 mmol, 2.0 eq) and $Fe(CF_3SO_3)_2.6H_2O$ (21.3 mg, 0.06 mmol, 1.0 eq) in nitromethane-ethanol (1:1, 20 cm^3) stirred under N_2. The turquoise-colored complex was stirred at 60 °C for 1 hour, filtered off and crystallized at RT by slow evaporation of solvent. Yield of dark blue single-crystals was 38 % after 8 weeks. Elemental analysis for $[Fe(L1)_2](CF_3SO_3)_2 \cdot 0.75CH_3CH_2OH \cdot CH_3NO_2$ ($C_{54.5}H_{41.5}FeN_{15}F_6O_{8.75}S_2$; M_w= 1280.42 g.mol^{-1}) found % (expected %): C 51.01 (51.13); N 16.92 (16.26); H 3.20 (3.35); S 5.01 (4.96). ESI ToF MS: $[Fe(L1)_2](CF_3SO_3)^+$ m/z = 1035.1993 ($C_{51}H_{34}N_{14}FeO_3SF_3^+$ requires m/z = 1035.1956); $[Fe(L1)_2]^{2+}$ m/z = 443.1343 ($C_{50}H_{34}N_{14}Fe^{2+}$ requires m/z = 443.1215). FT−IR (ATR, $\tilde{\nu}_{max}$/cm^{-1}): 3062 (w, C-H_{ar}), 1607,1591, 1535 (m, C-C_{ar} and C_{ar}-N), 1487, 1458, 1433 (m, C_{ar}-NN and/or C-C_{ar}). UV–VIS (ethanol, λ/nm, 10^{-5} mol.L^{-1}): 330, 663. ^{1}H NMR (400 MHz, DMSO-d_6): δ(ppm) 13.11; 10.99; 9.34; 8.67; 8.16; 7.84; 7.76; 7.40; 6.98; 6.52.

Compound **C3** and compound **C4**

Ligand **L2** was dissolved in ethanol (30 cm^3) and heated up to 60 °C for 30 minutes stirred under N_2. The corresponding $Fe(BF_4)_2.6H_2O$ (19.8 mg, 0.056 mmol, 1.05 eq) for compound **C3** or $Fe(ClO_4)_2.6H_2O$ (22.3 mg, 0.06 mmol, 1.05 eq) for compound **C4** were dissolved in 5 cm^3 of ethanol and immediately added to the ligand solution. The dark green solutions of coordination compounds were stirred at 60 °C next 30 minutes, filtered off and retained for the slow evaporation at 5°C. Yield of dark green single-crystals was 49 % for **C3** and 53 % for **C4** after 2 weeks. Elemental analysis for $[Fe(L2)_2](BF_4)_2 \cdot C_2H_5OH \cdot 3H_2O$ ($C_{38}H_{38}FeN_{10}B_2F_8O_4$; M_w= 926.22 g.mol^{-1}) found % (expected %): C 50.92 (50.17); N 15.90 (15.09); H 4.07 (4.13). ESI ToF MS: $[Fe(L1)_2](BF_4)^+$ m/z = 744.2056 ($C_{36}H_{30}N_{10}FeBF_4^+$ requires m/z = 744.2065).FT−IR (ATR, $\tilde{\nu}_{max}$/cm^{-1}): 3073 (w, C-H_{ar}), 1608,1588, 1551 (m, C-C_{ar} and C_{ar}-N and/or N=N), 1470 (m, C_{ar}-N and/or C-C_{ar}). UV – VIS (ethanol, λ/nm,10^{-5} mol.L^{-1}): 329, 384, 679. ^{1}H NMR (400 MHz, DMSO-d_6): δ(ppm) 13.27; 8.54; 8.28; 8.05; 7.83; 7.72; 7.30; 7.22. Elemental analysis for $[Fe(L2)_2](ClO_4)_2 \cdot 2.2H_2O$ ($C_{36}H_{30.4}FeN_{10}O_{10.2}Cl_2$; M_w= 893.04 g.mol^{-1}) found % (expected %): C 49.21 (48.61); N 15.32 (15.75); H 4.07 (3.40). ESI ToF MS: $[Fe(L1)_2](ClO_4)^+$ m/z = 753.1209 ($C_{36}H_{30}N_{10}FeClO_4^+$ requires m/z = 753.1179). FT−IR (ATR, $\tilde{\nu}_{max}$/cm^{-1}): 3070 (w, C-H_{ar}), 1608, 1589 (m, C-C_{ar} and C_{ar}-N), 1470, 1456, 1435 (m, C_{ar}-NN and/or C-C_{ar}). UV – VIS (ethanol, λ/nm, 10^{-5} mol.L^{-1}): 329, 384, 679. ^{1}H NMR (400 MHz, DMSO-d_6): δ(ppm) 8.52; 8.27; 8.03; 7.82; 7.70; 7.29.

1.4 Spectral characterization of reported compound

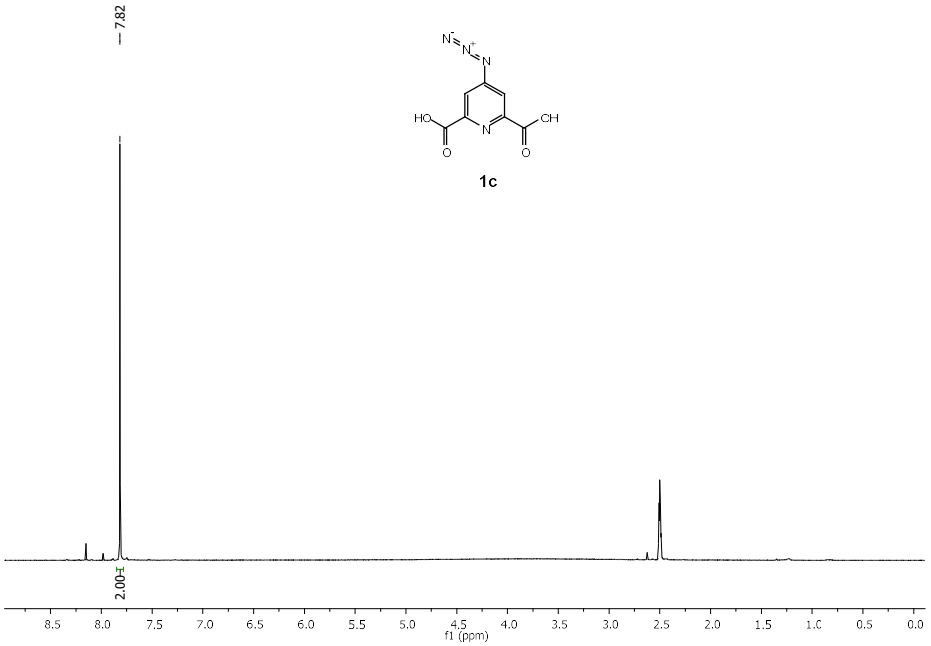

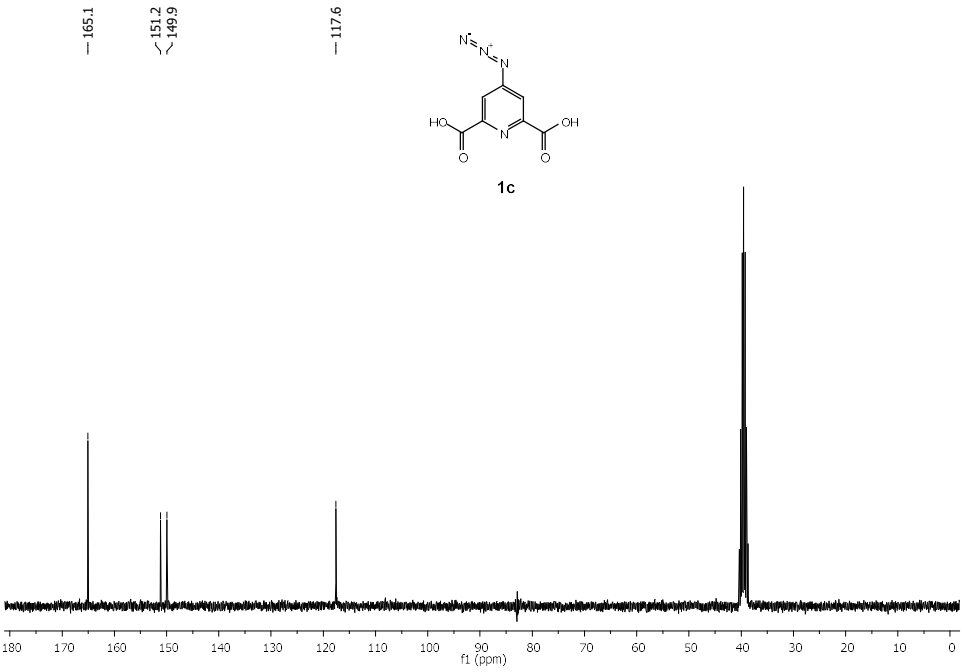

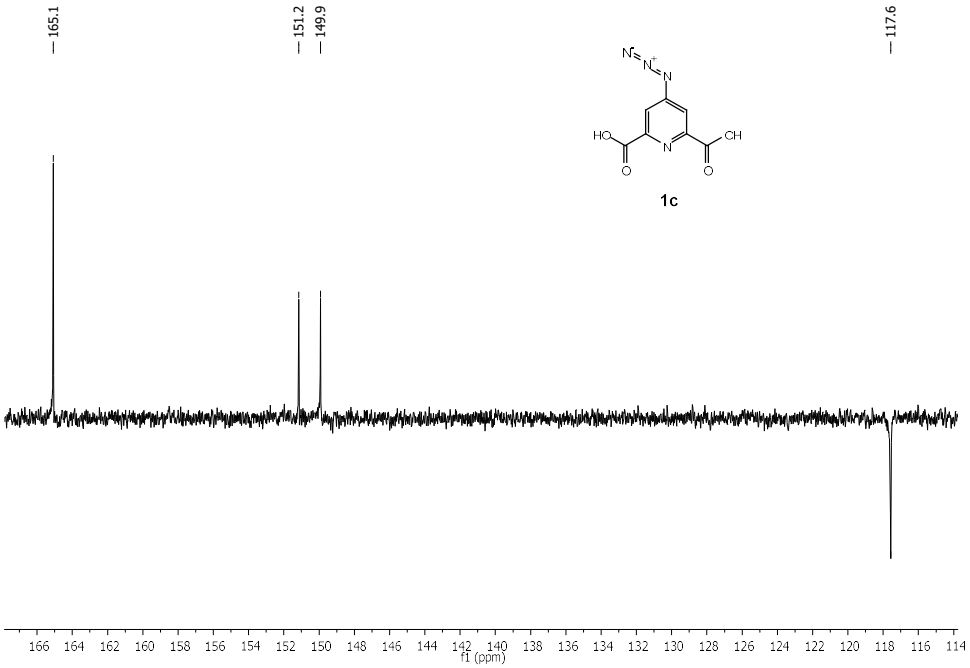
165.1
151.2
149.9
117.6
HO
OH
O
O
N
1c
166 164 162 160 158 156 154 152 150 148 146 144 142 140 138 136 134 132 130 128 126 124 122 120 118 116 114
f1 (ppm)

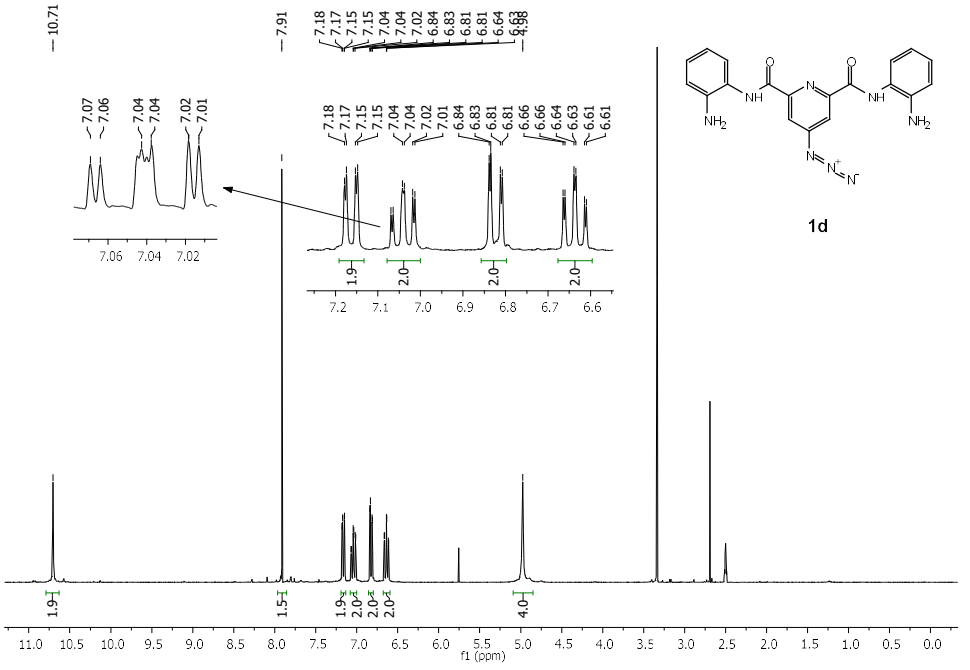
10.71
7.91
7.18
7.17
7.15
7.15
7.04
7.04
7.02
6.84
6.83
6.81
6.64
6.63
4.98
7.07
7.06
7.04
7.04
7.02
7.01
6.66
6.66
6.64
6.63
6.61
6.61
NH
NH
NH2
NH2
1d
1.9
1.5
1.9
2.0
2.0
4.0
11.0 10.5 10.0 9.5 9.0 8.5 8.0 7.5 7.0 6.5 6.0 5.5 5.0 4.5 4.0 3.5 3.0 2.5 2.0 1.5 1.0 0.5 0.0
f1 (ppm)

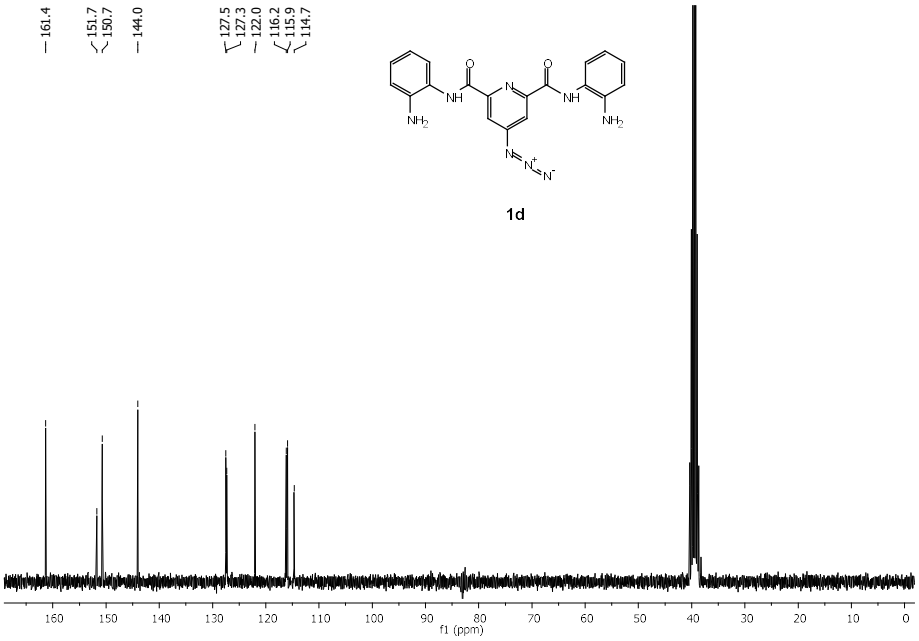
161.4
151.7
150.7
144.0
127.5
127.3
122.0
116.2
115.9
114.7
NH
O
N
NH
NH2
NH2
N+
N-
1d
160
150
140
130
120
110
100
90
80
70
60
50
40
30
20
10
0
f1 (ppm)

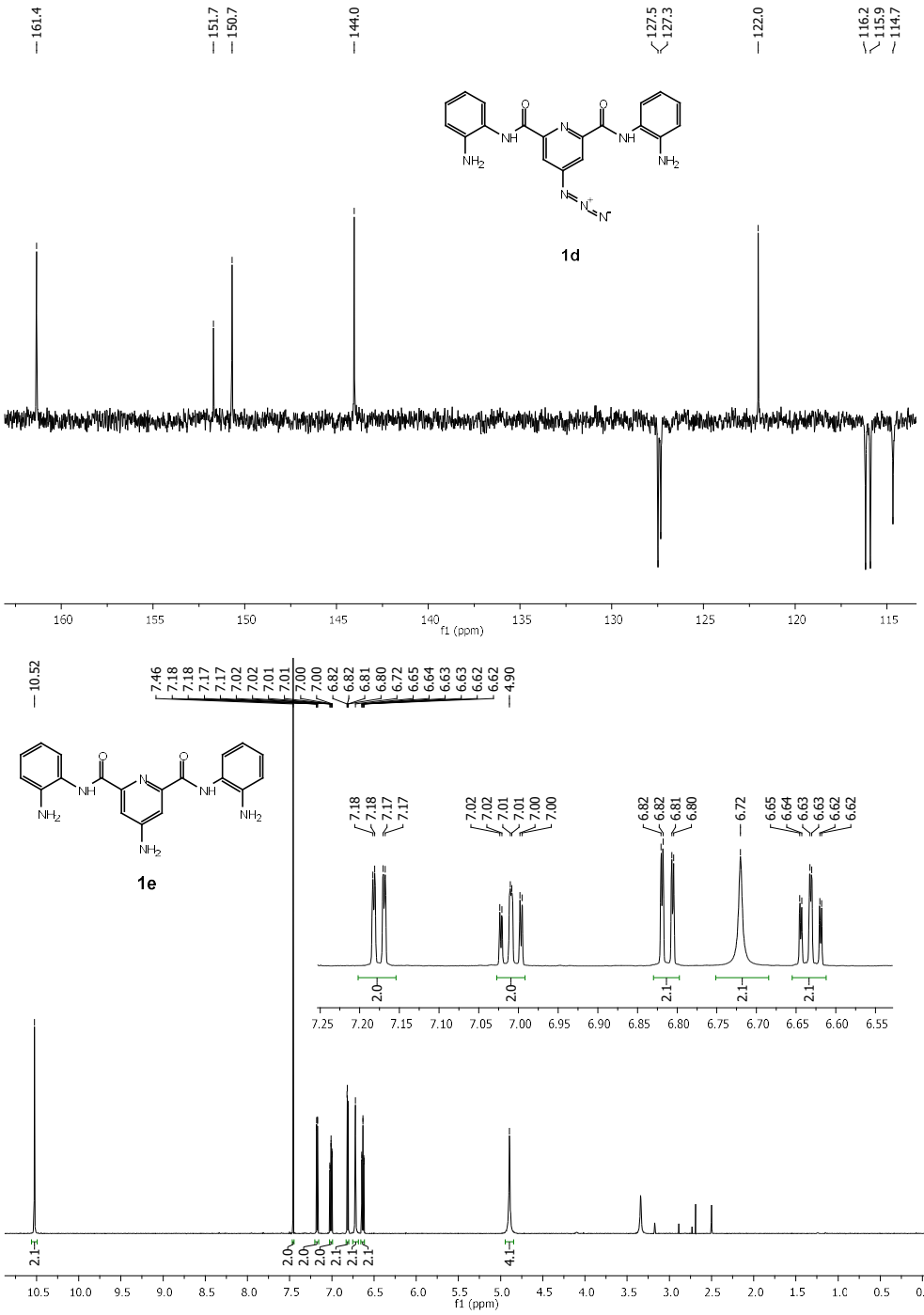
161.4
151.7
150.7
144.0
127.5
127.3
122.0
116.2
115.9
114.7
1d
f1 (ppm)
10.52
7.46
7.18
7.18
7.17
7.17
7.02
7.02
7.01
7.01
7.00
7.00
6.82
6.81
6.80
6.72
6.65
6.64
6.63
6.63
6.62
6.62
4.90
1e
2.0
2.0
2.1
2.1
2.1
2.1
2.0
2.0
2.1
2.1
2.1
4.1
f1 (ppm)

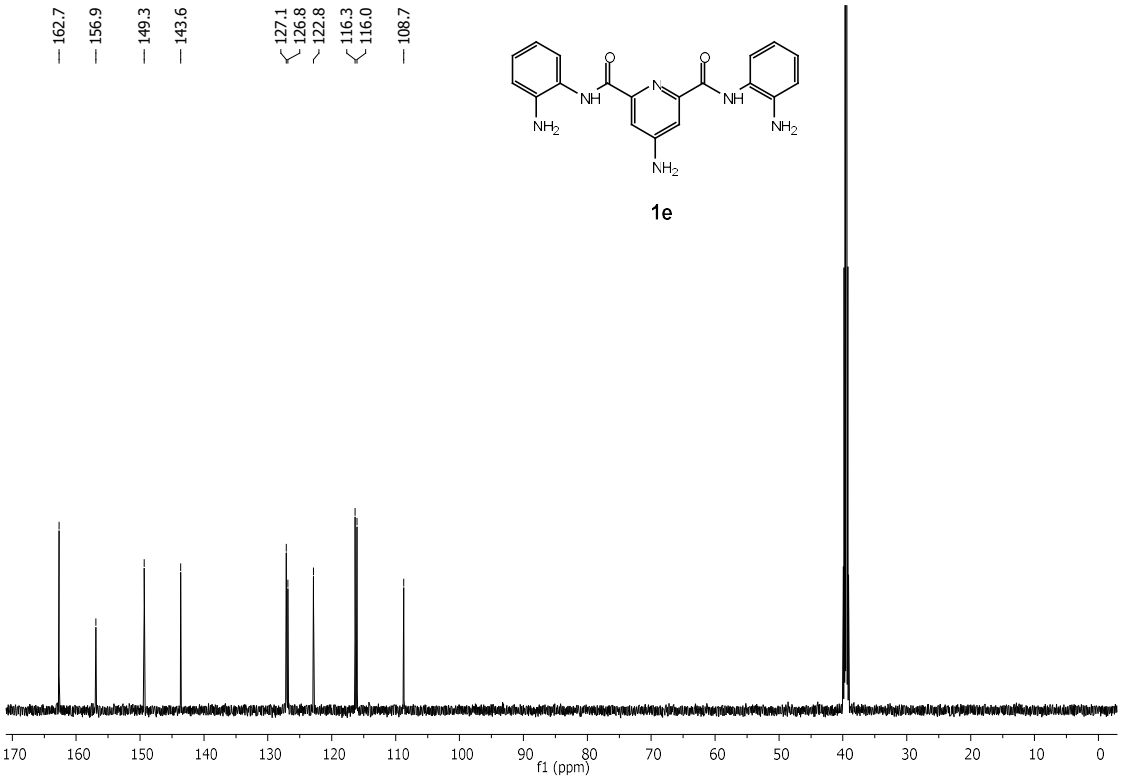
162.7
156.9
149.3
143.6
127.1
126.8
122.8
116.3
116.0
108.7
NH
NH
N
O
O
NH2
NH2
NH2
1e
170 160 150 140 130 120 110 100 90 80 70 60 50 40 30 20 10 0
f1 (ppm)

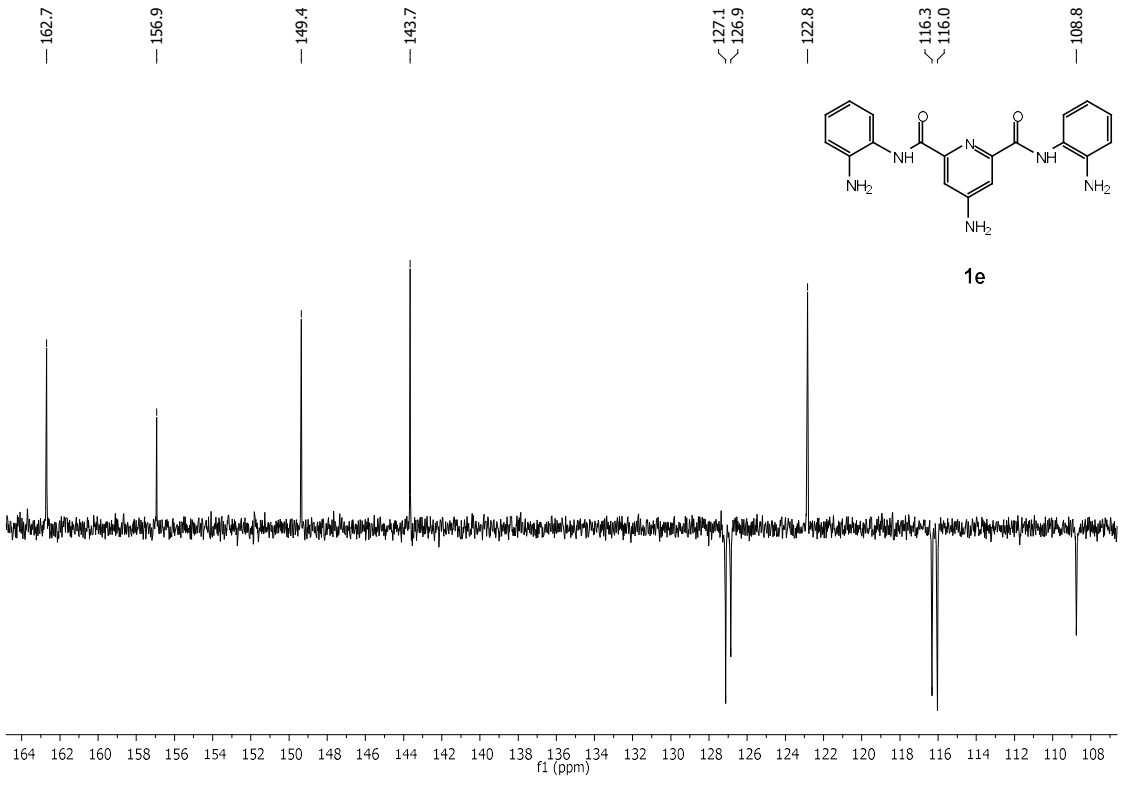
162.7
156.9
149.4
143.7
127.1
126.9
122.8
116.3
116.0
108.8
NH
NH
N
O
O
NH2
NH2
NH2
1e
164 162 160 158 156 154 152 150 148 146 144 142 140 138 136 134 132 130 128 126 124 122 120 118 116 114 112 110 108
f1 (ppm)

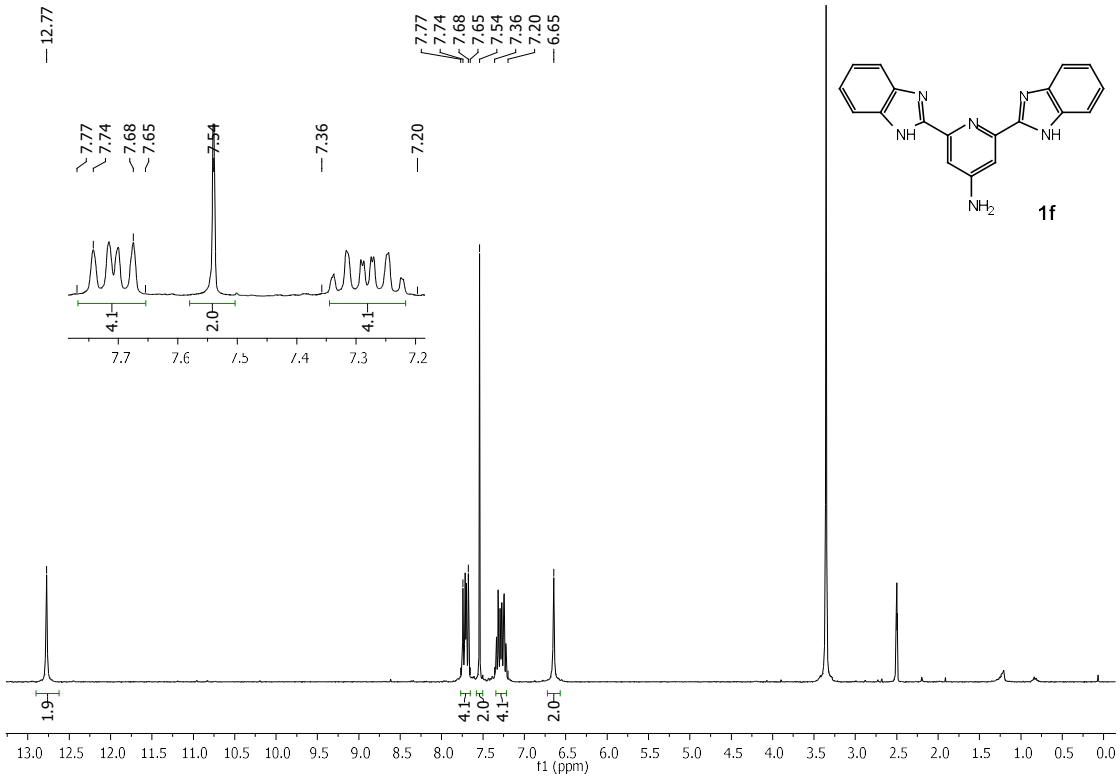
12.77
7.77
7.74
7.68
7.65
7.54
7.36
7.20
6.65
1.9
4.1
2.0
4.1
2.0
f1 (ppm)
1f

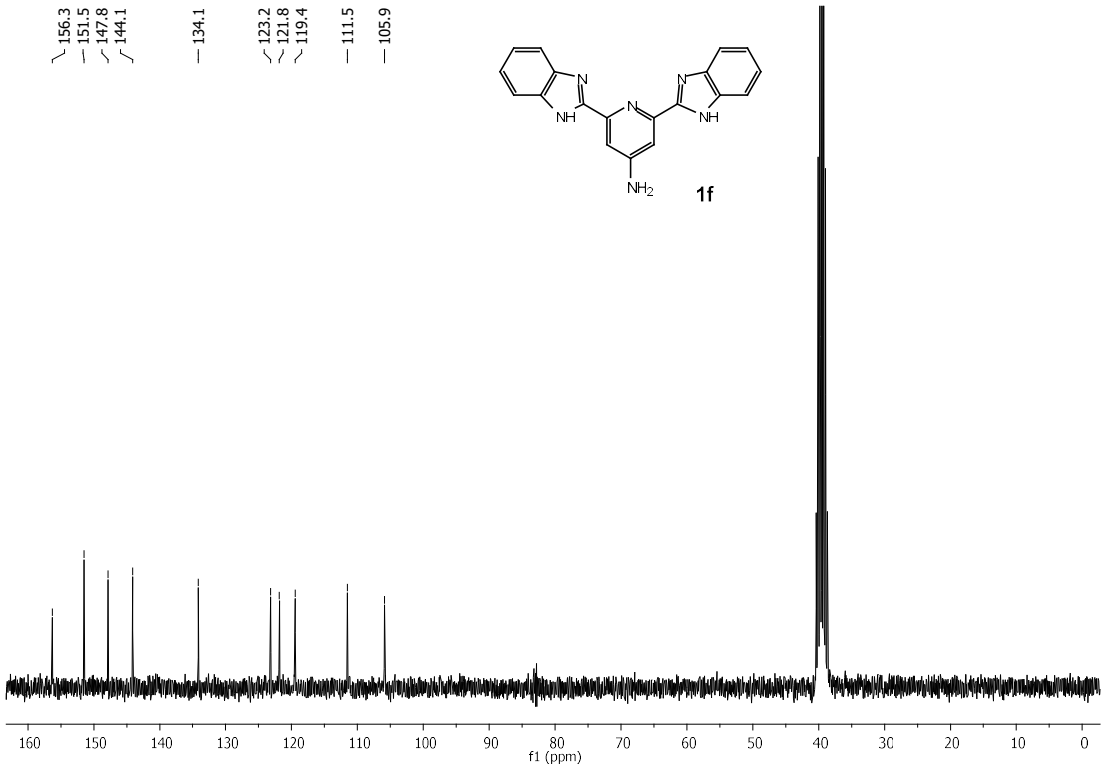
156.3
151.5
147.8
144.1
134.1
123.2
121.8
119.4
111.5
105.9
f1 (ppm)
1f

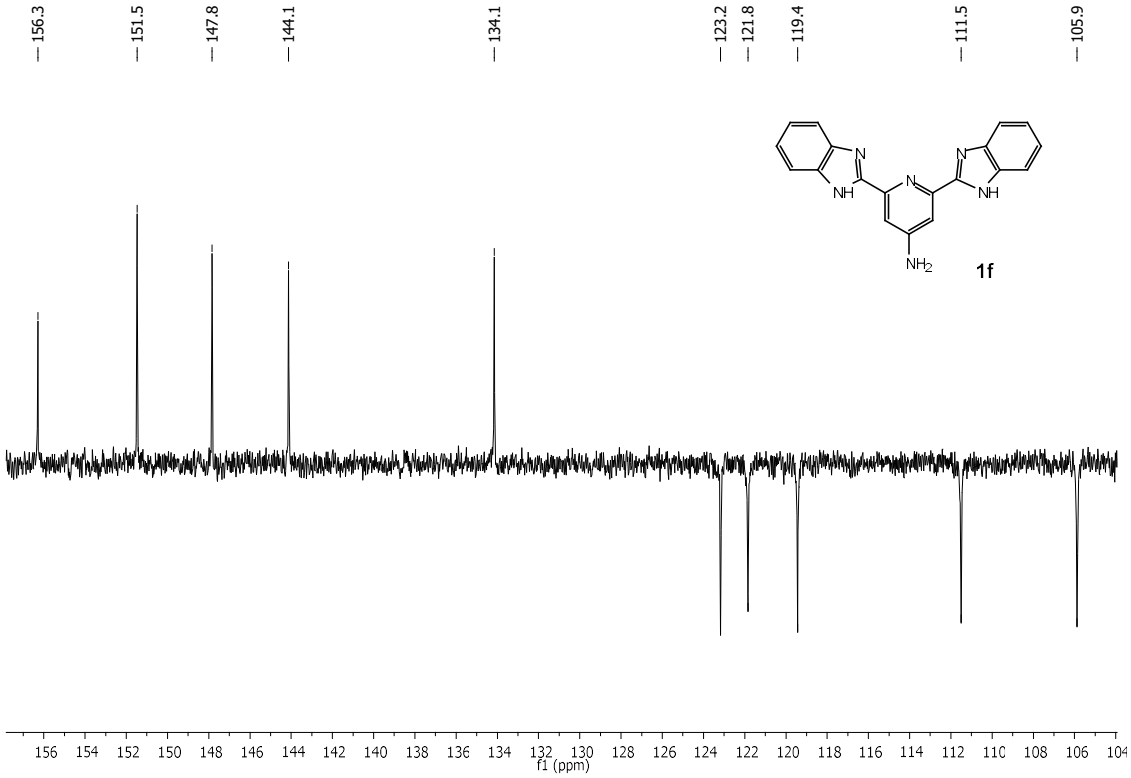
156.3
151.5
147.8
144.1
134.1
123.2
121.8
119.4
111.5
105.9
NH
N
NH2
1f
f1 (ppm)

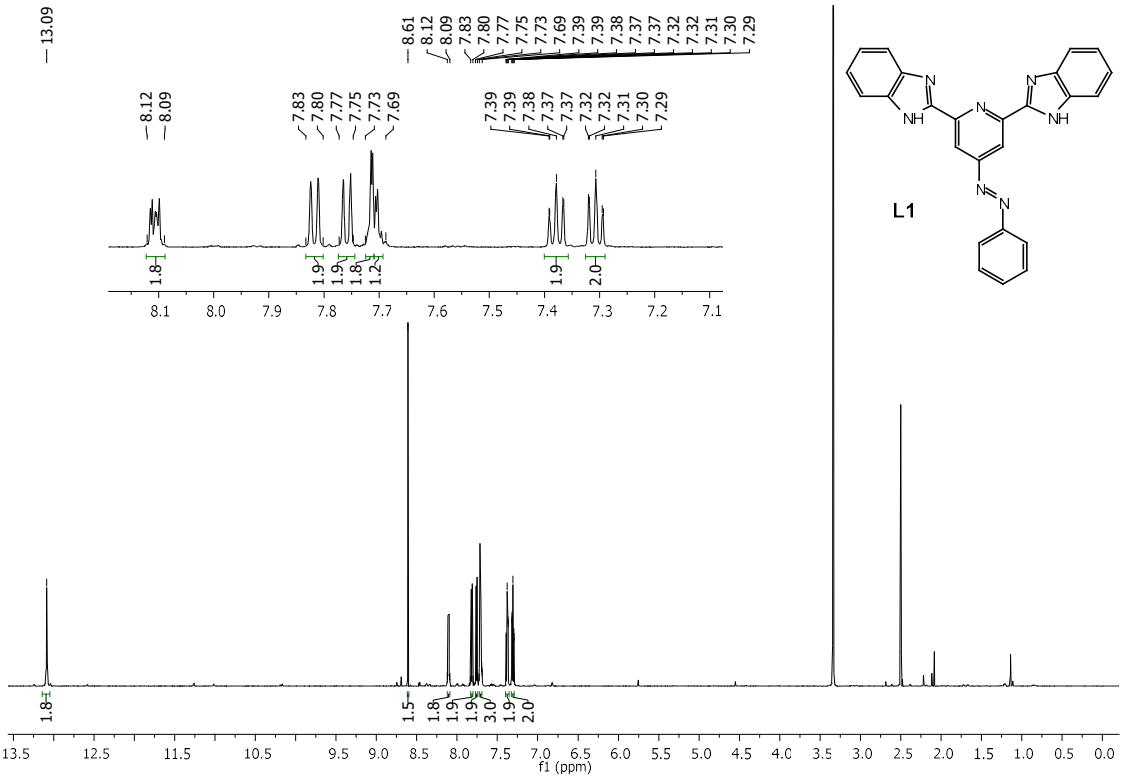
13.09
8.61
8.12
8.09
7.83
7.80
7.77
7.75
7.73
7.69
7.39
7.39
7.38
7.37
7.37
7.32
7.32
7.31
7.30
7.29
L1
f1 (ppm)

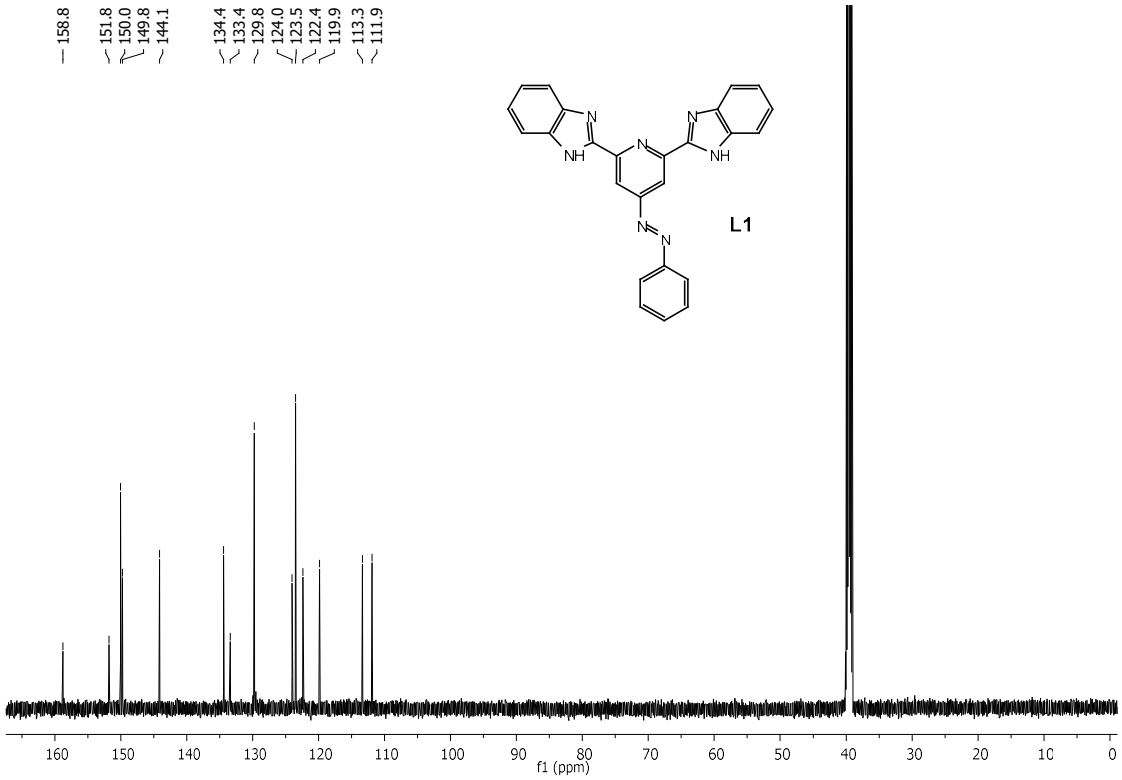
158.8
151.8
150.0
149.8
144.1
134.4
133.4
129.8
124.0
123.5
122.4
119.9
113.3
111.9
L1
160 150 140 130 120 110 100 90 80 70 60 50 40 30 20 10 0
f1 (ppm)

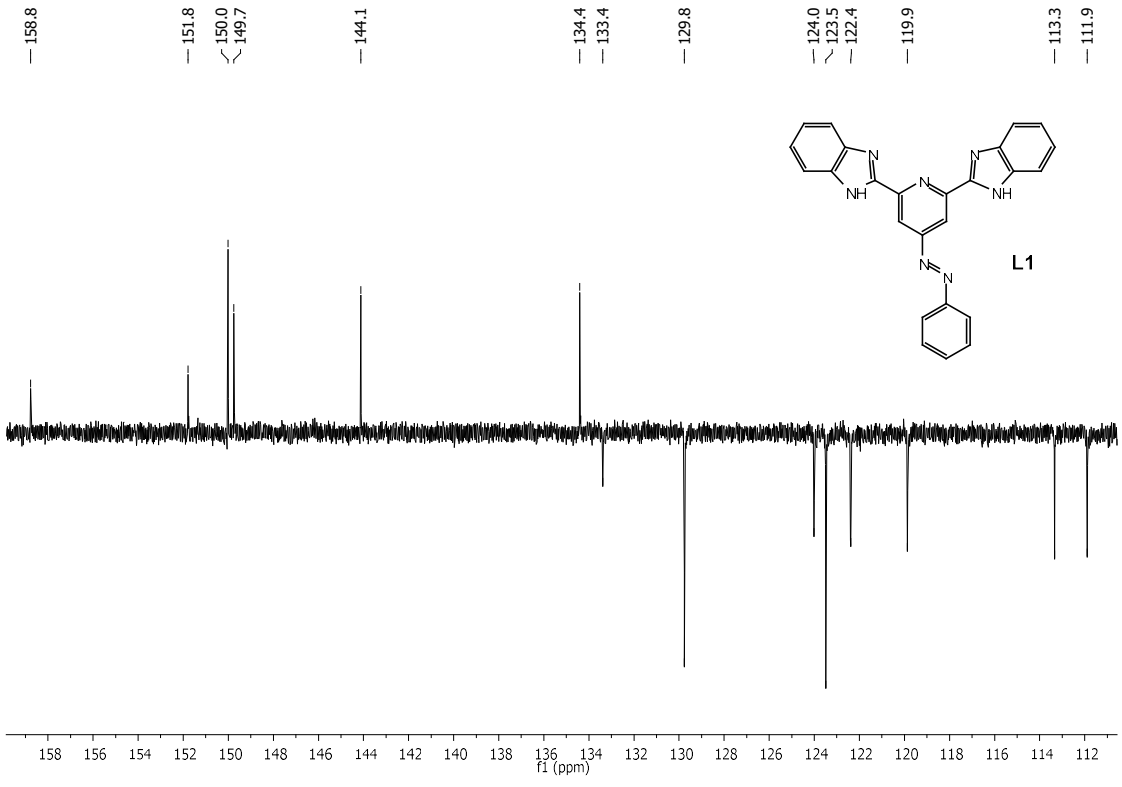
158.8
151.8
150.0
149.7
144.1
134.4
133.4
129.8
124.0
123.5
122.4
119.9
113.3
111.9
L1
158 156 154 152 150 148 146 144 142 140 138 136 134 132 130 128 126 124 122 120 118 116 114 112
f1 (ppm)

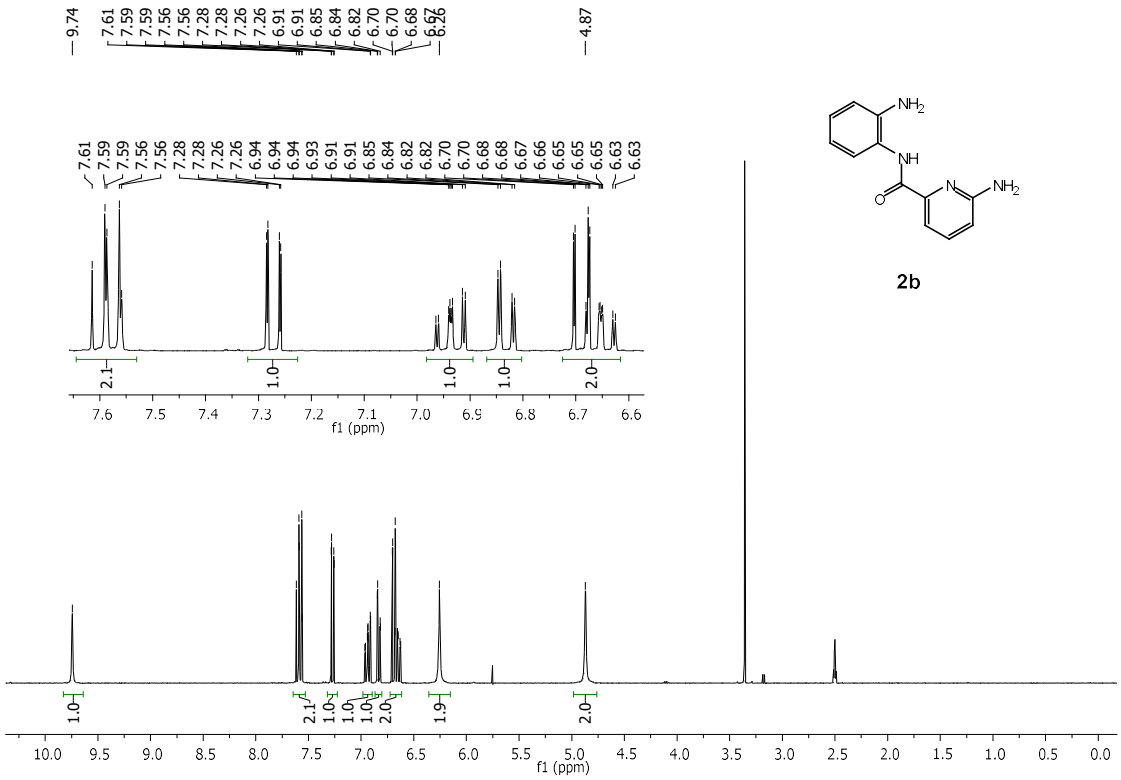
9.74
7.61
7.59
7.59
7.56
7.56
7.28
7.28
7.26
7.26
6.91
6.91
6.85
6.84
6.82
6.70
6.68
6.67
6.26
4.87
NH2
NH
N
NH2
O
2b
2.1
1.0
1.0
1.0
2.0
f1 (ppm)
1.0
2.1
1.0
1.0
2.0
1.9
2.0
f1 (ppm)

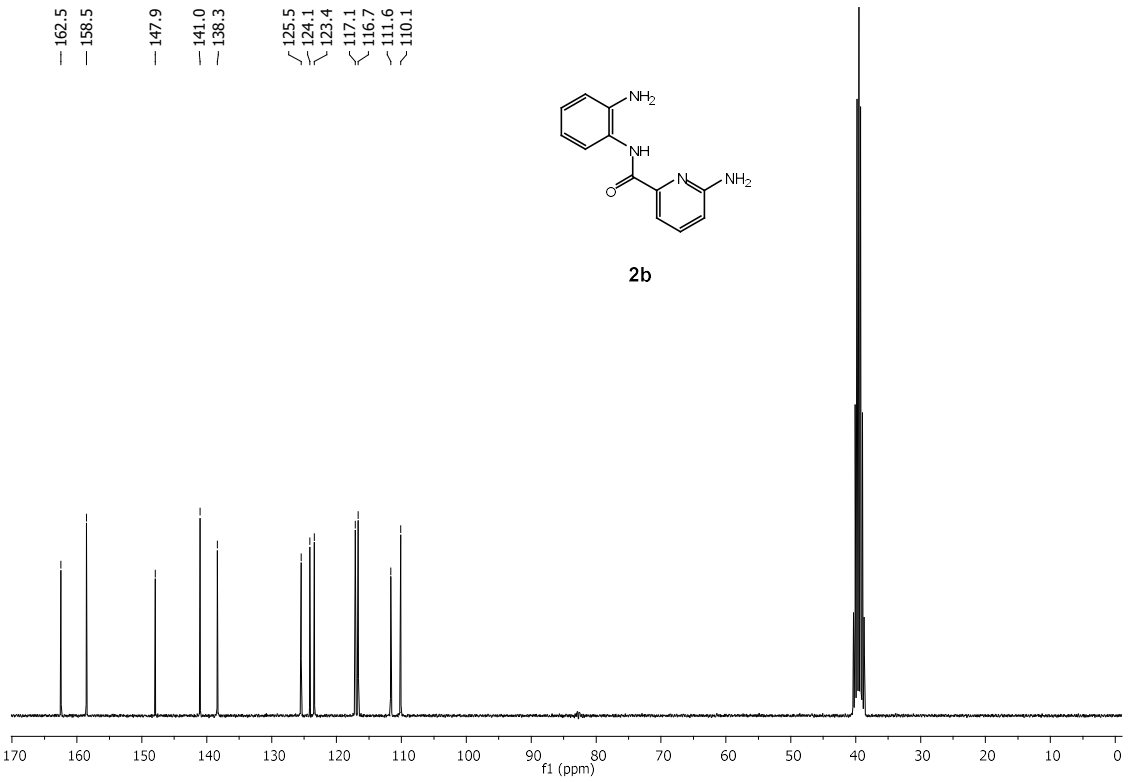
162.5
158.5
147.9
141.0
138.3
125.5
124.1
123.4
117.1
116.7
111.6
110.1
NH2
NH
N
NH2
O
2b
f1 (ppm)

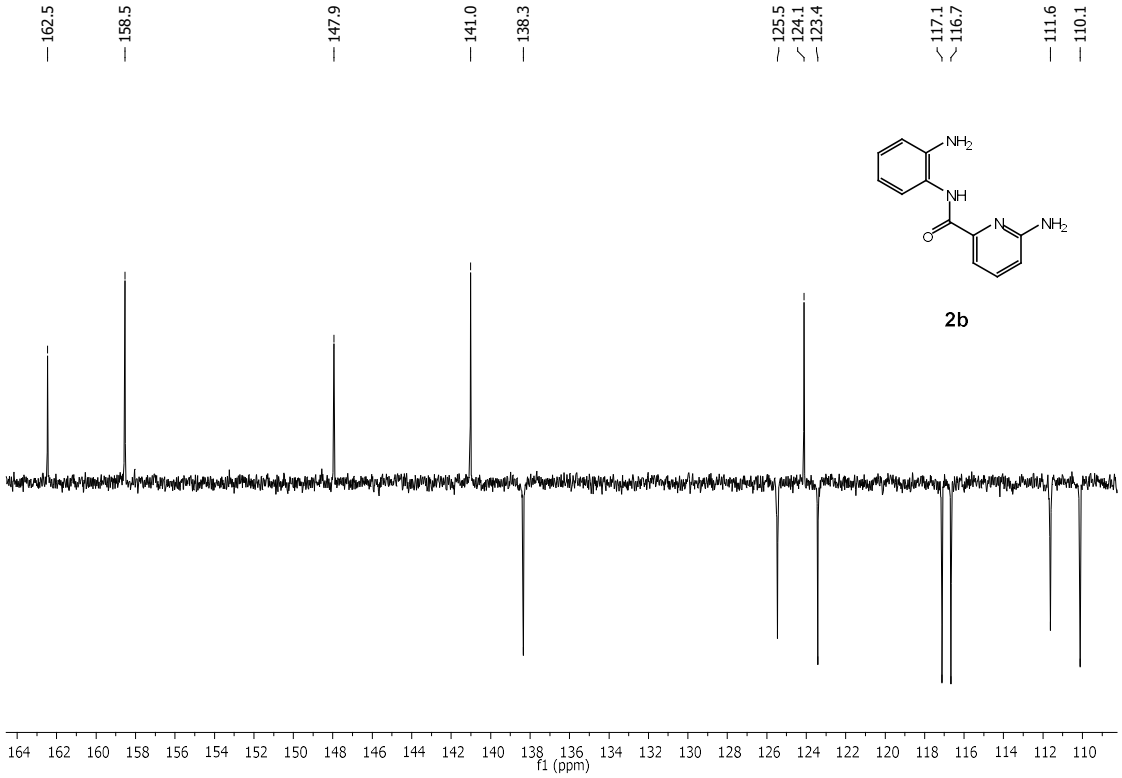
162.5
158.5
147.9
141.0
138.3
125.5
124.1
123.4
117.1
116.7
111.6
110.1
NH2
NH
O
N
NH2
2b
f1 (ppm)

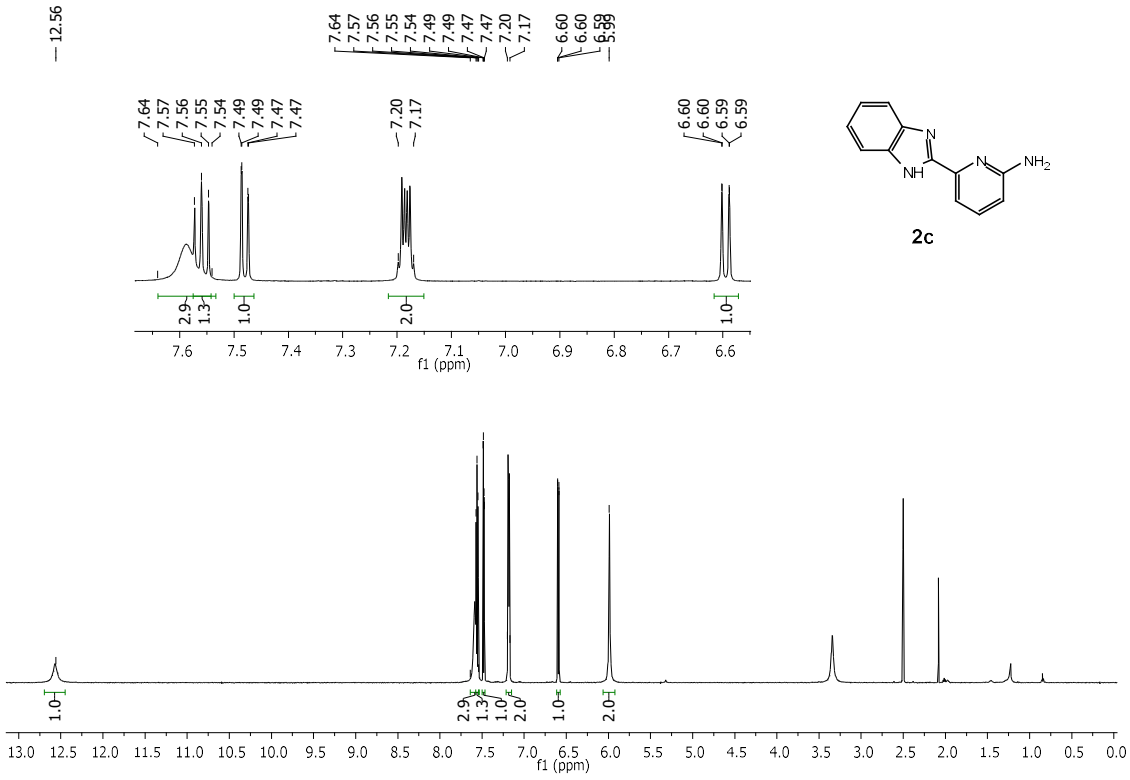
12.56
7.64
7.57
7.56
7.55
7.54
7.49
7.49
7.47
7.47
7.20
7.17
6.60
6.60
6.59
6.59
N
NH
N
NH2
2c
2.9
1.3
1.0
2.0
1.0
f1 (ppm)

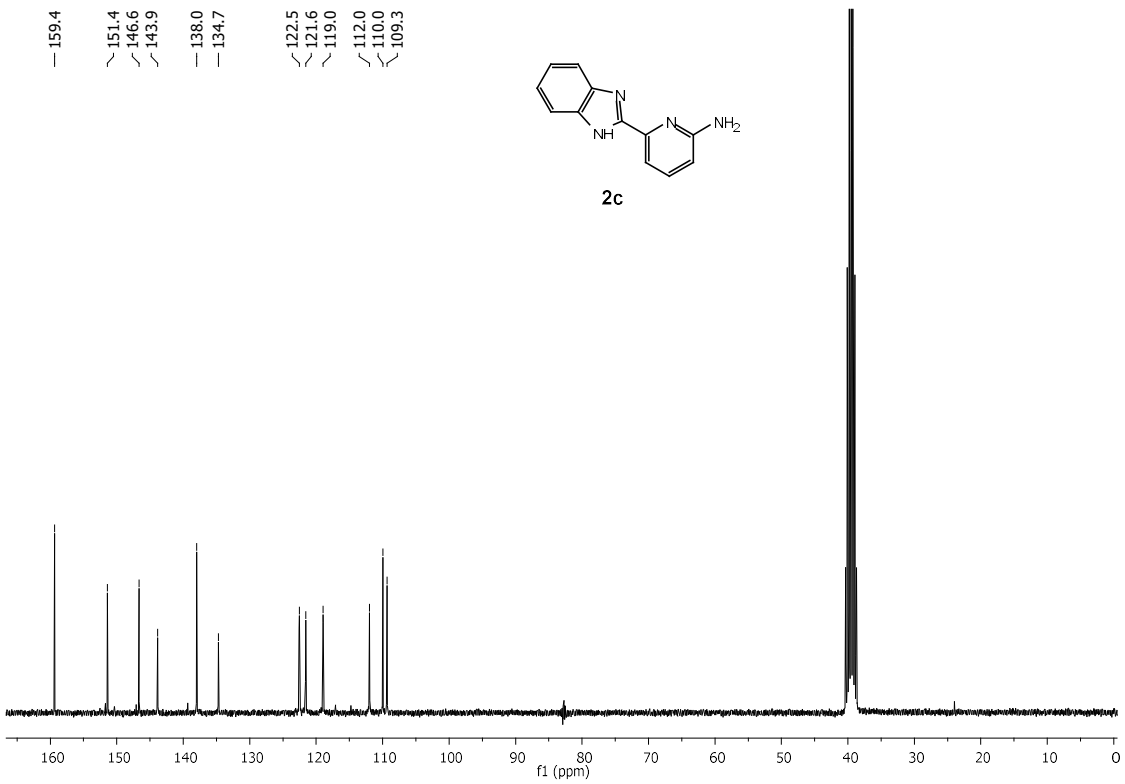
159.4
151.4
146.6
143.9
138.0
134.7
122.5
121.6
119.0
112.0
110.0
109.3
NH
N
N
NH2
2c
160
150
140
130
120
110
100
90
80
70
60
50
40
30
20
10
0
f1 (ppm)

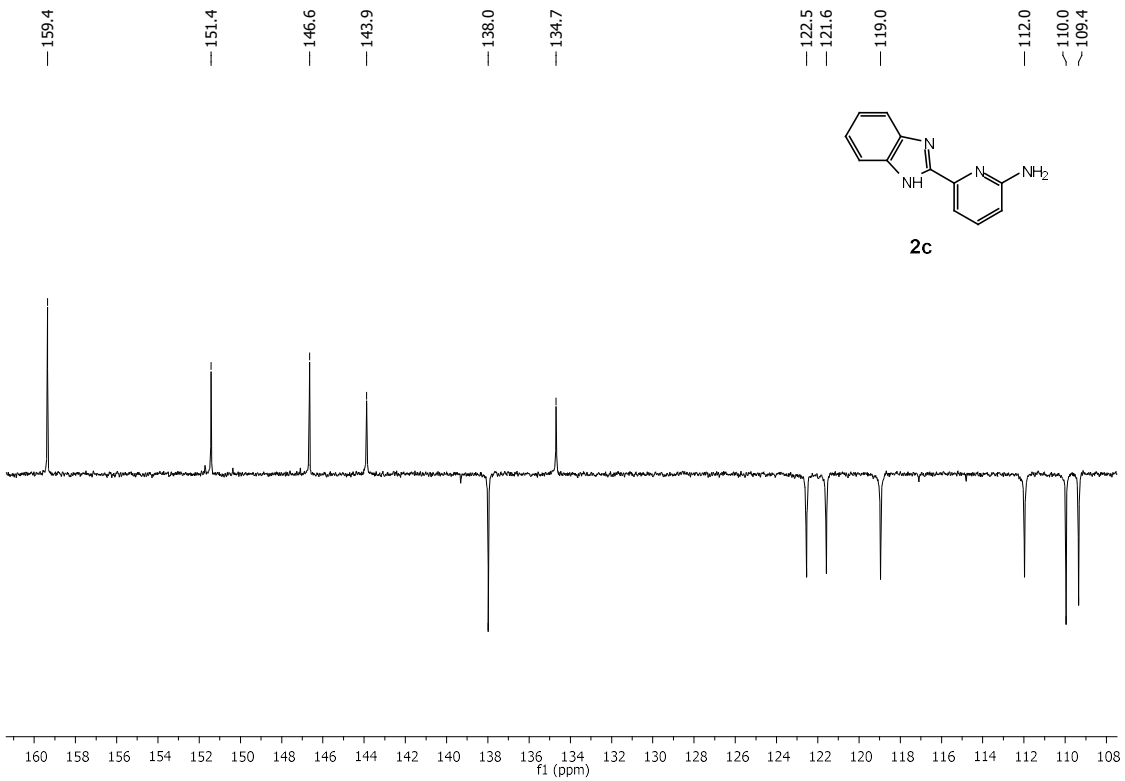
159.4
151.4
146.6
143.9
138.0
134.7
122.5
121.6
119.0
112.0
110.0
109.4
NH
N
N
NH2
2c
160
158
156
154
152
150
148
146
144
142
140
138
136
134
132
130
128
126
124
122
120
118
116
114
112
110
108
f1 (ppm)

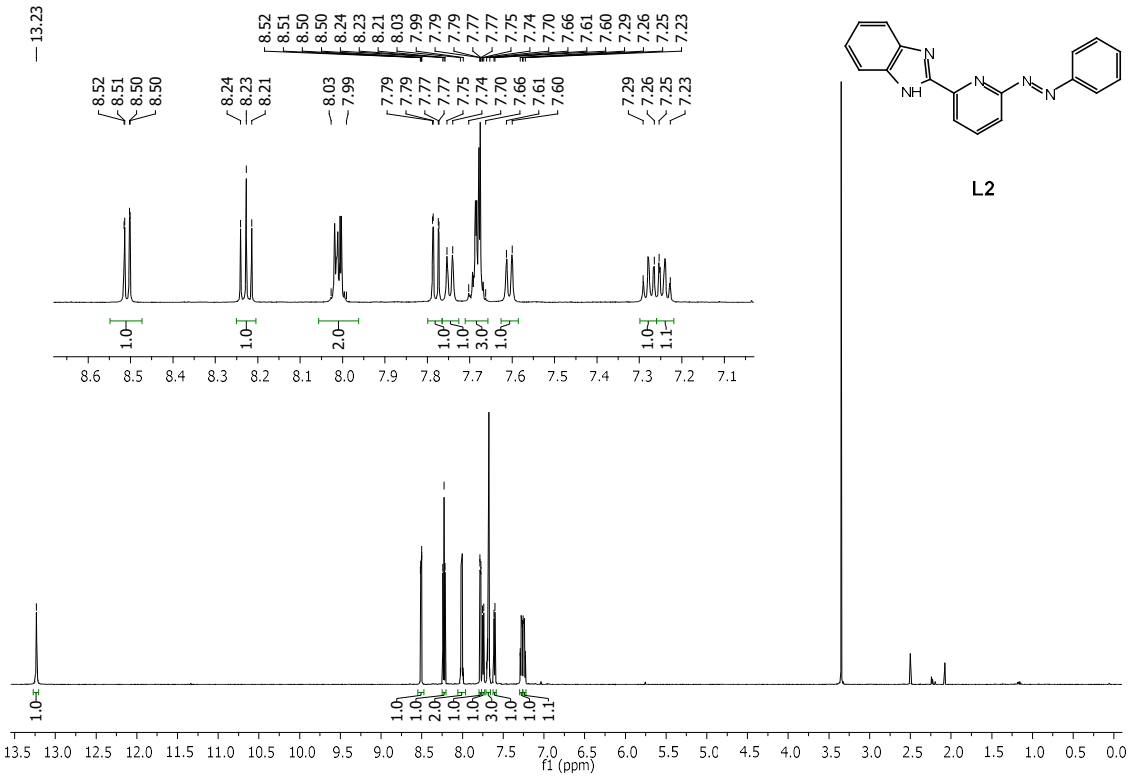
13.23
8.52
8.51
8.50
8.50
8.24
8.23
8.21
8.03
7.99
7.79
7.79
7.77
7.77
7.75
7.74
7.70
7.66
7.61
7.60
7.29
7.26
7.25
7.23
L2
f1 (ppm)

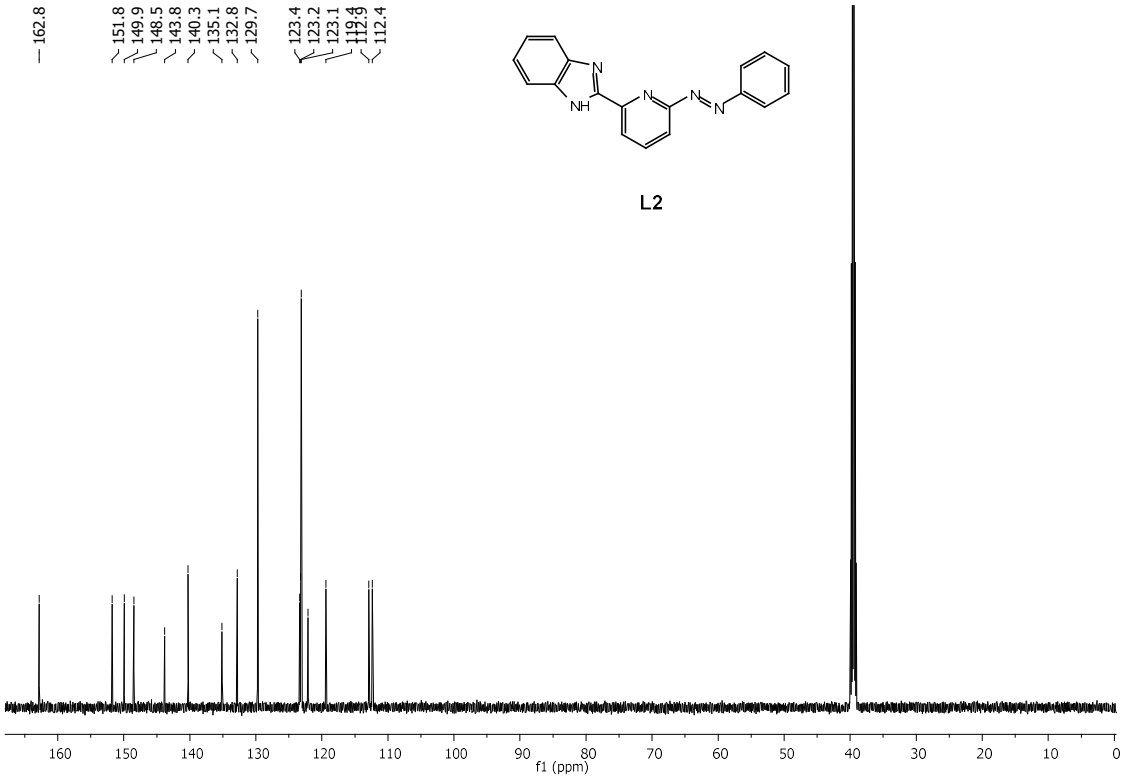
162.8
151.8
149.9
148.5
143.8
140.3
135.1
132.8
129.7
123.4
123.2
123.1
112.4
L2
f1 (ppm)

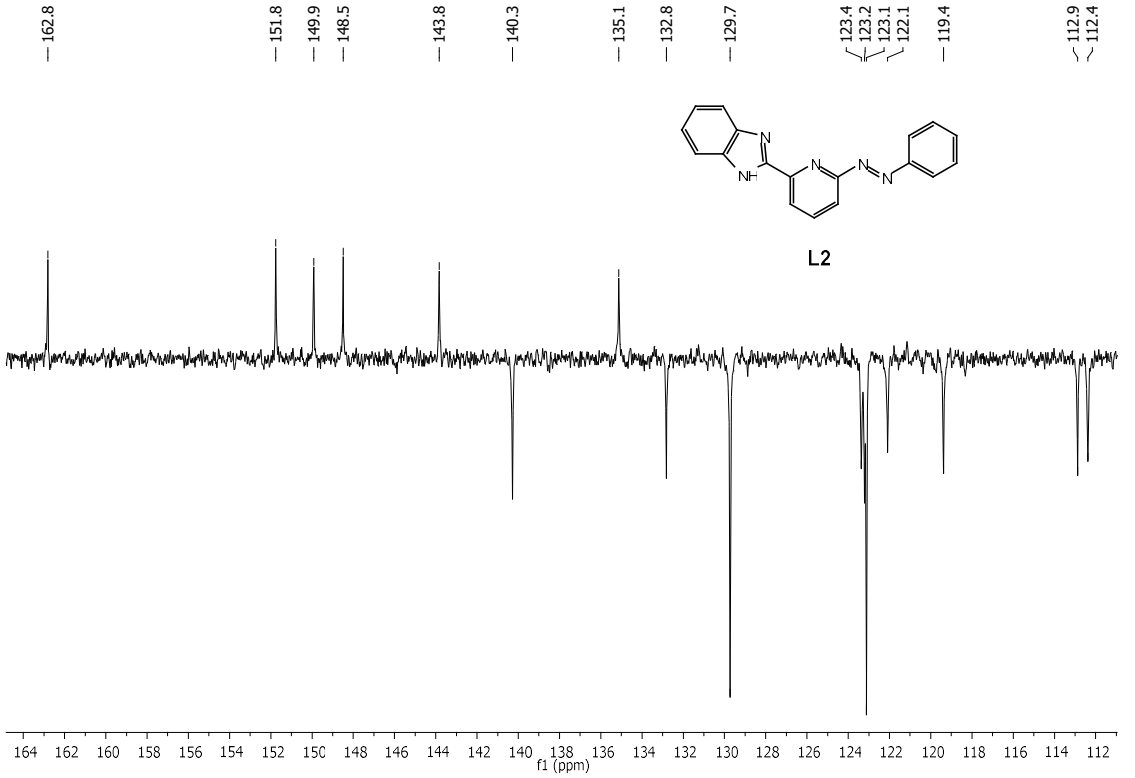
162.8
151.8
149.9
148.5
143.8
140.3
135.1
132.8
129.7
123.4
123.2
123.1
122.1
119.4
112.9
112.4
L2
f1 (ppm)

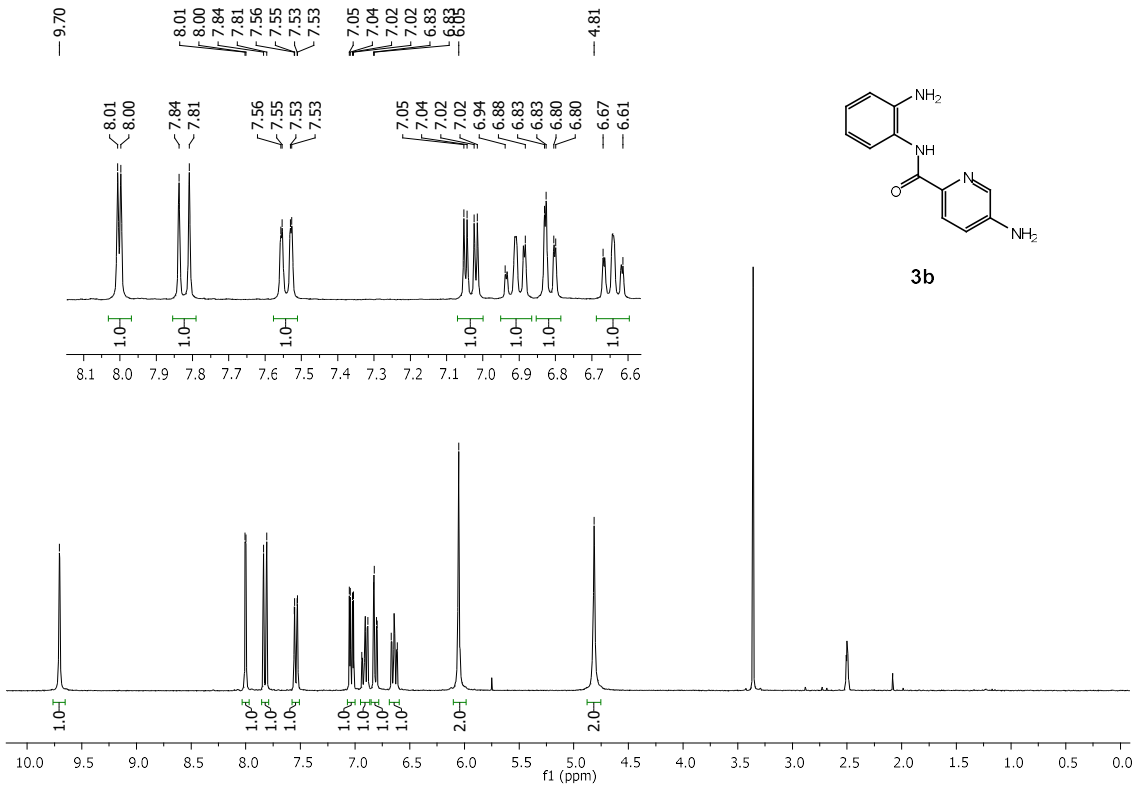
9.70
8.01
8.00
7.84
7.81
7.56
7.55
7.53
7.53
7.05
7.04
7.02
7.02
6.94
6.88
6.83
6.83
6.80
6.80
6.67
6.61
4.81
3b
f1 (ppm)

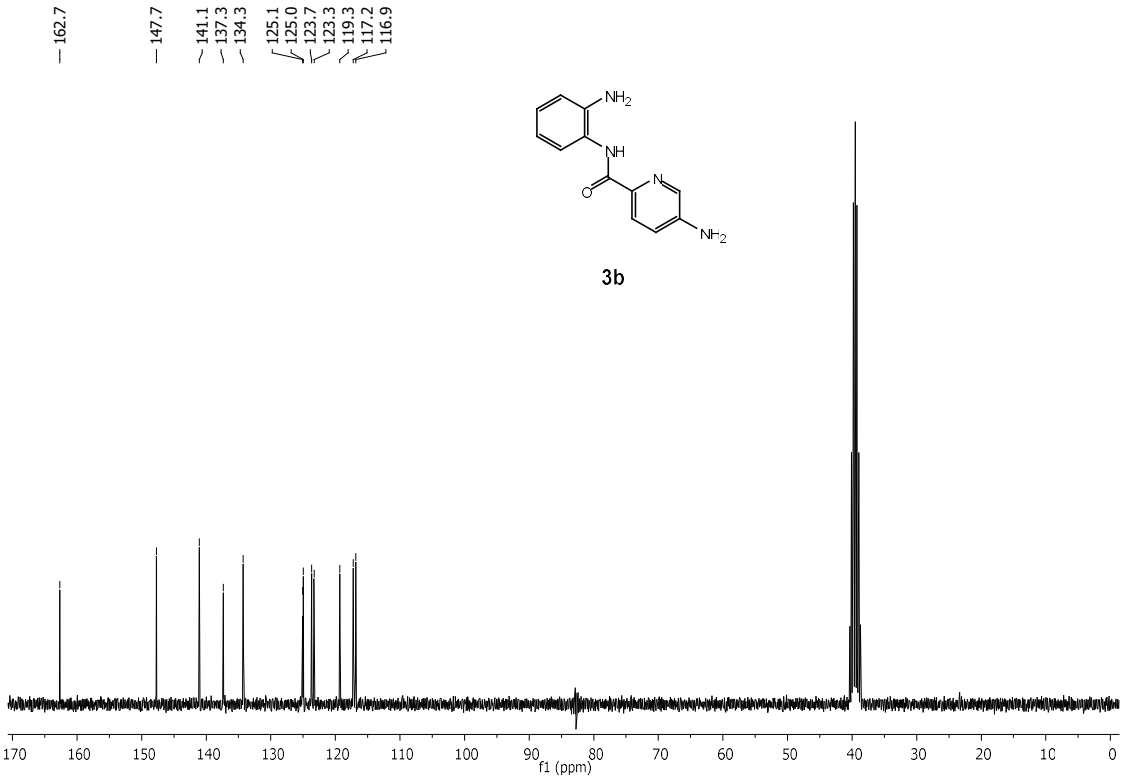
162.7
147.7
141.1
137.3
134.3
125.1
125.0
123.7
123.3
119.3
117.2
116.9
NH2
NH
O
N
NH2
3b
170
160
150
140
130
120
110
100
90
80
70
60
50
40
30
20
10
0
f1 (ppm)

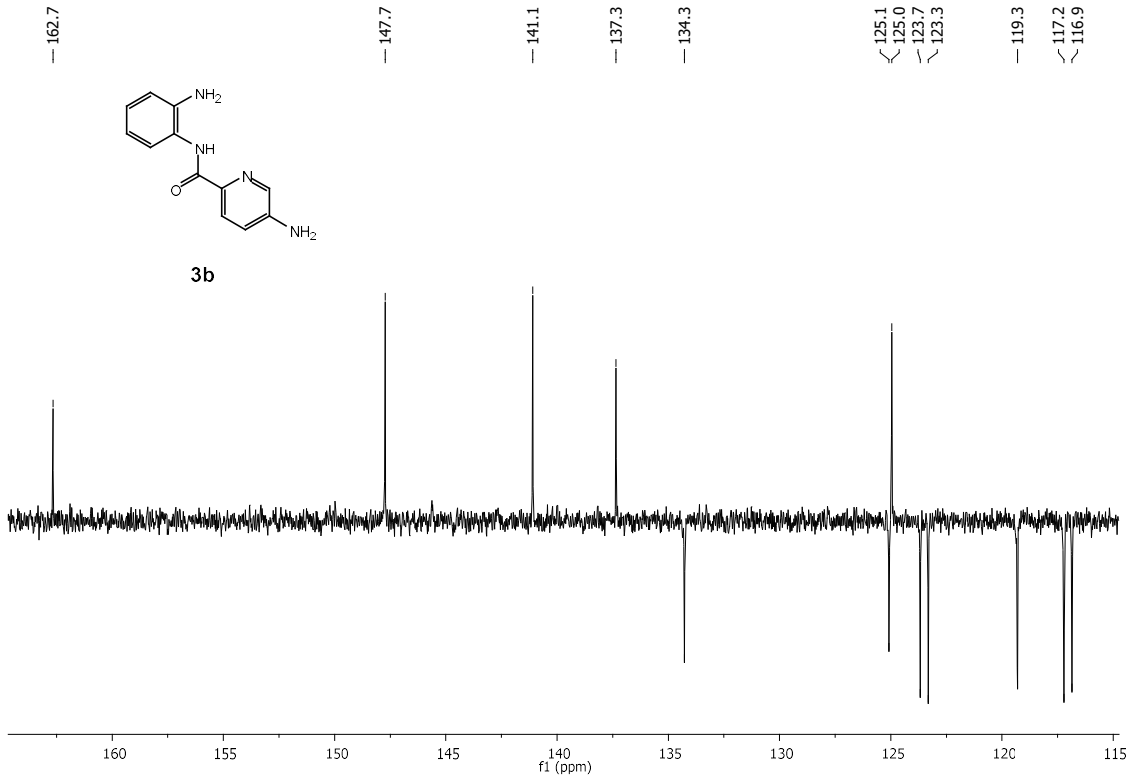
162.7
147.7
141.1
137.3
134.3
125.1
125.0
123.7
123.3
119.3
117.2
116.9
NH2
NH
O
N
NH2
3b
160
155
150
145
140
135
130
125
120
115
f1 (ppm)

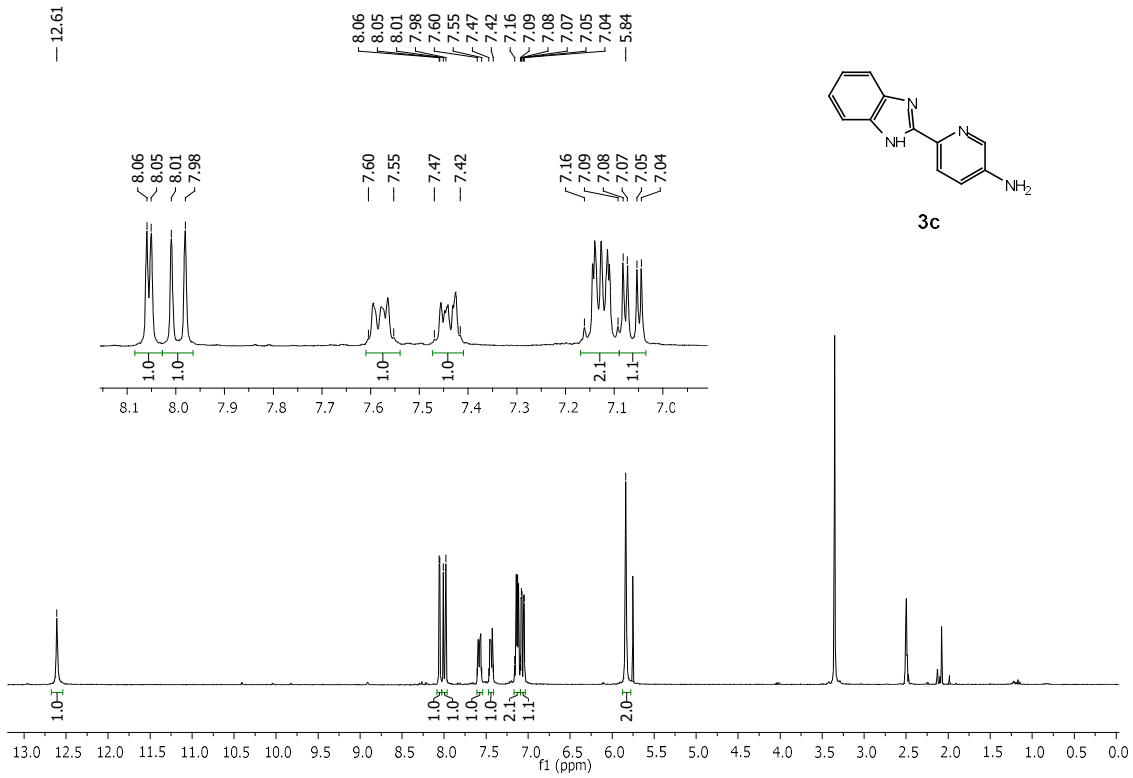
12.61
8.06
8.05
8.01
7.98
7.60
7.55
7.47
7.42
7.16
7.09
7.08
7.07
7.05
7.04
5.84
NH
N
NH2
3c
1.0
1.0
1.0
1.0
2.1
1.1
f1 (ppm)

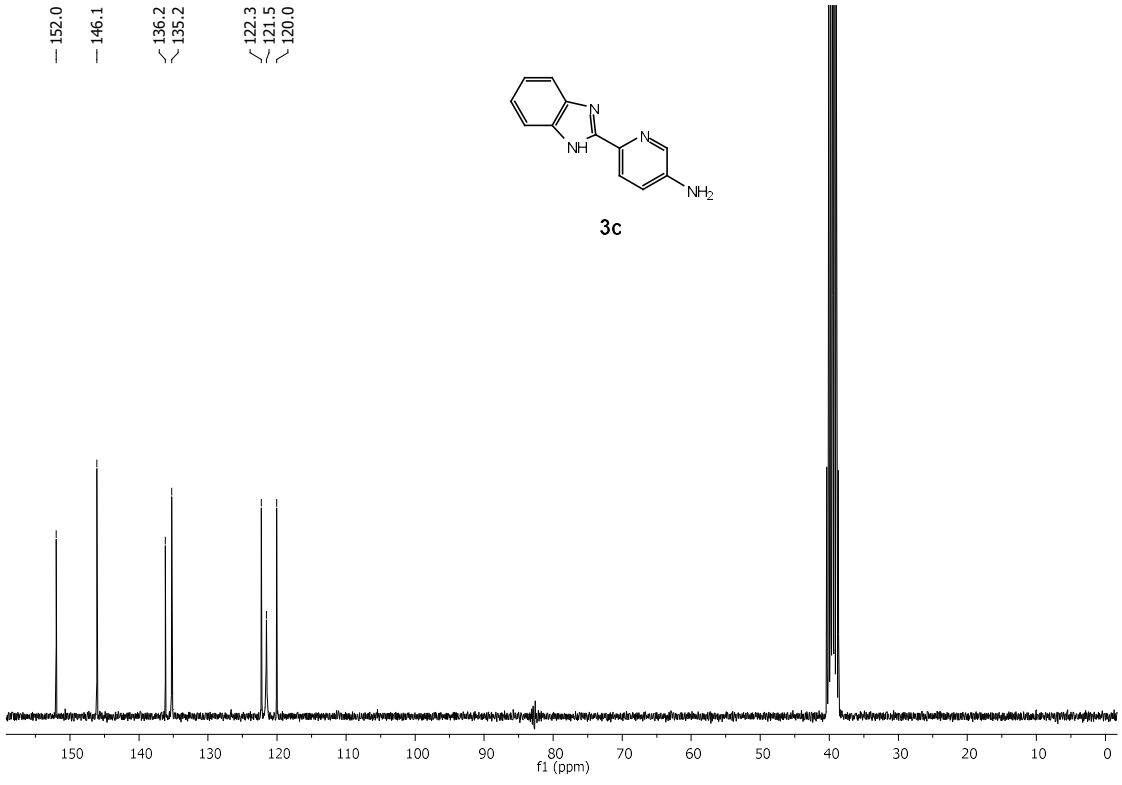
152.0
146.1
136.2
135.2
122.3
121.5
120.0
NH
N
NH2
3c
f1 (ppm)

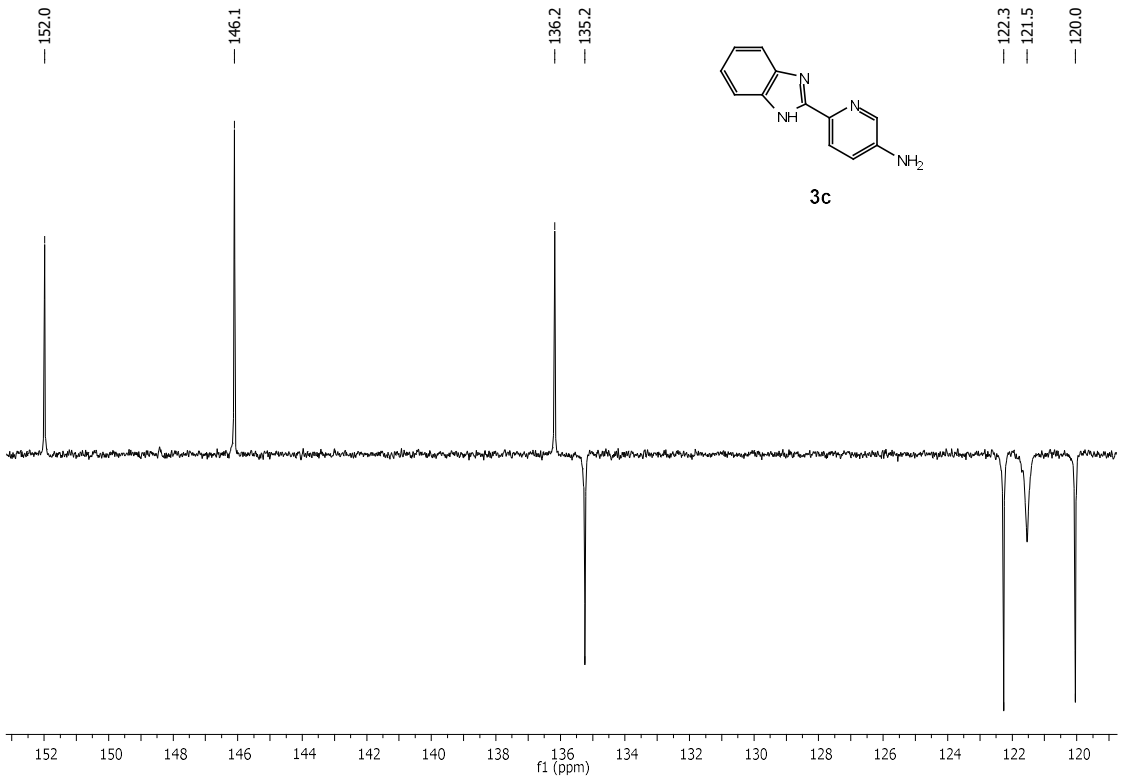
152.0
146.1
136.2
135.2
122.3
121.5
120.0
N
NH
N
NH2
3c
152 150 148 146 144 142 140 138 136 134 132 130 128 126 124 122 120
f1 (ppm)

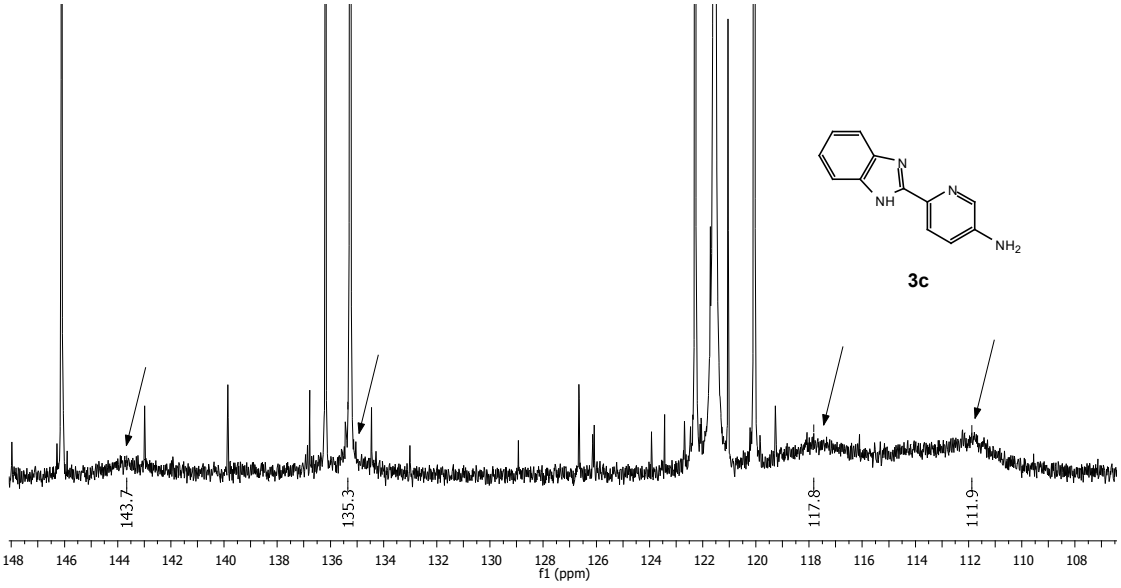
N
NH
N
NH2
3c
143.7
135.3
117.8
111.9
148 146 144 142 140 138 136 134 132 130 128 126 124 122 120 118 116 114 112 110 108
f1 (ppm)

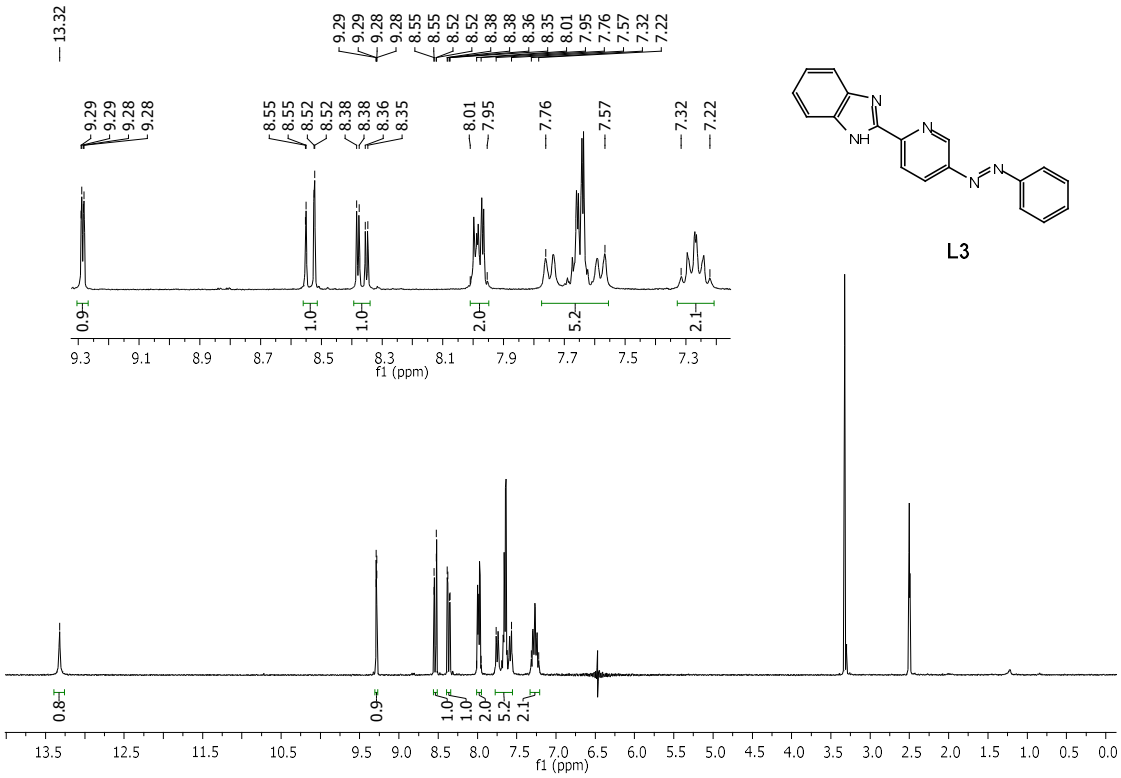
13.32
9.29
9.29
9.28
9.28
8.55
8.55
8.52
8.52
8.38
8.38
8.36
8.35
8.01
7.95
7.76
7.57
7.32
7.22
0.9
1.0
1.0
2.0
5.2
2.1
f1 (ppm)
L3

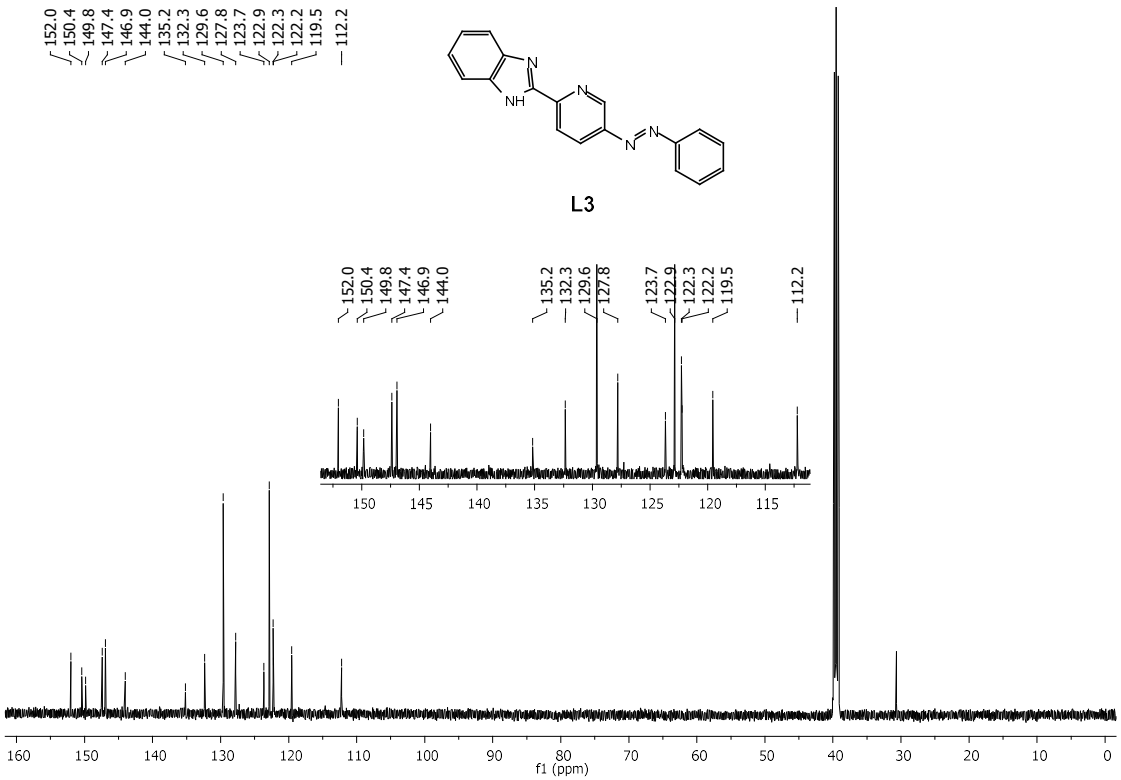
152.0
150.4
149.8
147.4
146.9
144.0
135.2
132.3
129.6
127.8
123.7
122.9
122.3
122.2
119.5
112.2
L3
f1 (ppm)

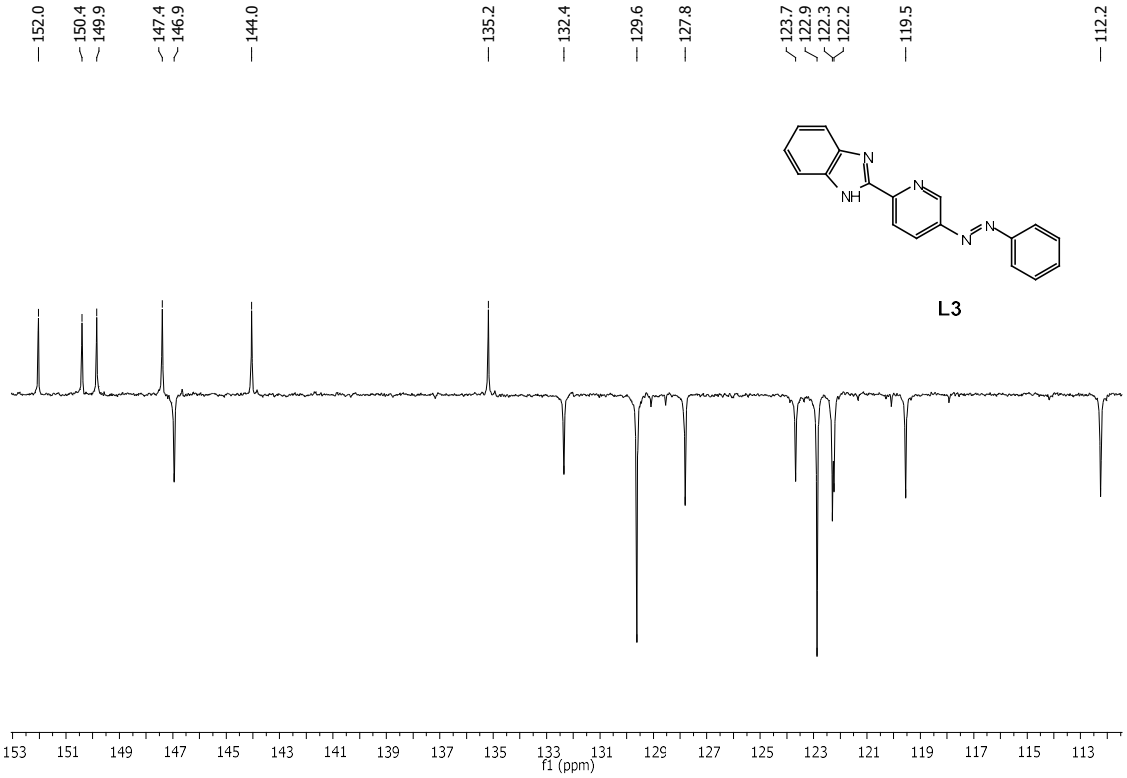
152.0
150.4
149.9
147.4
146.9
144.0
135.2
132.4
129.6
127.8
123.7
122.9
122.3
122.2
119.5
112.2
N
NH
N
N
N
L3
153 151 149 147 145 143 141 139 137 135 133 131 129 127 125 123 121 119 117 115 113
f1 (ppm)

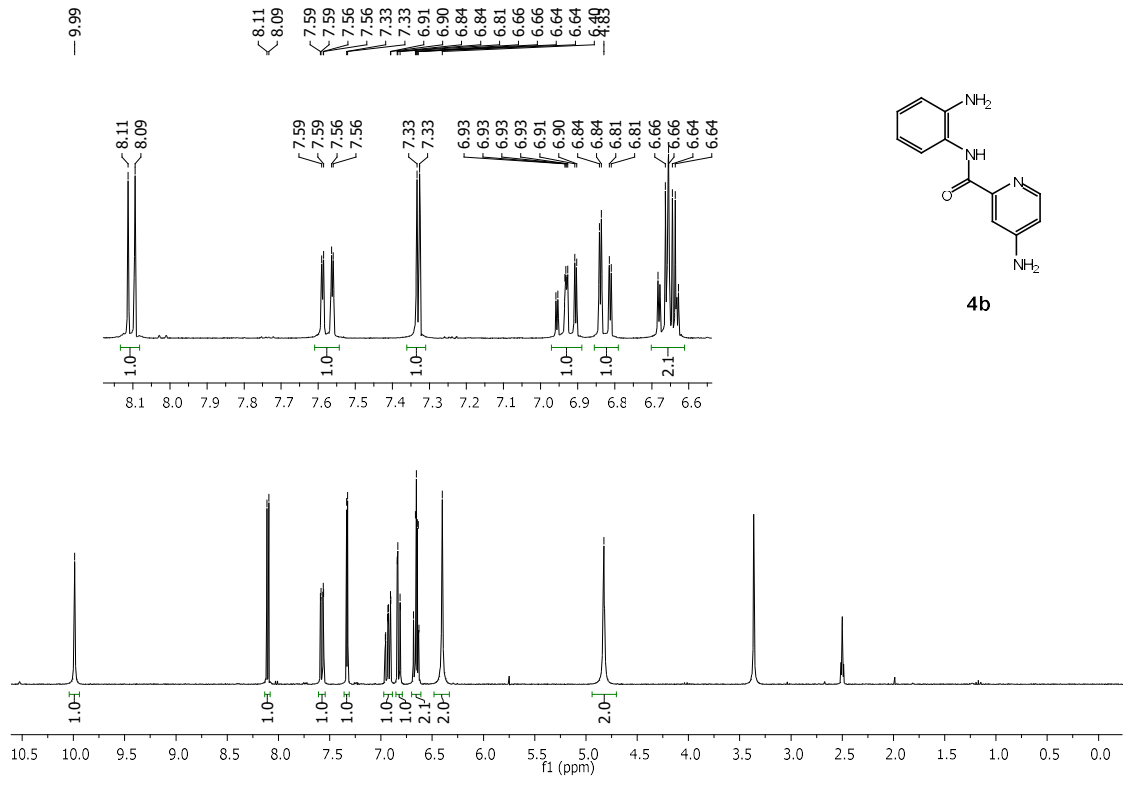
9.99
8.11
8.09
7.59
7.59
7.56
7.56
7.33
7.33
6.91
6.90
6.84
6.84
6.81
6.66
6.66
6.64
6.64
6.40
4.83
NH2
NH
O
N
NH2
4b
1.0
1.0
1.0
1.0
1.0
2.1
8.1 8.0 7.9 7.8 7.7 7.6 7.5 7.4 7.3 7.2 7.1 7.0 6.9 6.8 6.7 6.6
1.0
1.0
1.0
1.0
1.0
2.1
2.0
2.0
10.5 10.0 9.5 9.0 8.5 8.0 7.5 7.0 6.5 6.0 5.5 5.0 4.5 4.0 3.5 3.0 2.5 2.0 1.5 1.0 0.5 0.0
f1 (ppm)

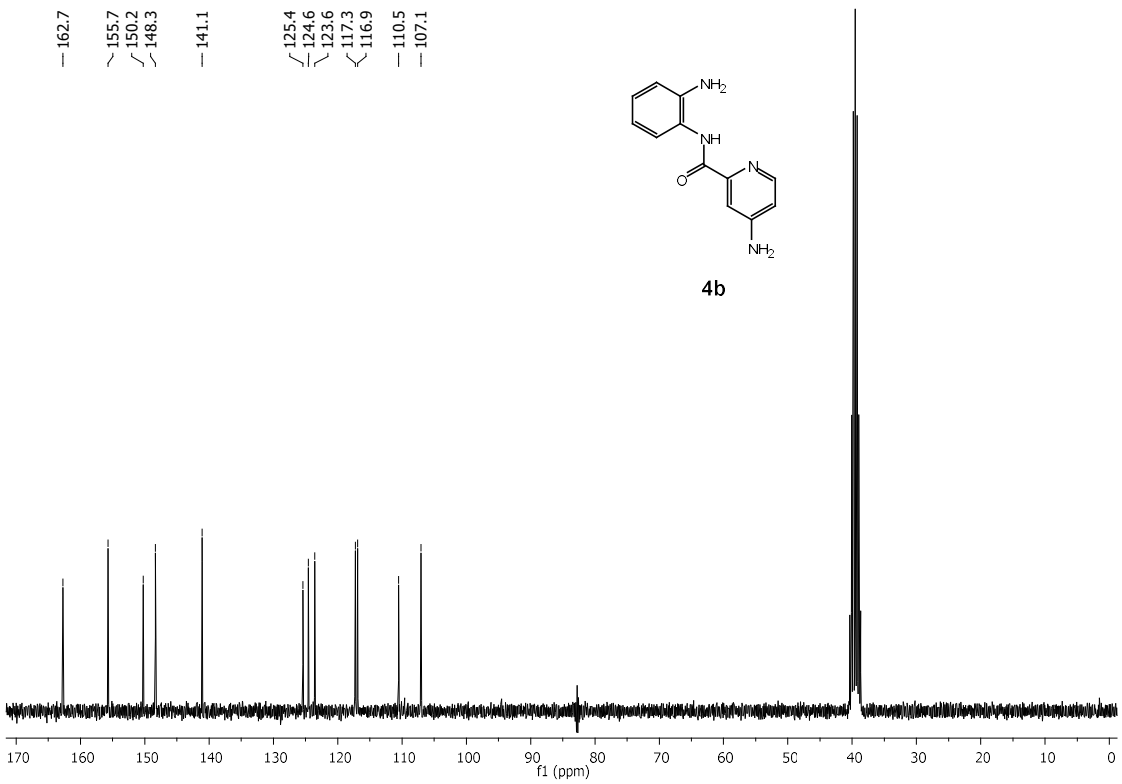
162.7
155.7
150.2
148.3
141.1
125.4
124.6
123.6
117.3
116.9
110.5
107.1
NH2
NH
O
N
NH2
4b
170 160 150 140 130 120 110 100 90 80 70 60 50 40 30 20 10 0
f1 (ppm)

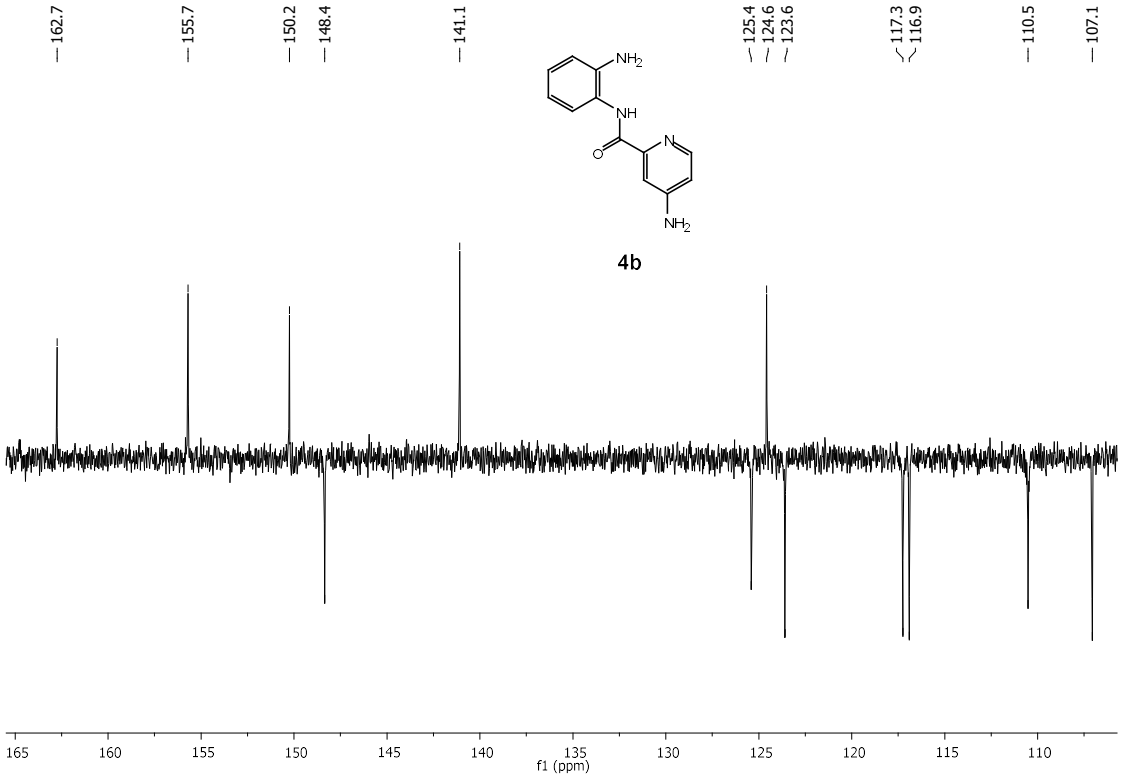
162.7
155.7
150.2
148.4
141.1
125.4
124.6
123.6
117.3
116.9
110.5
107.1
NH2
NH
O
N
NH2
4b
165 160 155 150 145 140 135 130 125 120 115 110
f1 (ppm)

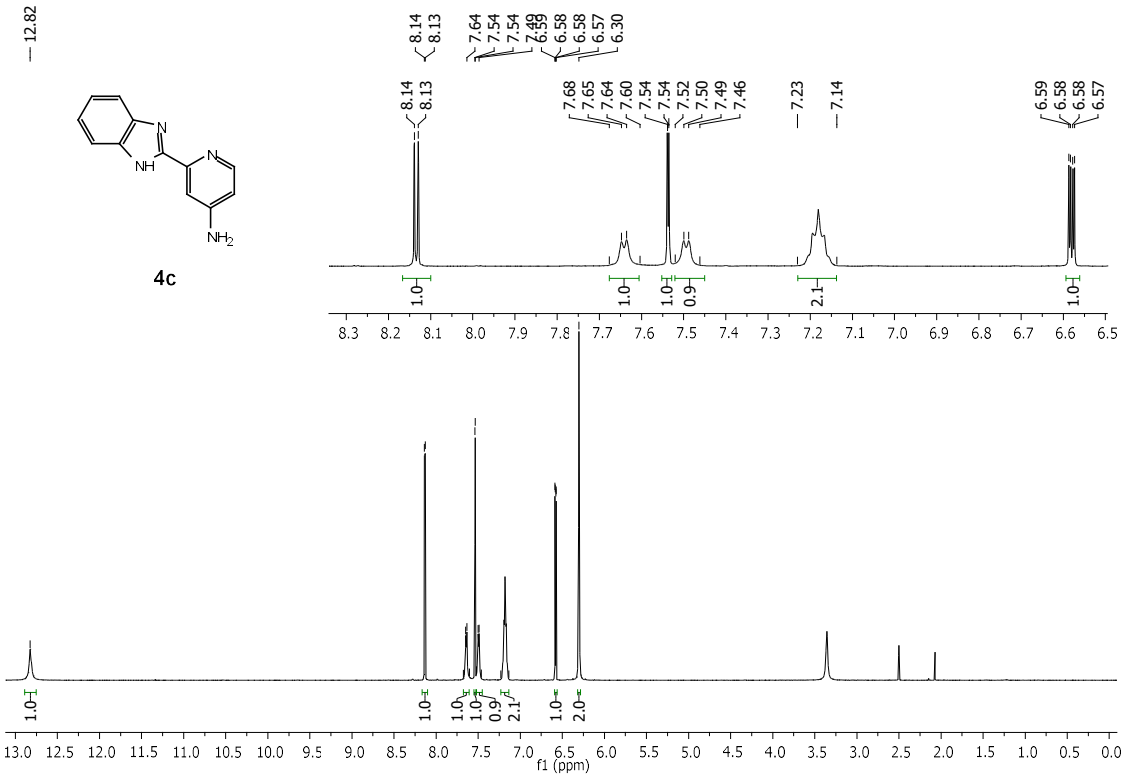
12.82
8.14
8.13
7.64
7.54
7.54
7.49
6.59
6.58
6.57
6.30
7.68
7.65
7.64
7.60
7.54
7.54
7.52
7.50
7.49
7.46
7.23
7.14
6.59
6.58
6.58
6.57
NH
NH2
4c
1.0
1.0
1.0
0.9
2.1
1.0
f1 (ppm)

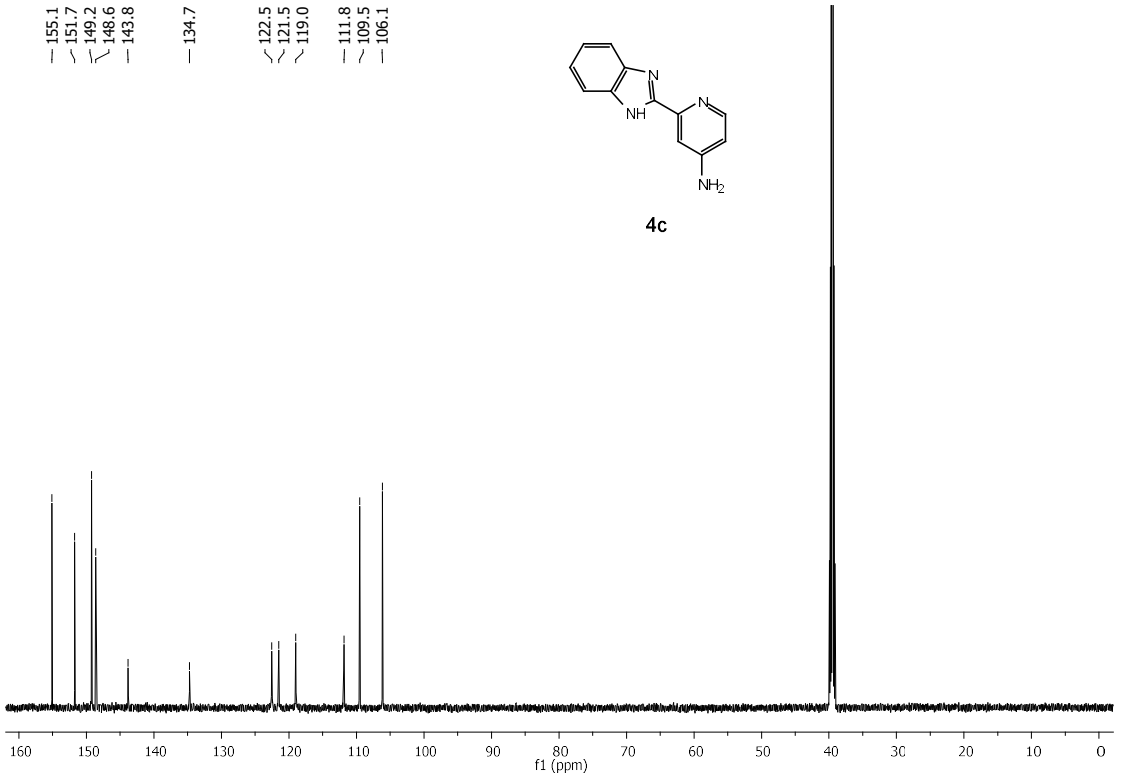
155.1
151.7
149.2
148.6
143.8
134.7
122.5
121.5
119.0
111.8
109.5
106.1
NH
NH2
4c
f1 (ppm)

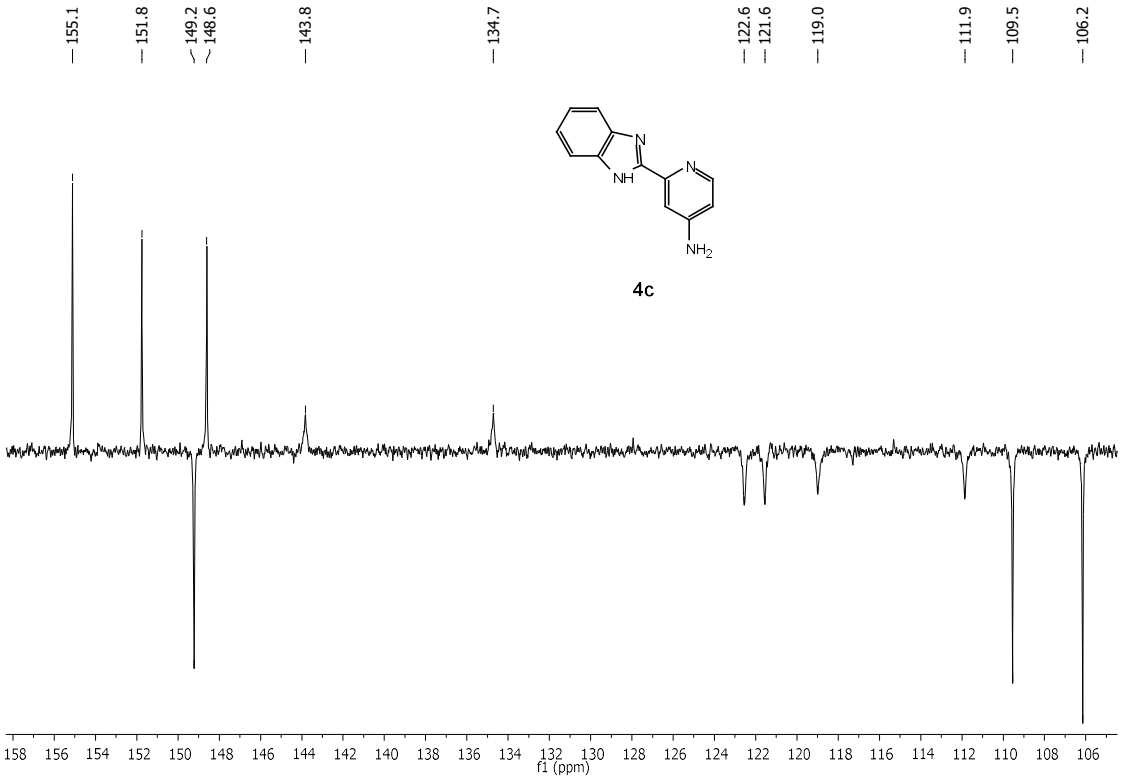
155.1
151.8
149.2
148.6
143.8
134.7
122.6
121.6
119.0
111.9
109.5
106.2
NH
N
N
NH2
f1 (ppm)

4c

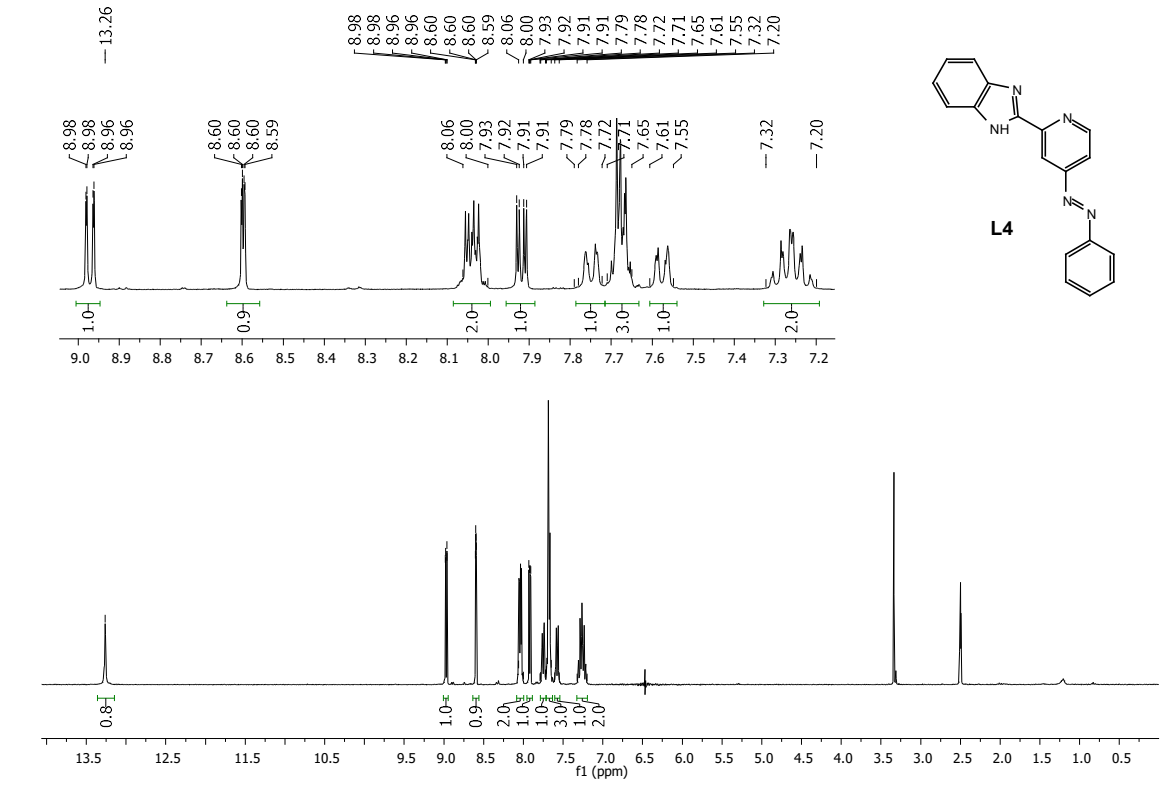
13.26
8.98
8.98
8.96
8.96
8.60
8.60
8.60
8.59
8.06
8.00
7.93
7.92
7.91
7.91
7.79
7.78
7.72
7.71
7.65
7.61
7.55
7.32
7.20
1.0
0.9
2.0
1.0
1.0
3.0
1.0
2.0
f1 (ppm)

NH
N
N
N

L4

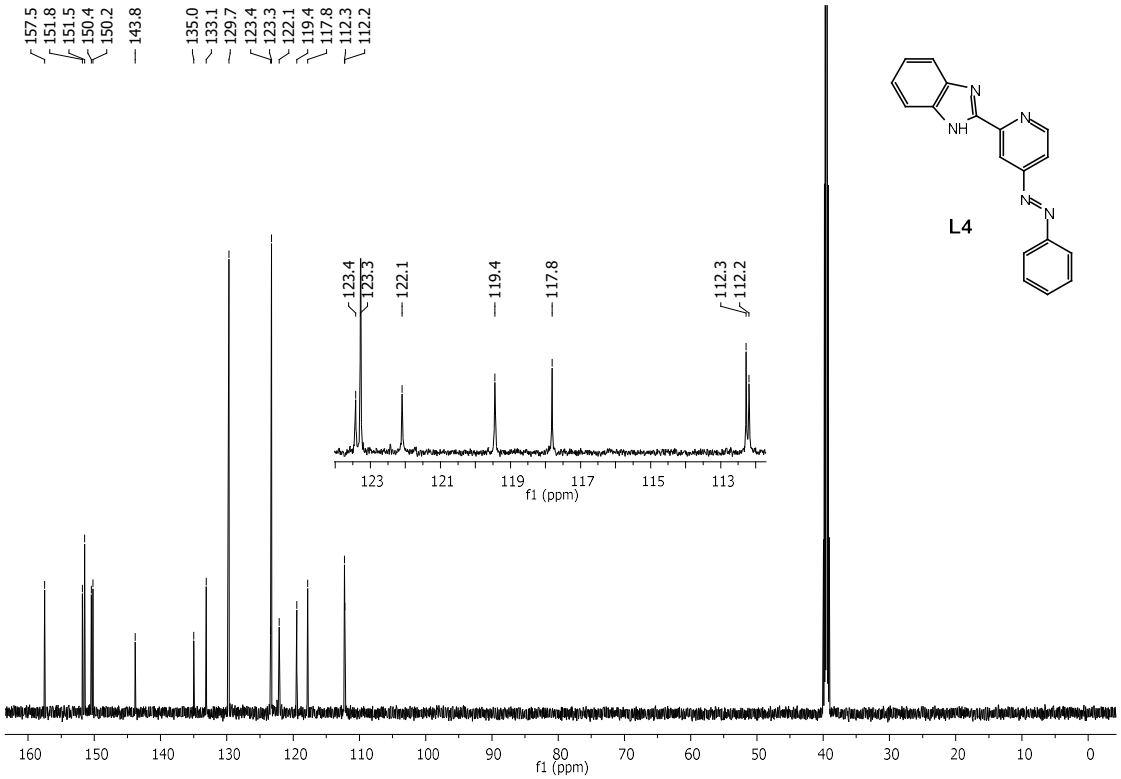
157.5
151.8
151.5
150.4
150.2
143.8
135.0
133.1
129.7
123.4
123.3
122.1
119.4
117.8
112.3
112.2
L4
f1 (ppm)

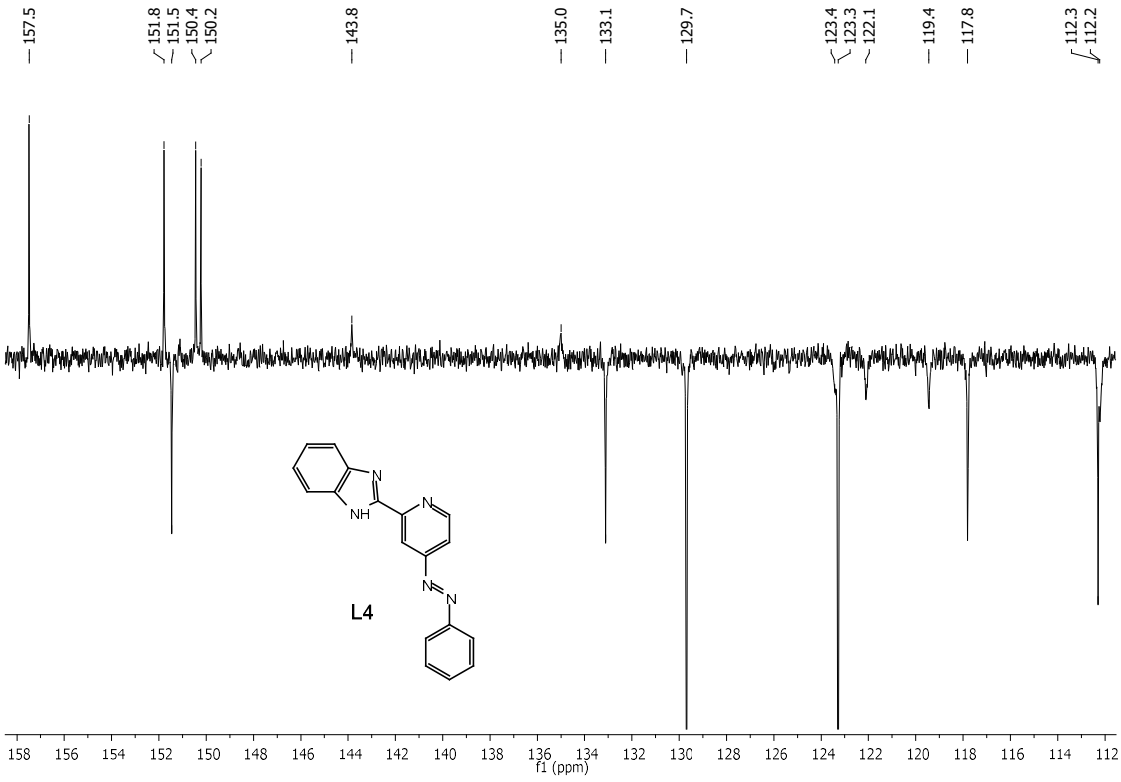
157.5
151.8
151.5
150.4
150.2
143.8
135.0
133.1
129.7
123.4
123.3
122.1
119.4
117.8
112.3
112.2
L4
f1 (ppm)

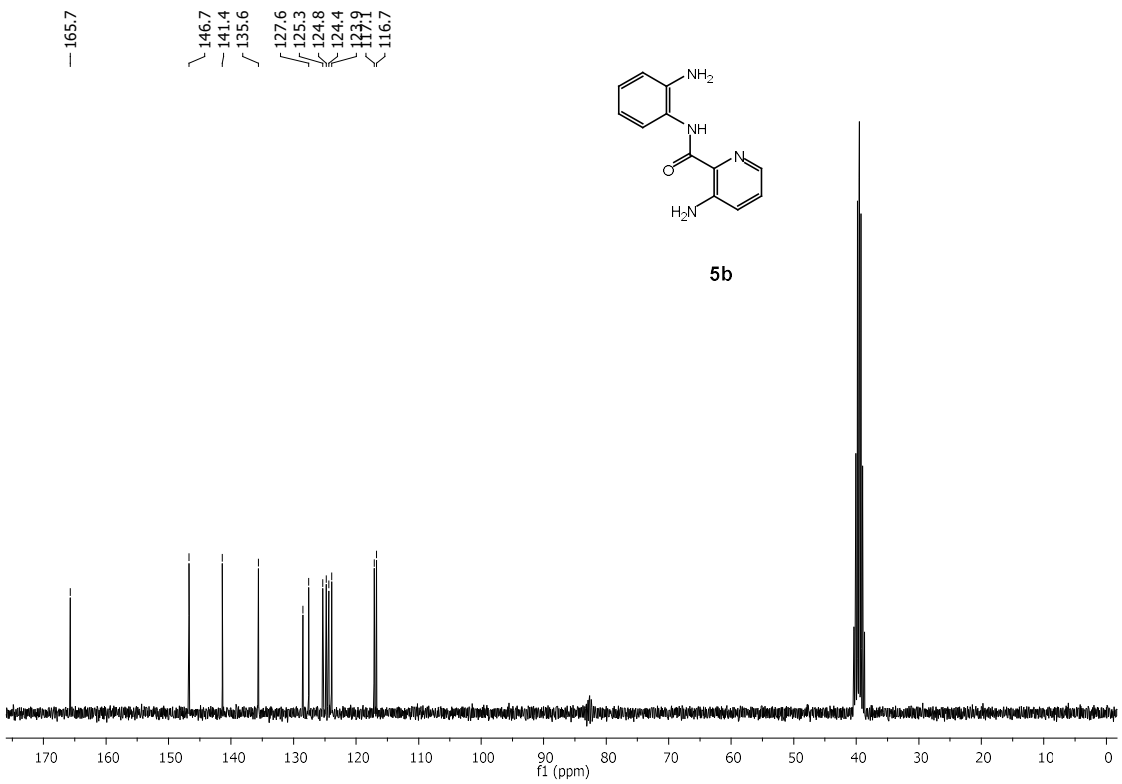
165.7
146.7
141.4
135.6
127.6
125.3
124.8
124.4
123.9
117.1
116.7
NH2
NH
O
N
H2N
5b
170 160 150 140 130 120 110 100 90 80 70 60 50 40 30 20 10 0
f1 (ppm)

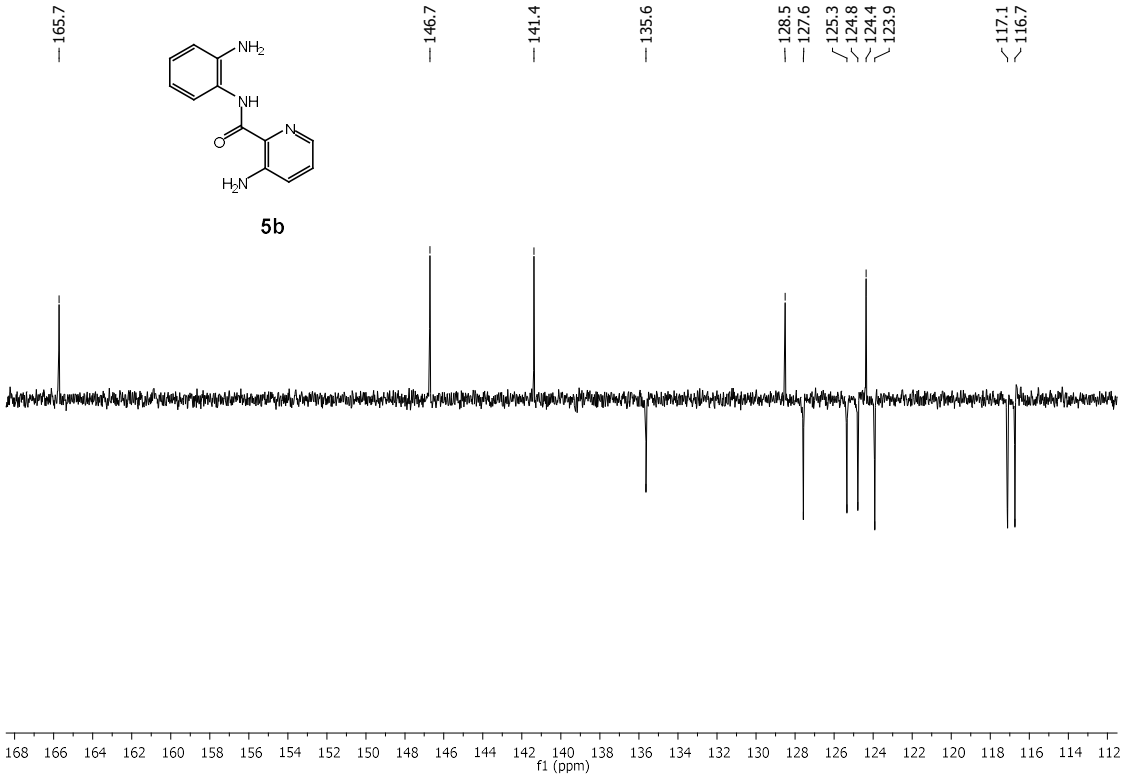
165.7
146.7
141.4
135.6
128.5
127.6
125.3
124.8
124.4
123.9
117.1
116.7
NH2
NH
O
N
H2N
5b
168 166 164 162 160 158 156 154 152 150 148 146 144 142 140 138 136 134 132 130 128 126 124 122 120 118 116 114 112
f1 (ppm)

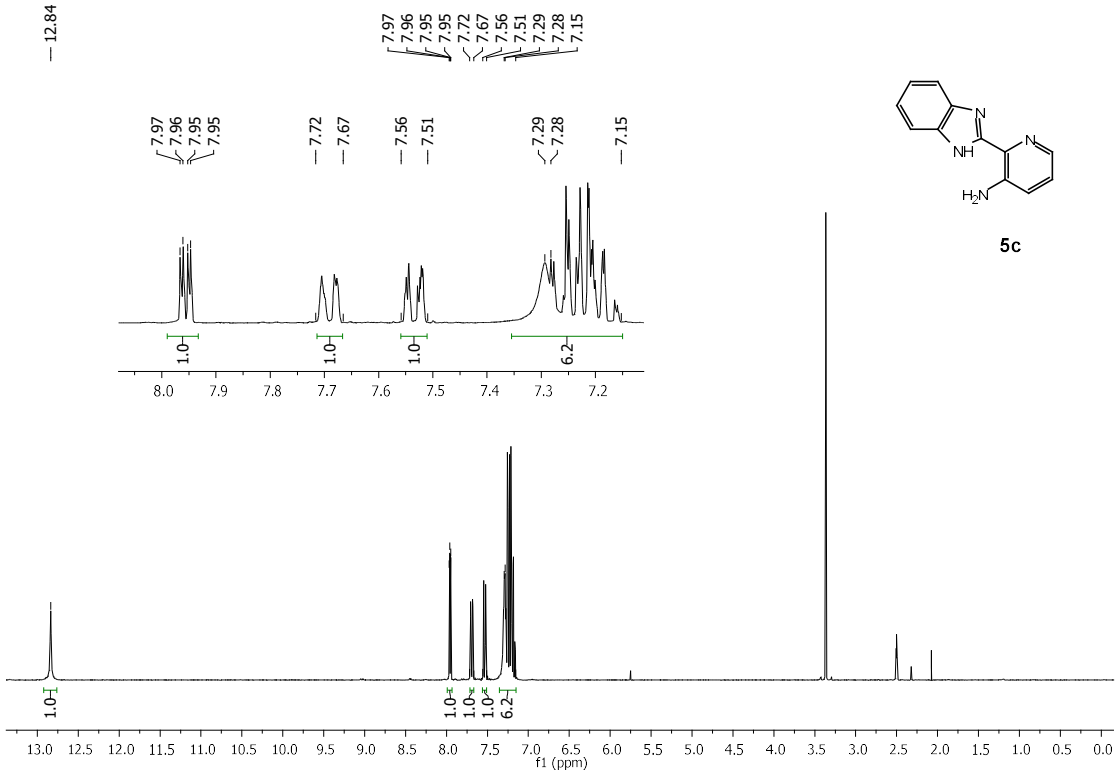
12.84
7.97
7.96
7.95
7.95
7.72
7.67
7.56
7.51
7.29
7.28
7.15
1.0
1.0
1.0
6.2
1.0
1.0
1.0
6.2
f1 (ppm)
5c

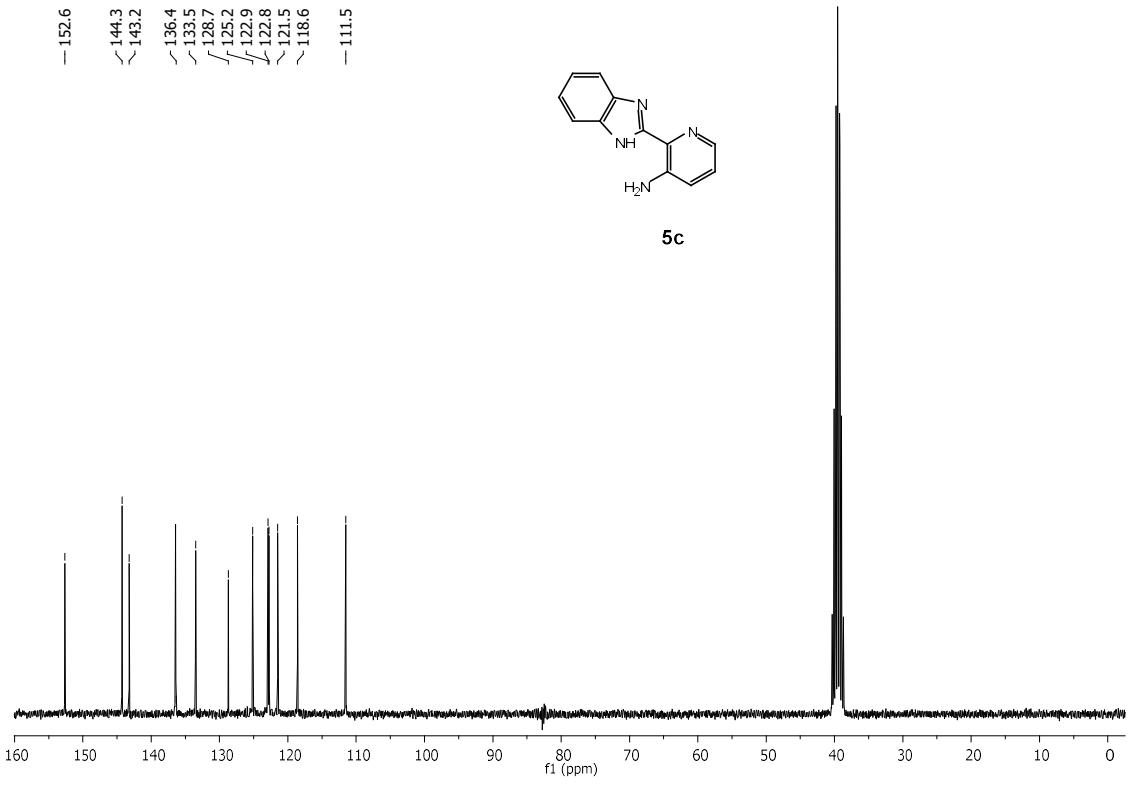
152.6
144.3
143.2
136.4
133.5
128.7
125.2
122.9
122.8
121.5
118.6
111.5
f1 (ppm)
5c

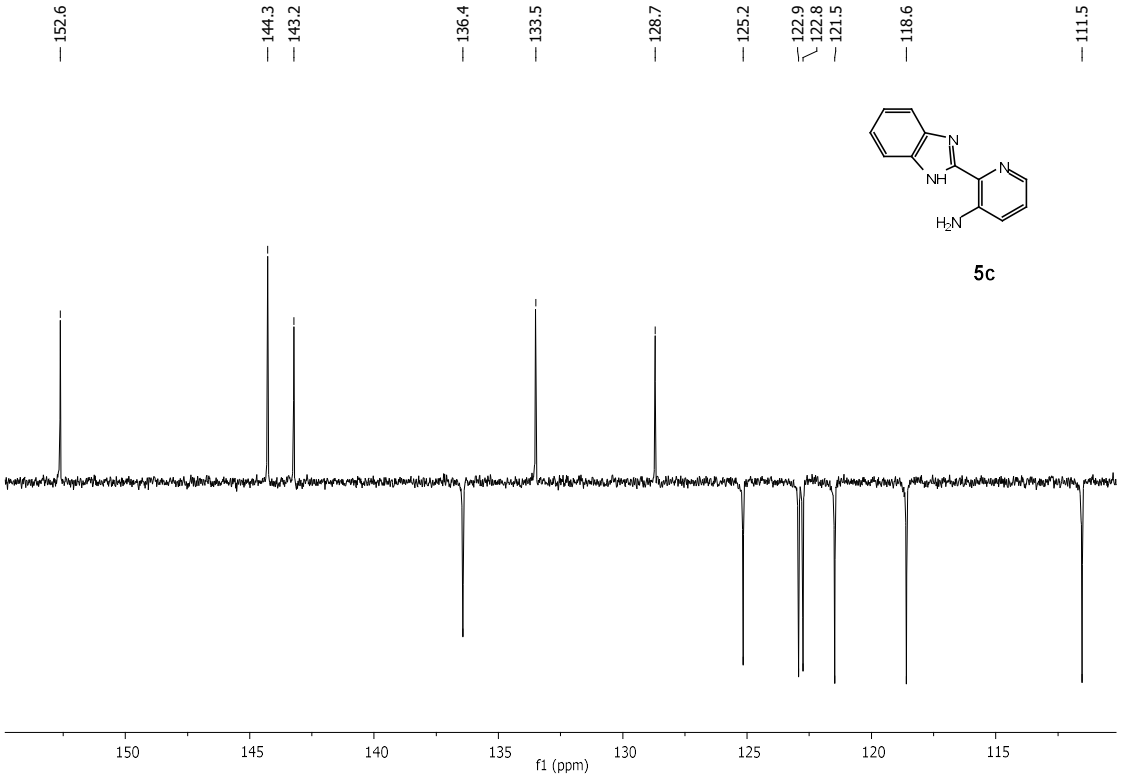
152.6
144.3
143.2
136.4
133.5
128.7
125.2
122.9
122.8
121.5
118.6
111.5
N
NH
N
H2N
5c
150
145
140
135
130
125
120
115
f1 (ppm)

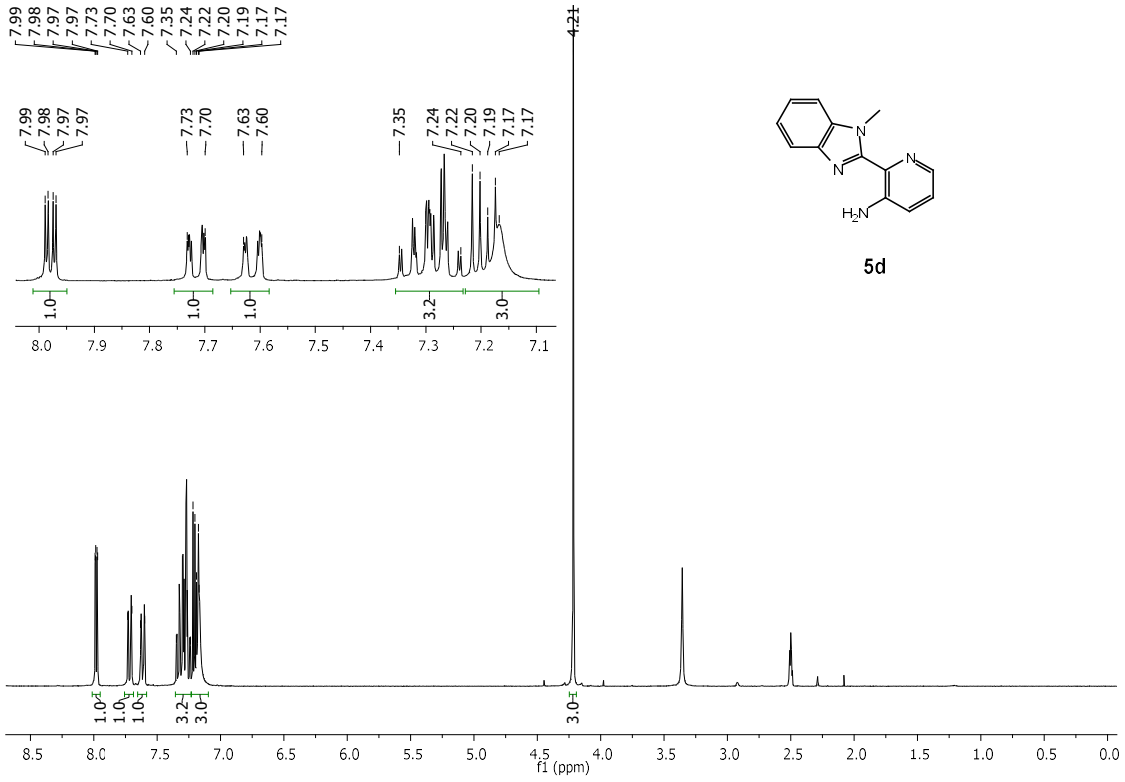
7.99
7.98
7.97
7.97
7.73
7.70
7.63
7.60
7.35
7.24
7.22
7.20
7.19
7.17
7.17
4.21
N
N
N
H2N
5d
1.0
1.0
1.0
3.2
3.0
3.0
8.5
8.0
7.5
7.0
6.5
6.0
5.5
5.0
4.5
4.0
3.5
3.0
2.5
2.0
1.5
1.0
0.5
0.0
f1 (ppm)

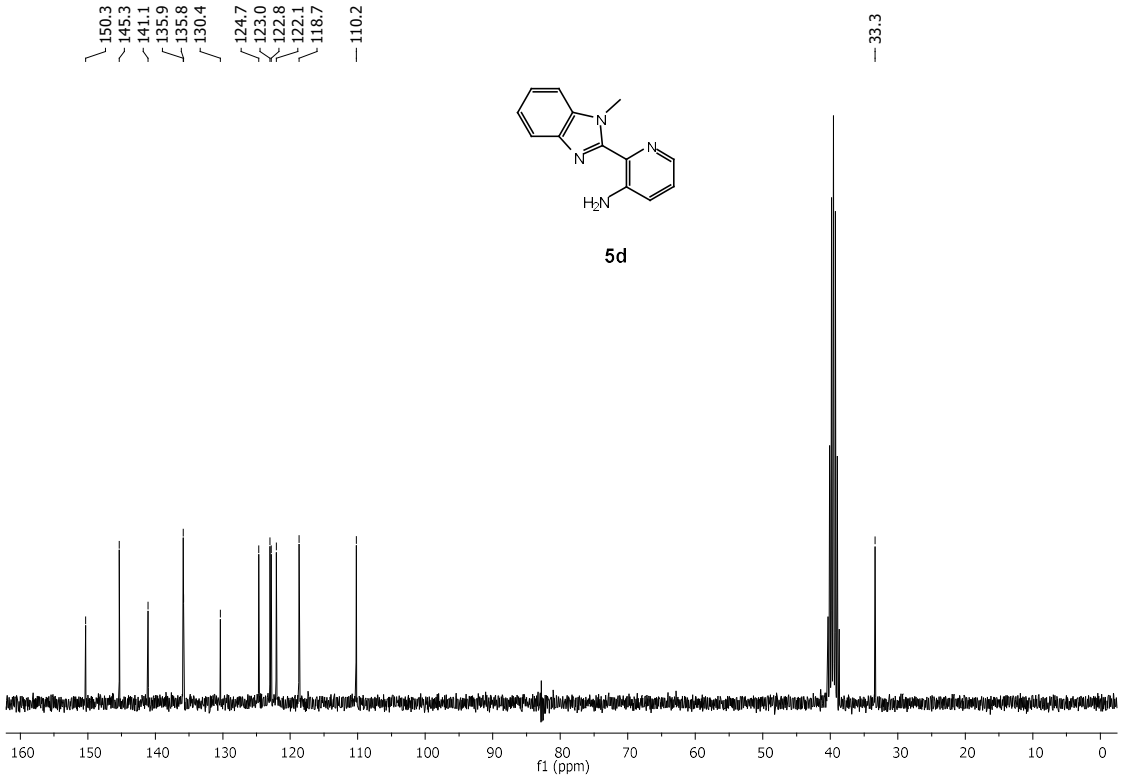
150.3
145.3
141.1
135.9
135.8
130.4
124.7
123.0
122.8
122.1
118.7
110.2
33.3
5d
160
150
140
130
120
110
100
90
80
70
60
50
40
30
20
10
0
f1 (ppm)

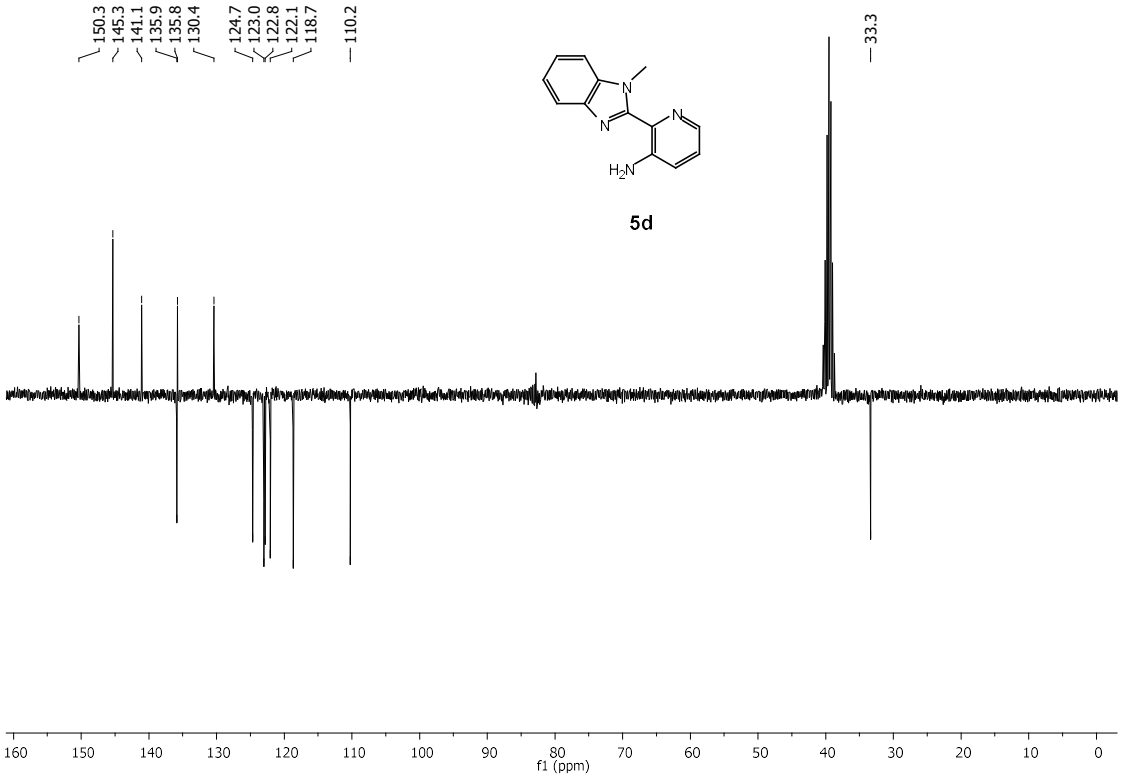
150.3
145.3
141.1
135.9
135.8
130.4
124.7
123.0
122.8
122.1
118.7
110.2
33.3
5d
160
150
140
130
120
110
100
90
80
70
60
50
40
30
20
10
0
f1 (ppm)

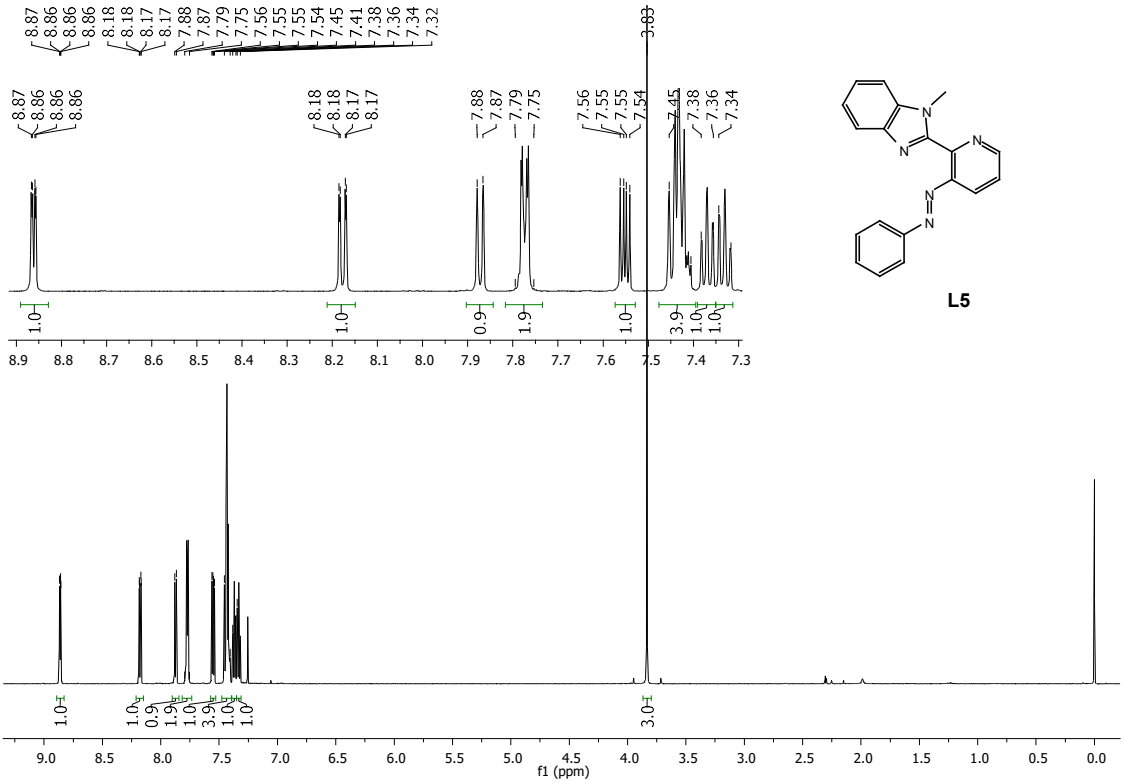
8.87
8.86
8.86
8.86
8.18
8.18
8.17
8.17
7.88
7.87
7.79
7.75
7.56
7.55
7.55
7.54
7.45
7.41
7.38
7.36
7.34
7.32
3.83
L5
f1 (ppm)

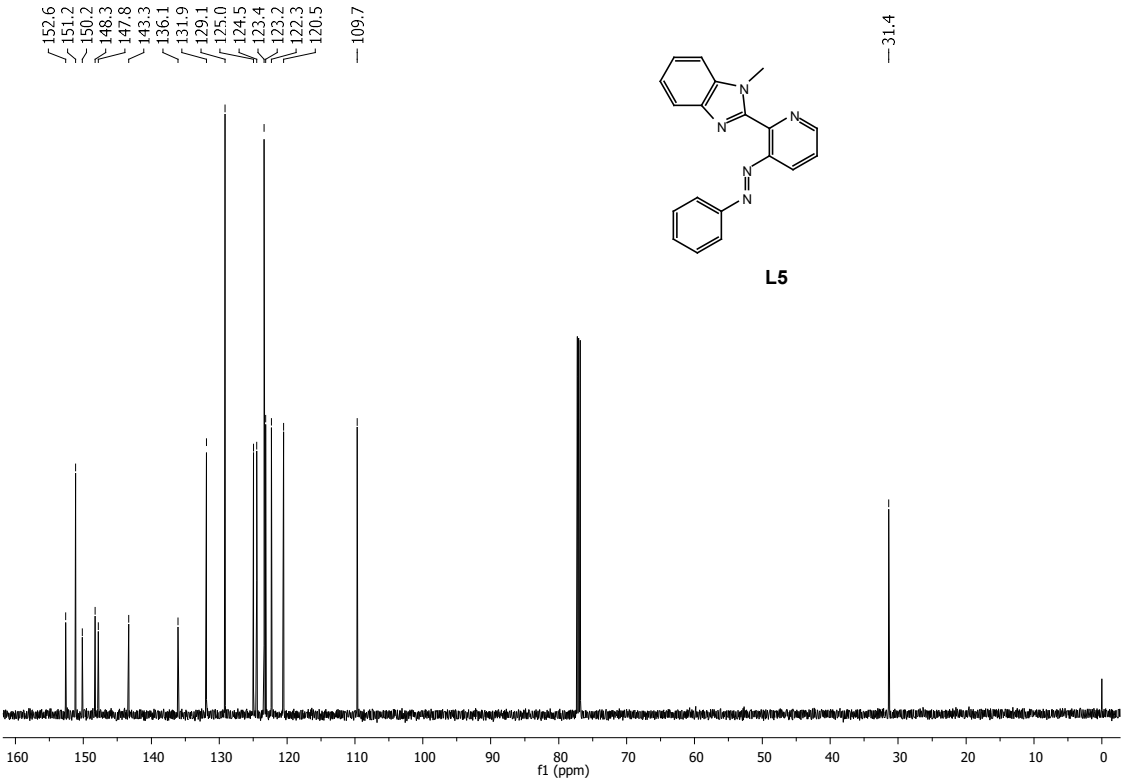
152.6
151.2
150.2
148.3
147.8
143.3
136.1
131.9
129.1
125.0
124.5
123.4
123.2
122.3
120.5
109.7
31.4
L5
f1 (ppm)

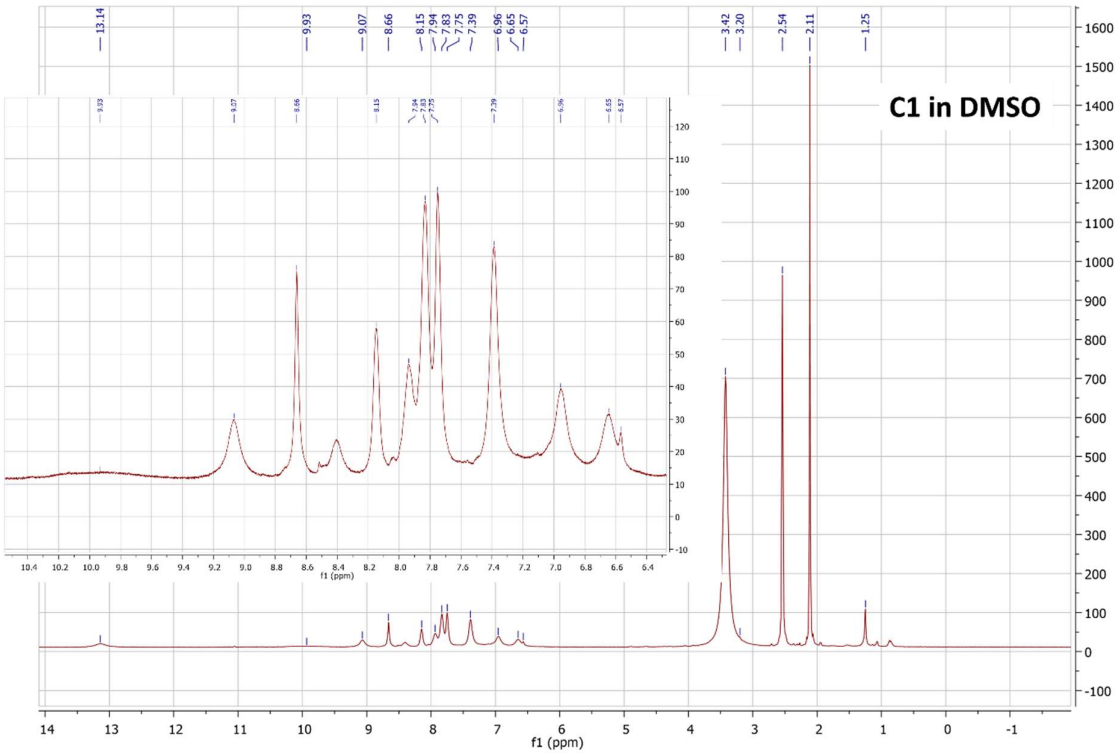
C1 in DMSO
13.14
9.93
9.07
8.66
8.15
7.94
7.83
7.75
7.39
6.96
6.65
6.57
3.42
3.20
2.54
2.11
1.25
f1 (ppm)

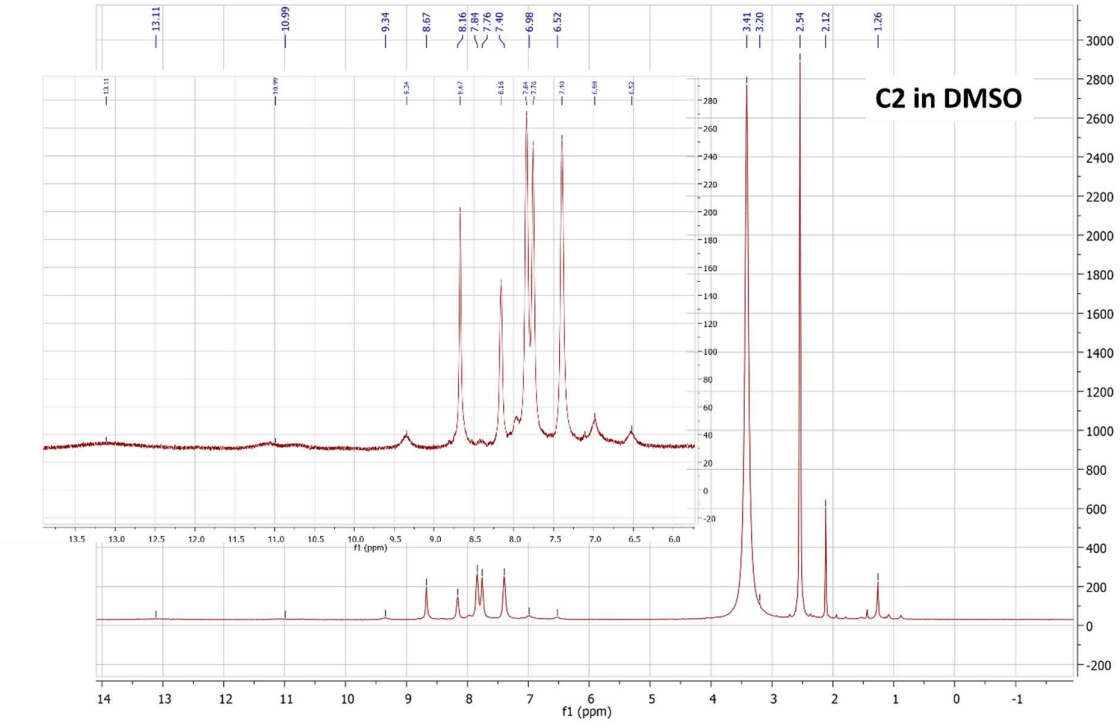
C2 in DMSO
13.11
10.99
9.34
8.67
8.16
7.84
7.76
7.40
6.98
6.52
3.41
3.20
2.54
2.12
1.26
f1 (ppm)

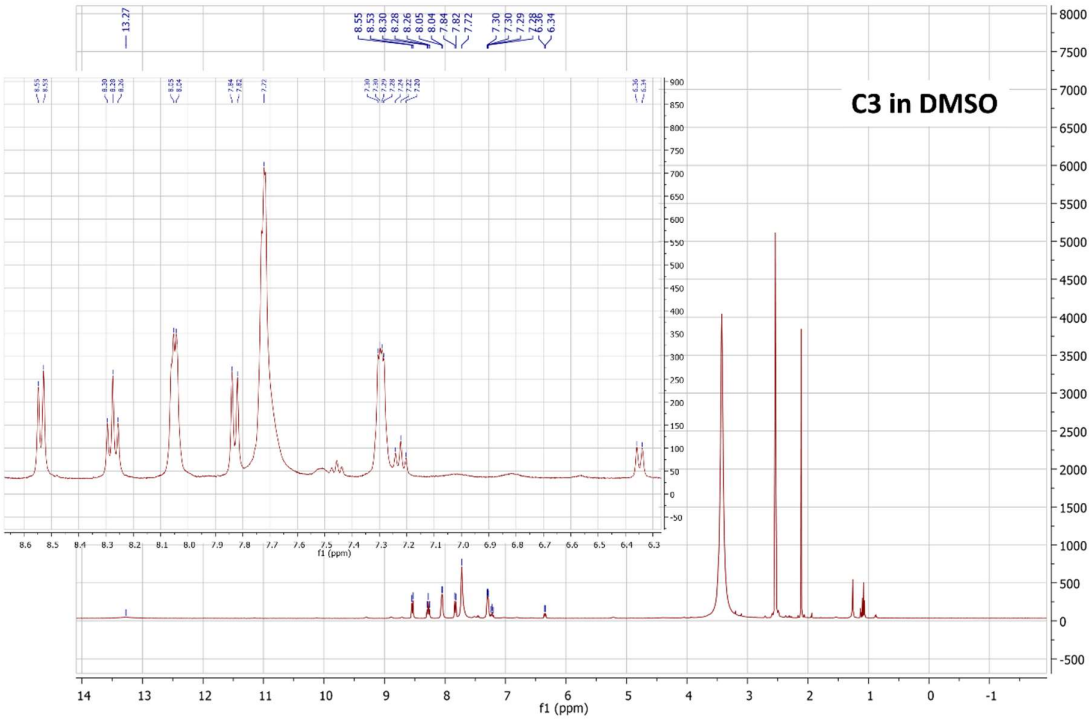

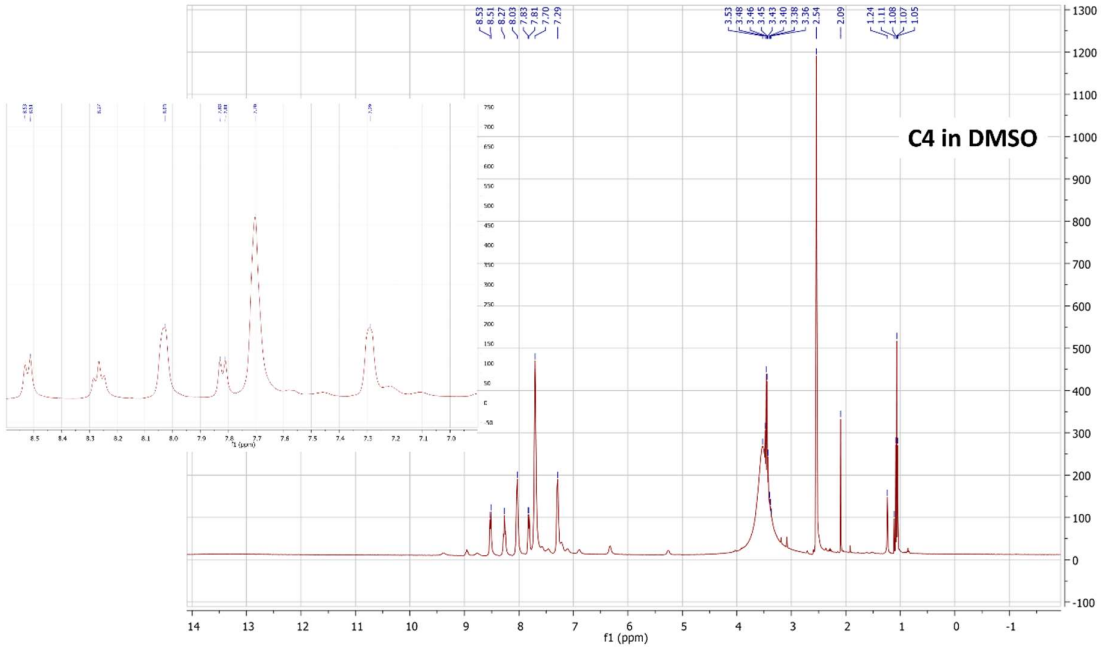

Figure S1. NMR spectra of reported organic and coordination compounds.

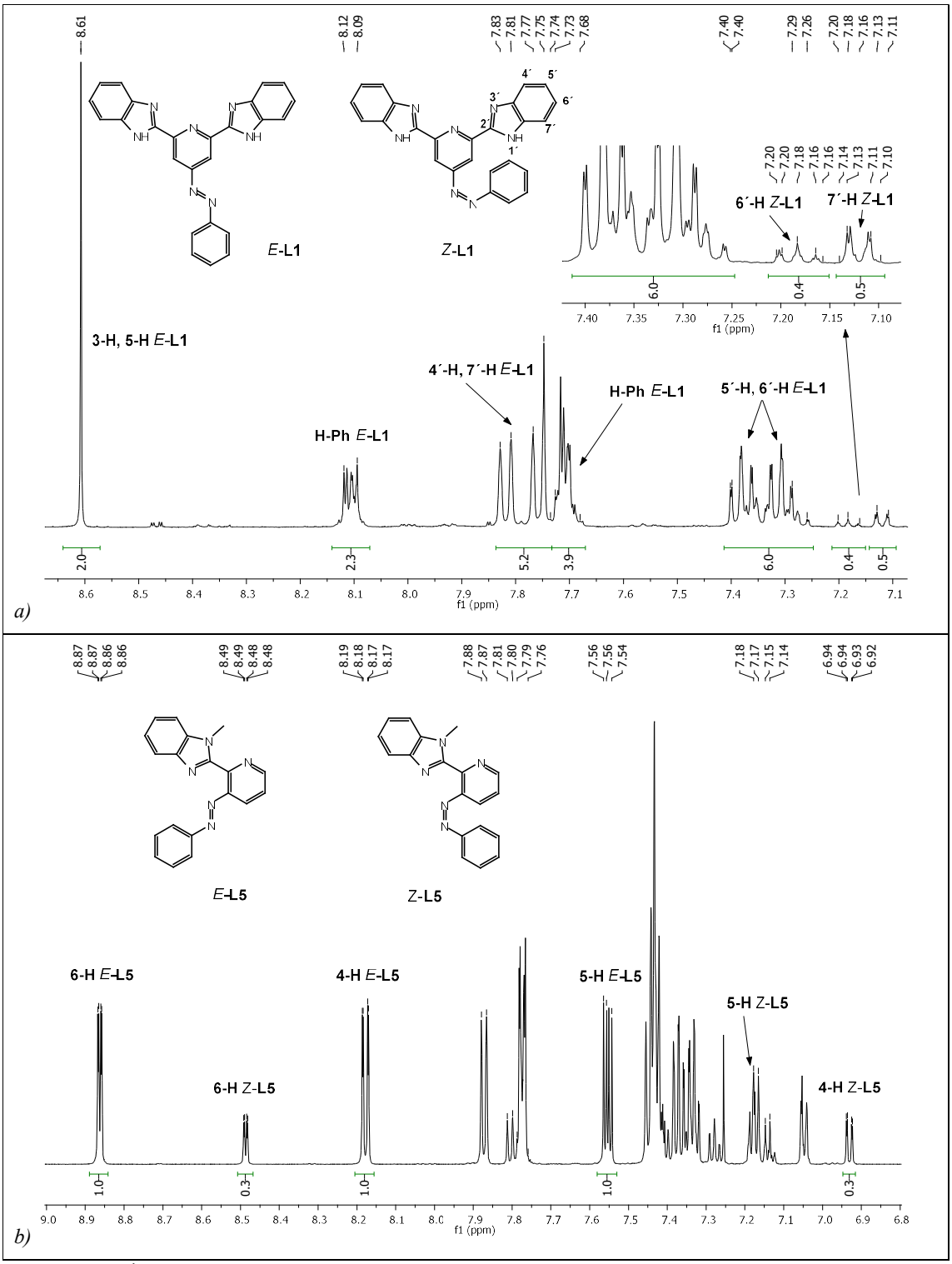

Figure S2. a) ^{1}H NMR spectrum of **L1** in DMSO-d_6 (400 MHz) after exposure to sunlight within 7 days. b) ^{1}H NMR spectrum of **L5** in $CDCl_3$ (600 MHz) after exposure to sunlight within 12 hours.

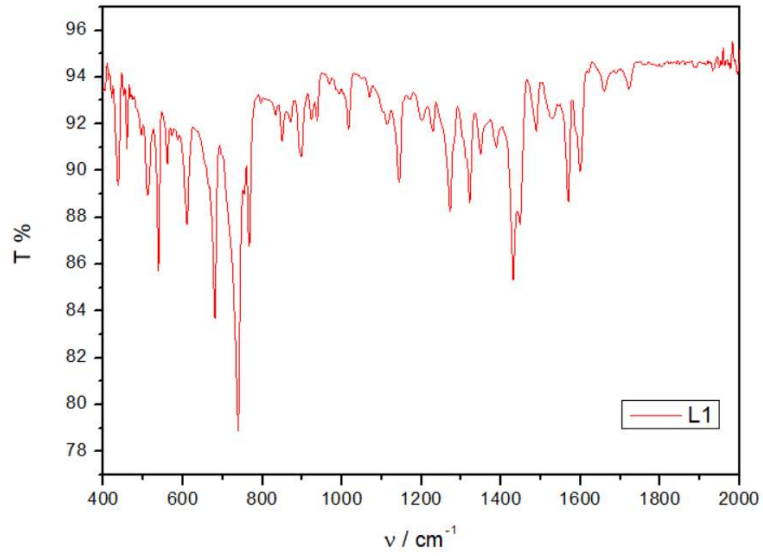
T %
ν / cm-1
L1

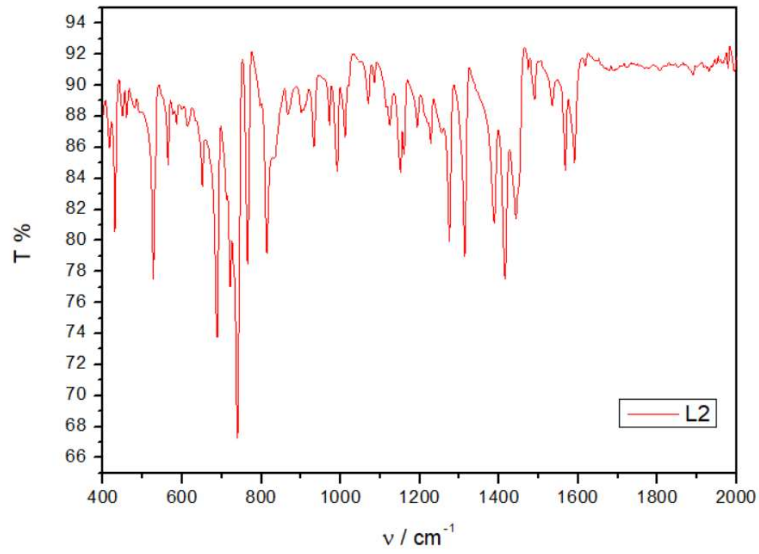
T %
ν / cm-1
L2

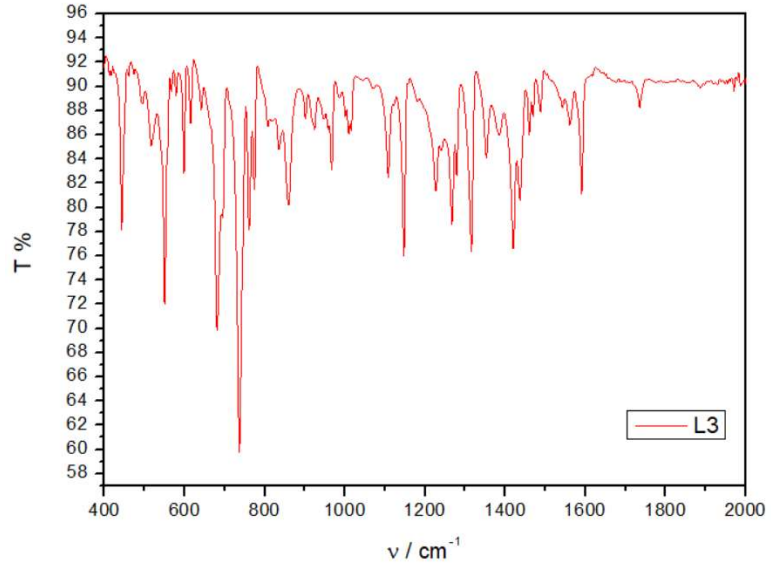
T %
ν / cm-1
L3

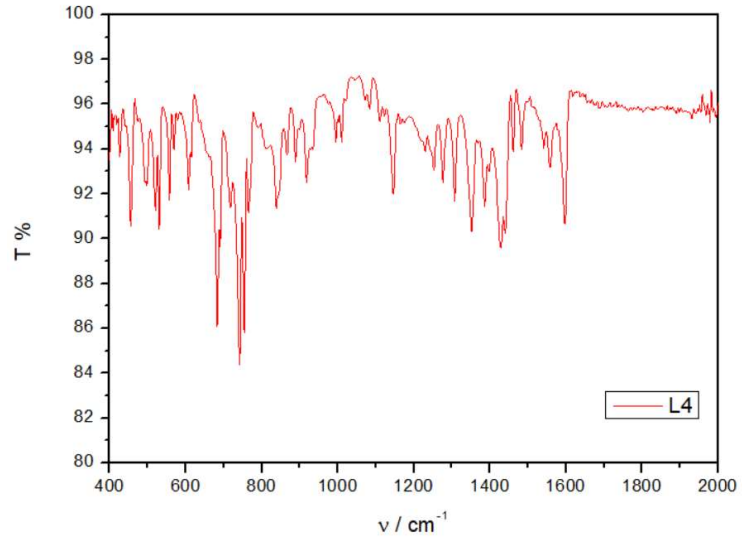
T %
ν / cm-1
L4

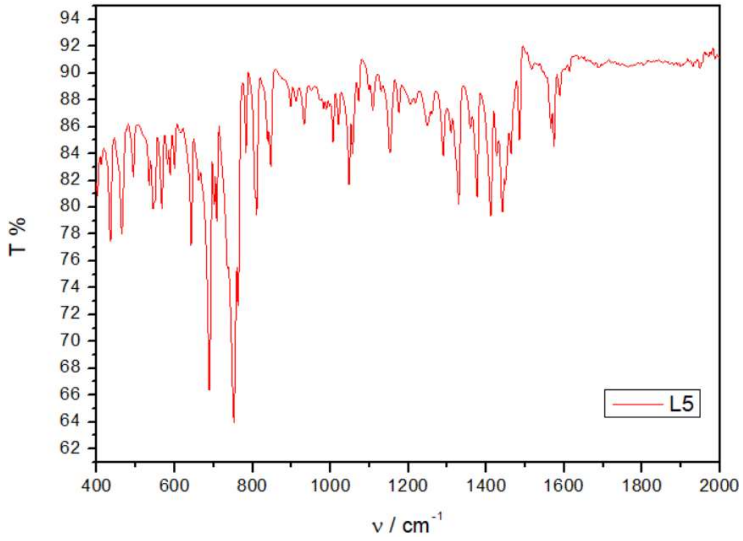
T %
ν / cm-1
L5

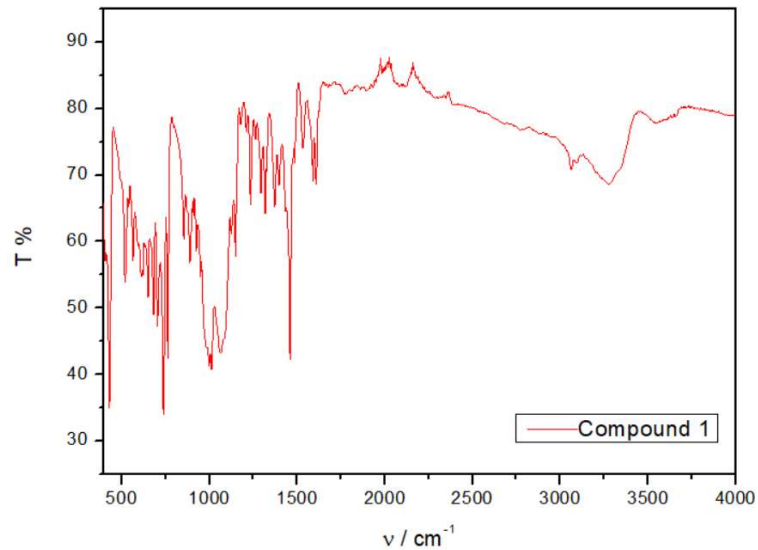
T %
ν / cm-1
Compound 1

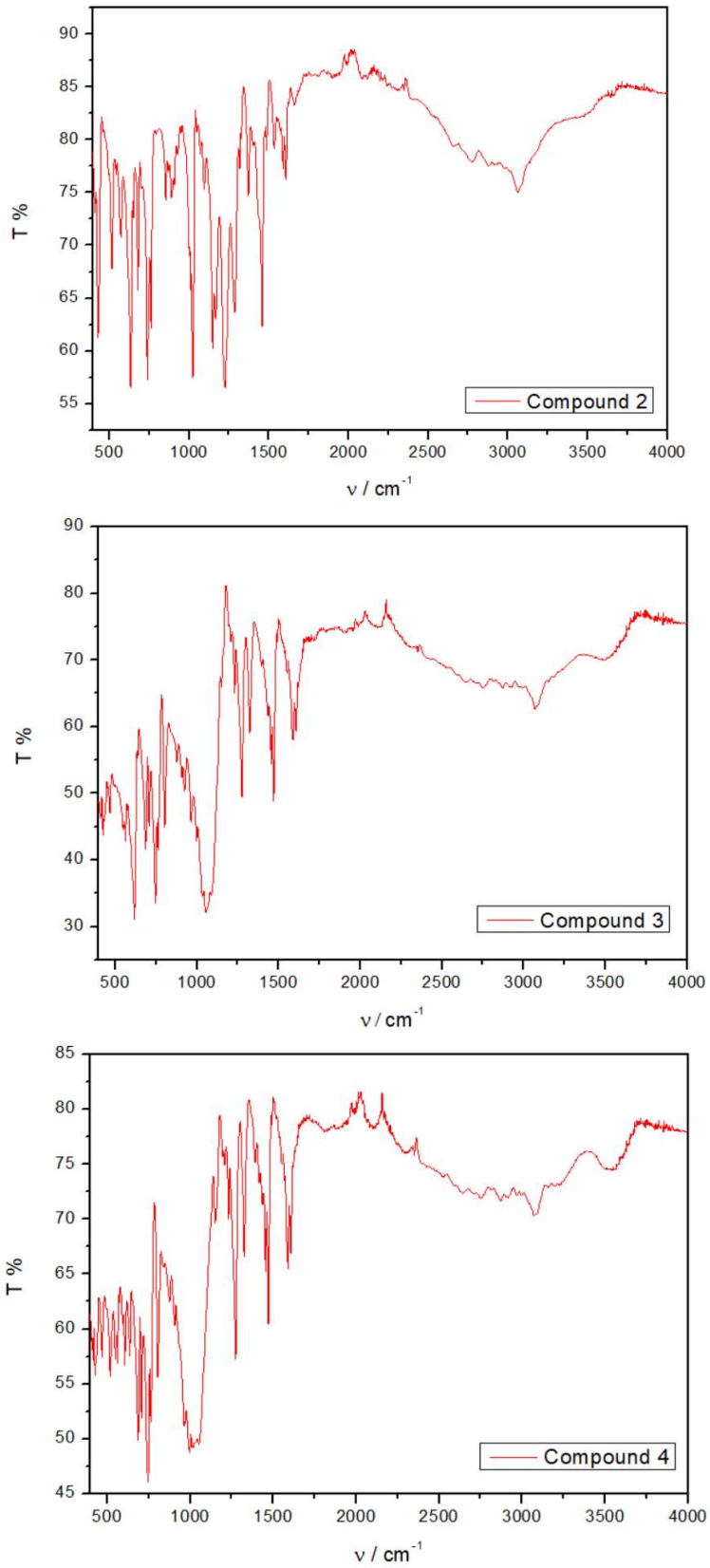

Figure S3. FTIR spectra of ligands **L1-L5** and coordination compounds **C1- C4**.

SI 2. Supplementary structural information

Table S1. Selected crystallographic parameters for ligands **L1**, **L4** and **L5** at 100 K.

	L1	**L4**	**L5**
Formula	$C_{56}H_{48}N_{16}O_2$	$C_{18}H_{13}N_5$	$C_{19}H_{15}N_5$
M_w/ g mol^{-1}	977.10	299.33	313.36
Temperature / K	100	100	100
Wavelength / Å	1.54186	1.54186	1.54186
Crystal system	triclinic	triclinic	monoclinic
Space group	*P*-1	*P*-1	$P2_1/c$
a / Å	10.5322(4)	10.1146(5)	8.0886(2)
b / Å	11.0246(4)	11.3094(5)	14.0373(4)
c / Å	12.4797(4)	15.8785(7)	13.5453(4)
α /°	103.400(3)	89.644(4)	90
β /°	106.838(3)	73.862(4)	96.285(2)
γ /°	112.929(3)	74.458(4)	90
V / Å^3	1175.70(9)	1676.39(14)	1528.72(7)
Z; ρ_{calc} / g.cm^{-3}	2; 1.380	4; 1.186	4; 1.362
μ (Cu-K$_\alpha$)/mm^{-1}	0.718	0.595	0.676
F(000)	512.0	624.0	656.0
Crystal size / mm	0.21 × 0.11 × 0.07	0.25 × 0.08 × 0.04	0.29 × 0.24 × 0.03
θ range for the data collection / °	8.042 to 143.278	5.81 to 143.738	9.102 to 143.708
Final *R* indices [$I > 2\sigma(I)$][a]	R_1 = 0.0443, wR_2 = 0.1320	R_1 = 0.0370, wR_2 = 0.0957	R_1 = 0.0353, wR_2 = 0.1125
R indices (all data)[a]	R_1 = 0.0568, wR_2 = 0.1320	R_1 = 0.0577, wR_2 = 0.0957	R_1 = 0.0396, wR_2 = 0.1160
GoF on F^2	1.085	0.922	0.983
CCDC number	2178235	2178236	2178237

Table S2. Selected crystallographic parameters for coordination compounds **C1-C4** at the corresponding temperature.

	C1	**C2**	**C3**	**C4**
Formula	$C_{50}H_{36}FeN_{14}OB_2F_8$	$C_{54}H_{41}FeN_{15}F_6O_8S_2$	$C_{38}H_{36}FeN_{10}O_4B_2F_8$	$C_{36}H_{26}FeN_{10}O_8Cl_2$
M_w/ g mol^{-1}	1078.40	1243.23	926.22	853.42
Temperature / K	100	100	110	100
Wavelength / Å	1.54186	1.54186	0.71073	1.54186
Crystal system	Triclinic	triclinic	monoclinic	Monoclinic
Space group	*P*-1	*P*-1	$P2_1/n$	$P2_1/n$
a / Å	12.1509(9)	13.2426(4)	12.3214(6)	13.23290(10)
b / Å	12.4816(6)	14.0283(4)	15.2951(8)	16.50510(10)
c / Å	16.3600(8)	15.6093(5)	21.4537(11)	17.50870(10)
α /°	95.525(4)	76.494(2)	90	90
β /°	100.998(5)	87.725(3)	96.579(11)	92.7200(10)
γ /°	106.255(5)	82.131(2)	90	90
V / Å^3	2308.6(2)	2792.93(15)	4016.5(4)	3819.77(4)
Z; ρ_{calc} / g.cm^{-3}	2; 1.551	2; 1.478	4; 1.532	4; 1.484

μ / mm^{-1}	3.406	3.526	0.468	5.016
F(000)	1100.0	1274.0	1896.0	1744.0
Crystal size / mm	0.32 × 0.2 × 0.02	0.20×0.107×0.02	0.18 × 0.10 × 0.02	0.45×0.28×0.15
θ range for the data collection / °	8.998 to 100.86	5.824 to 143.332	4.658 to 50.052	45.468 to 144
Final R indices $[I > 2\sigma(I)]^a$	R_1 =0.1486, wR_2 = 0.3858	R_1 =0.0853, wR_2 = 0.2278	R_1 = 0.0479, wR_2 = 0.1348	R_1 =0.0469, wR_2 = 0.1233
R indices (all data)^a	R_1 =0.1850, wR_2 = 0.4314	R_1 =0.1720, wR_2 = 0.2766	R_1 = 0.0575, wR_2 = 0.1431	R_1 =0.0478, wR_2 = 0.1241
GoF on F^2	1.108	0.946	1.050	1.070
CCDC number	2178231	2178232	2178233	2178234

***a*) L1**

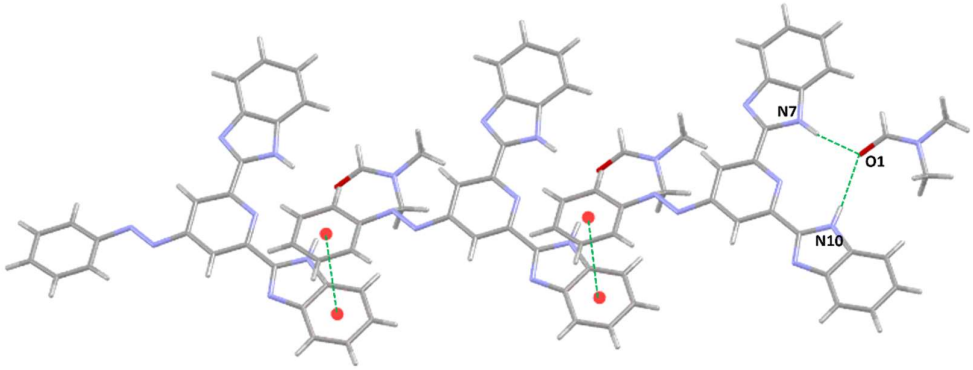

***b*) L4**

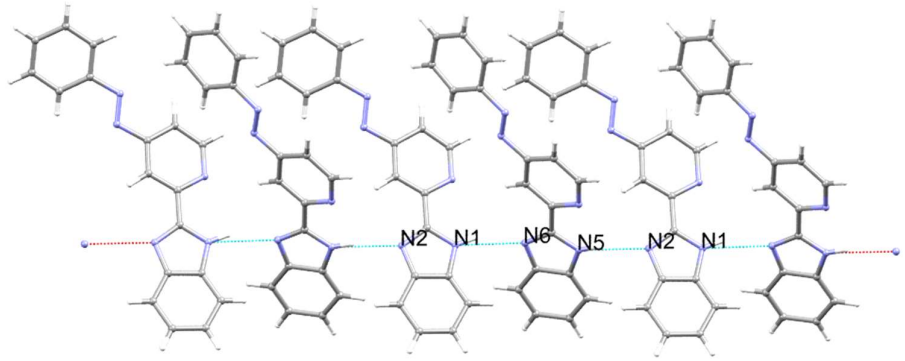

c) **L5**

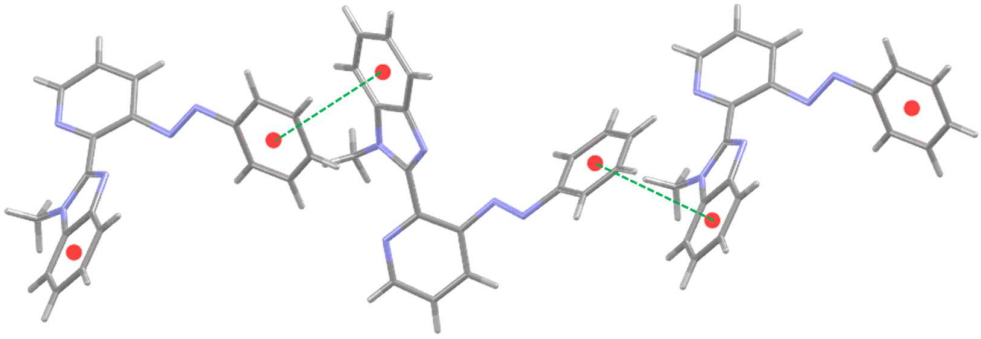

Figure S4 Noncovalent contacts (green dashed lines) in crystal structures of reported organic ligands a) **L1**: O1···N7=2.891(4) Å, O1···N10=3.184(4) Å, distance between two centroid C20 C21 C22 C23 C24 C25 = 3.911(3) Å; b) **L4**: N1-H···N6=2.896(2) Å and N5-H···N2=2.890(2) Å; c) **L5**: Distances between two centroid C13C14C15C16C17C18=4.067(3) Å.

a) ***b***)

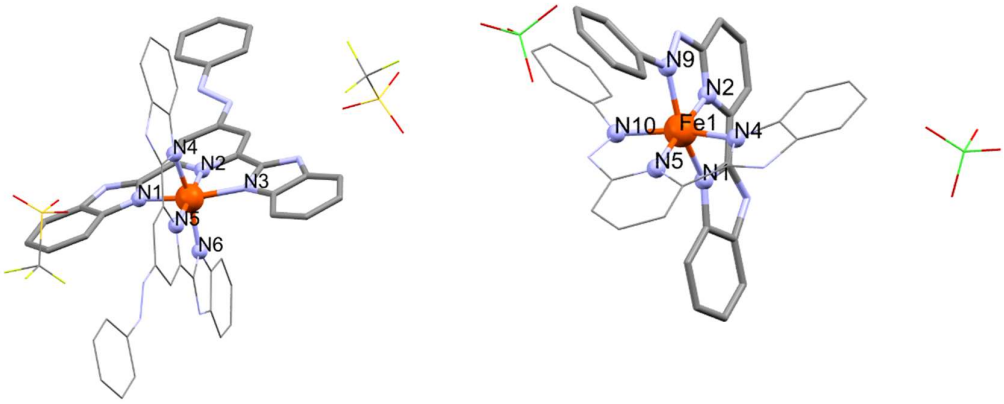

Figure S5. The units of a) **C2** and b) **C4**. The hydrogen atoms and lattice solvent molecules are omitted for clarity. Color code: C- grey; N-blue; O-red; S-yellow; Fe- orange; Cl-green.

Table S3 Bond distances and distortion parameters.

Compound	**Fe-N1**	**Fe-N2**	**Fe-N3**	**Fe-N4**	**Fe-N5**	**Fe-N6**	**Σ /º**	**Θ /º**
C1	1.954(9)	1.91(1)	1.985(8)	1.990(8)	1.895(9)	1.990(9)	79	259
C2	1.977(1)	1.904(1)	1.983(1)	1.997(1)	1.887(1)	1.964(1)	83	272
	Fe-N1	**Fe-N2**	**Fe-N4**	**Fe-N5**	**Fe-N9**	**Fe-N10**	**Σ /º**	**Θ /º**
C3	1.989(2)	1.882(2)	1.998(2)	1.875(2)	1.939(2)	1.959(2)	104	320
C4	2.002(2)	1.876(2)	1.999(2)	1.878(2)	1.968(2)	1.956(2)	109	328

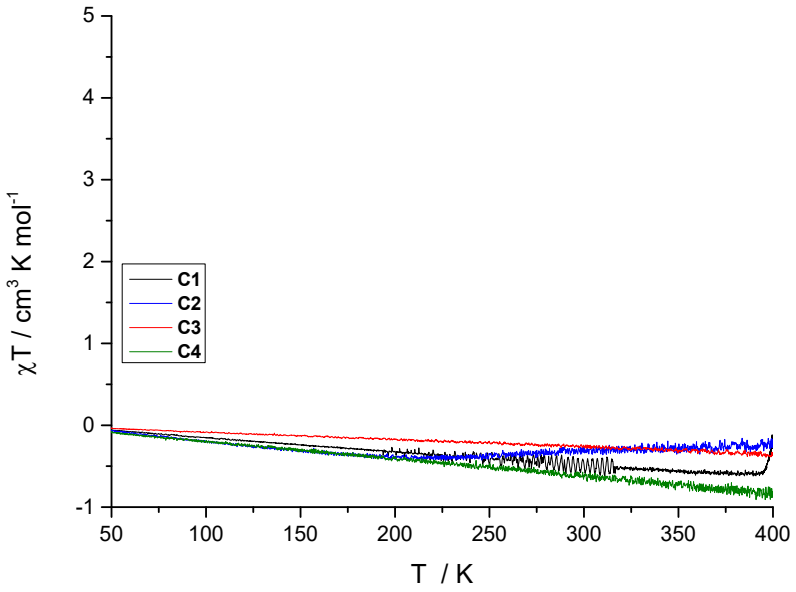

Figure S6. Diamagnetic properties of **C1-C4**.

SI 3. UV-VIS spectroscopy and calculations

a)

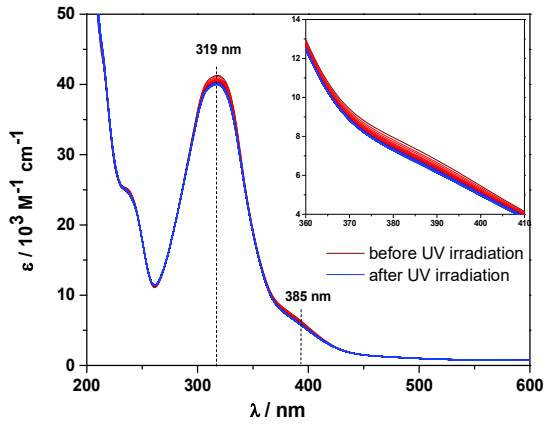

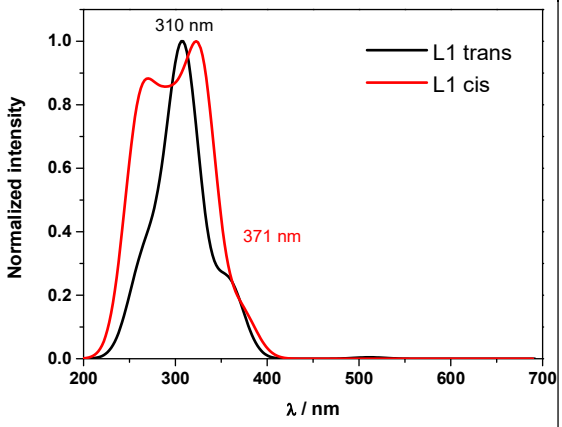

b)

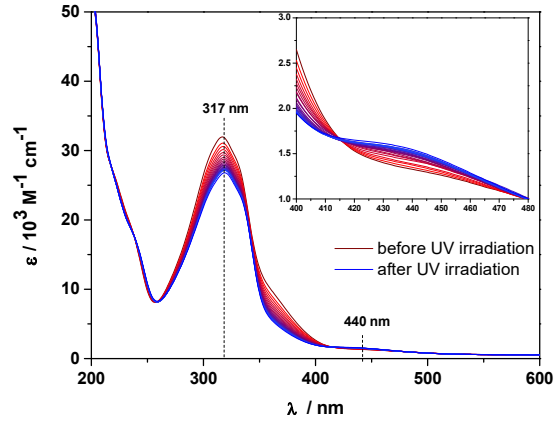

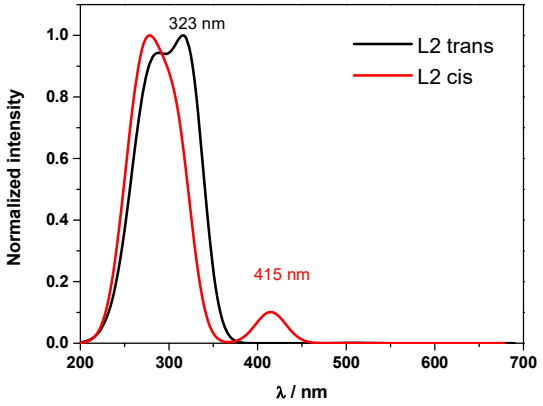

c)

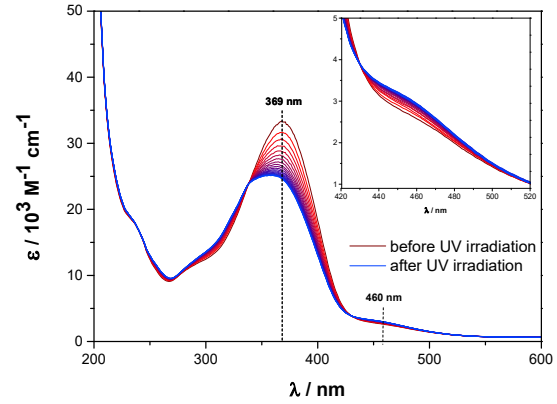

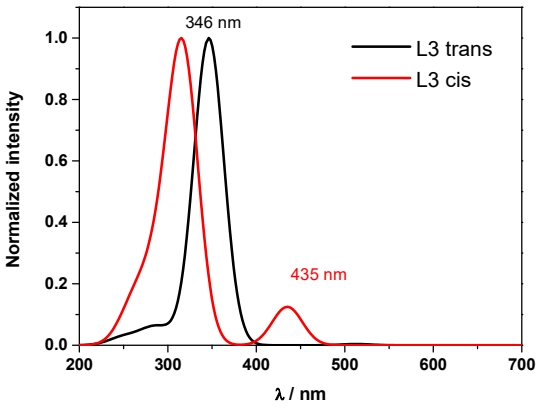

d)

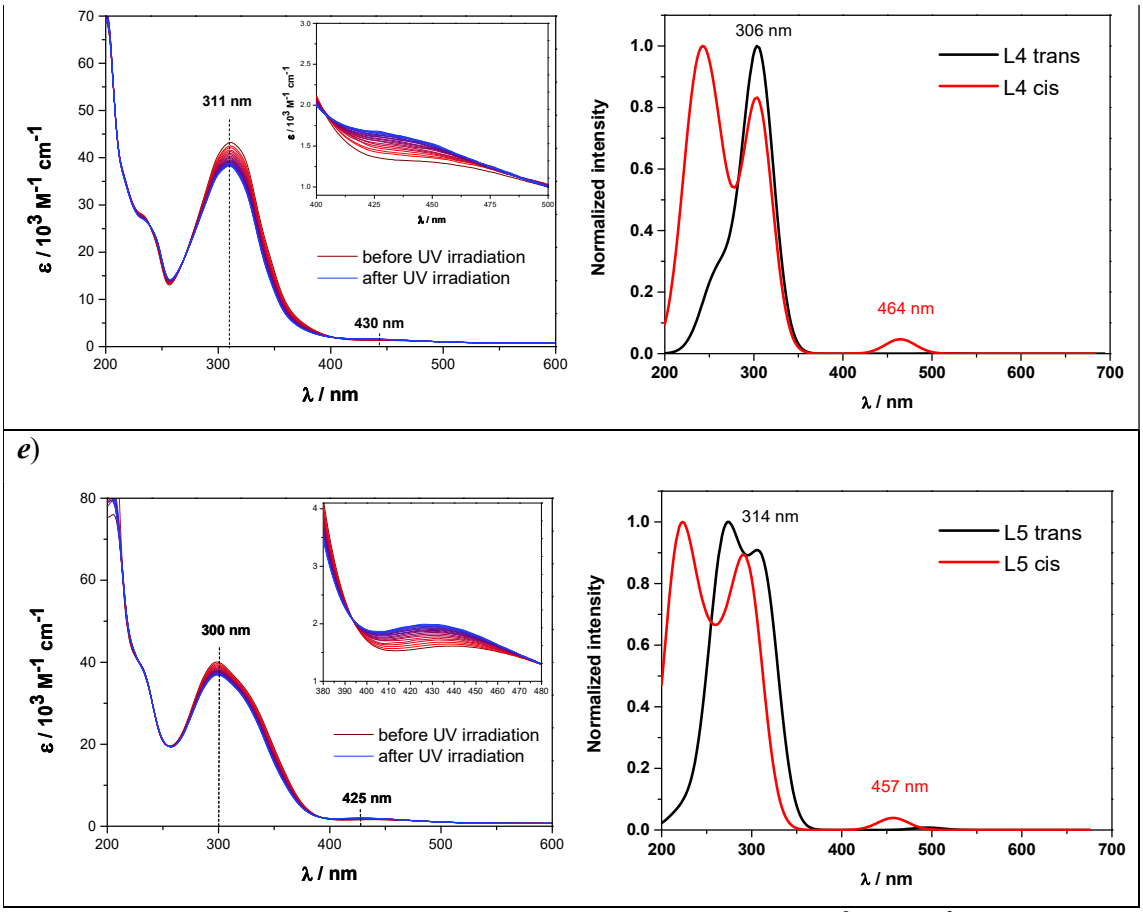

Figure S7 Left: Experimental UV-VIS spectra of compounds *a*) **L1** ($4.87.10^{-5}$ mol.dm^{-3}), *b*) **L2** ($6.26.10^{-5}$ mol.dm^{-3}), *c*) **L3** ($5.65.10^{-5}$ mol.dm^{-3}), *d*) **L4** ($4.78.10^{-5}$ mol.dm^{-3}), and *e*) **L5** ($4.81.10^{-5}$ mol.dm^{-3}) in ethanol. The solutions were irradiated for 5 minutes by UV (scan collected every 15 seconds, in total 40 scans for one cycle). Right: Simulated electronic spectra for *E* and *Z* isomers of **L1-L5**.

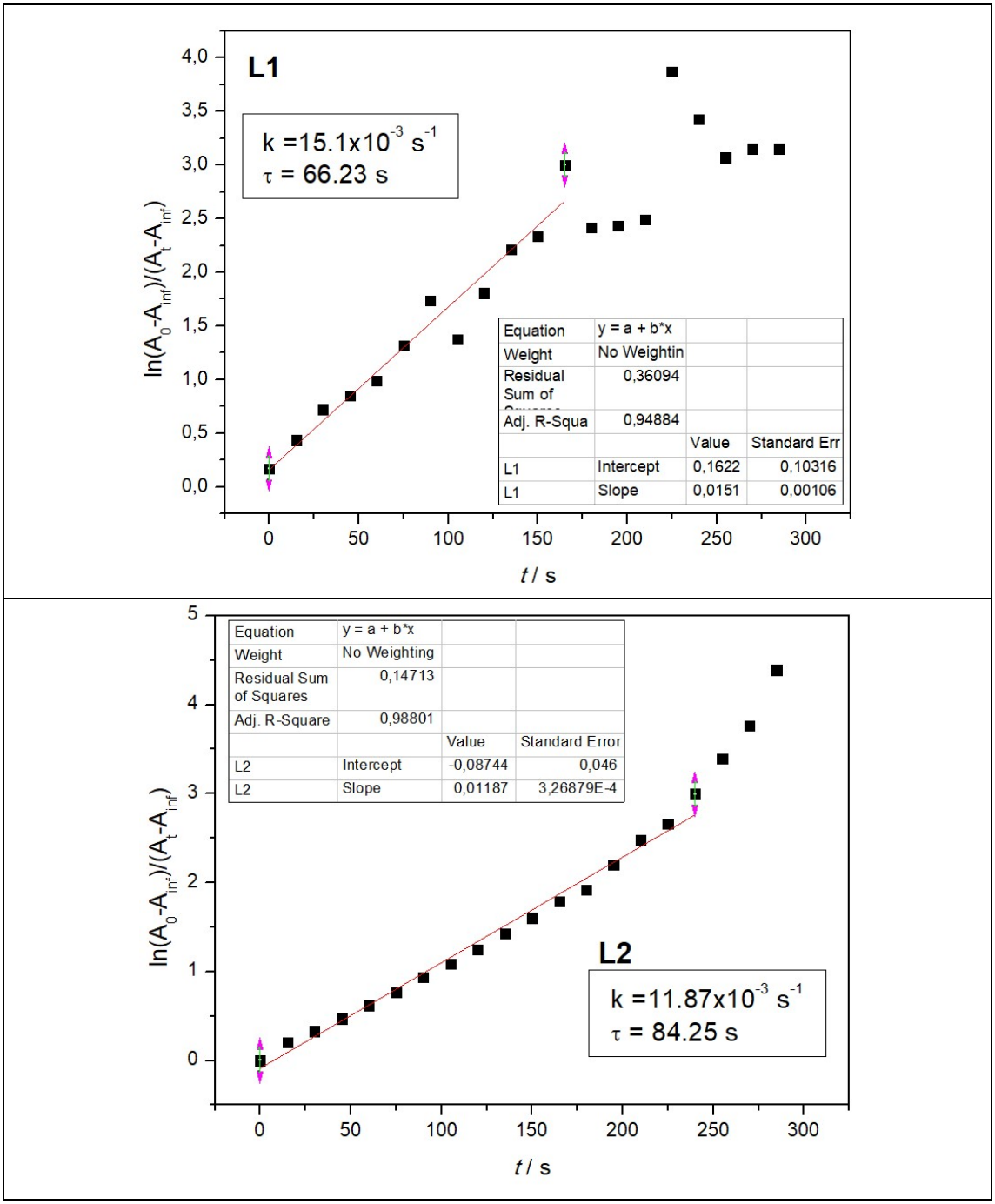
L1
k =15.1x10-3 s-1
τ = 66.23 s
ln(A0-Ainf)/(At-Ainf)
t / s
Equation y = a + b*x
Weight No Weightin
Residual Sum of 0,36094
Adj. R-Squa 0,94884
Value Standard Err
L1 Intercept 0,1622 0,10316
L1 Slope 0,0151 0,00106
Equation y = a + b*x
Weight No Weighting
Residual Sum of Squares 0,14713
Adj. R-Square 0,98801
Value Standard Error
L2 Intercept -0,08744 0,046
L2 Slope 0,01187 3,26879E-4
L2
k =11.87x10-3 s-1
τ = 84.25 s

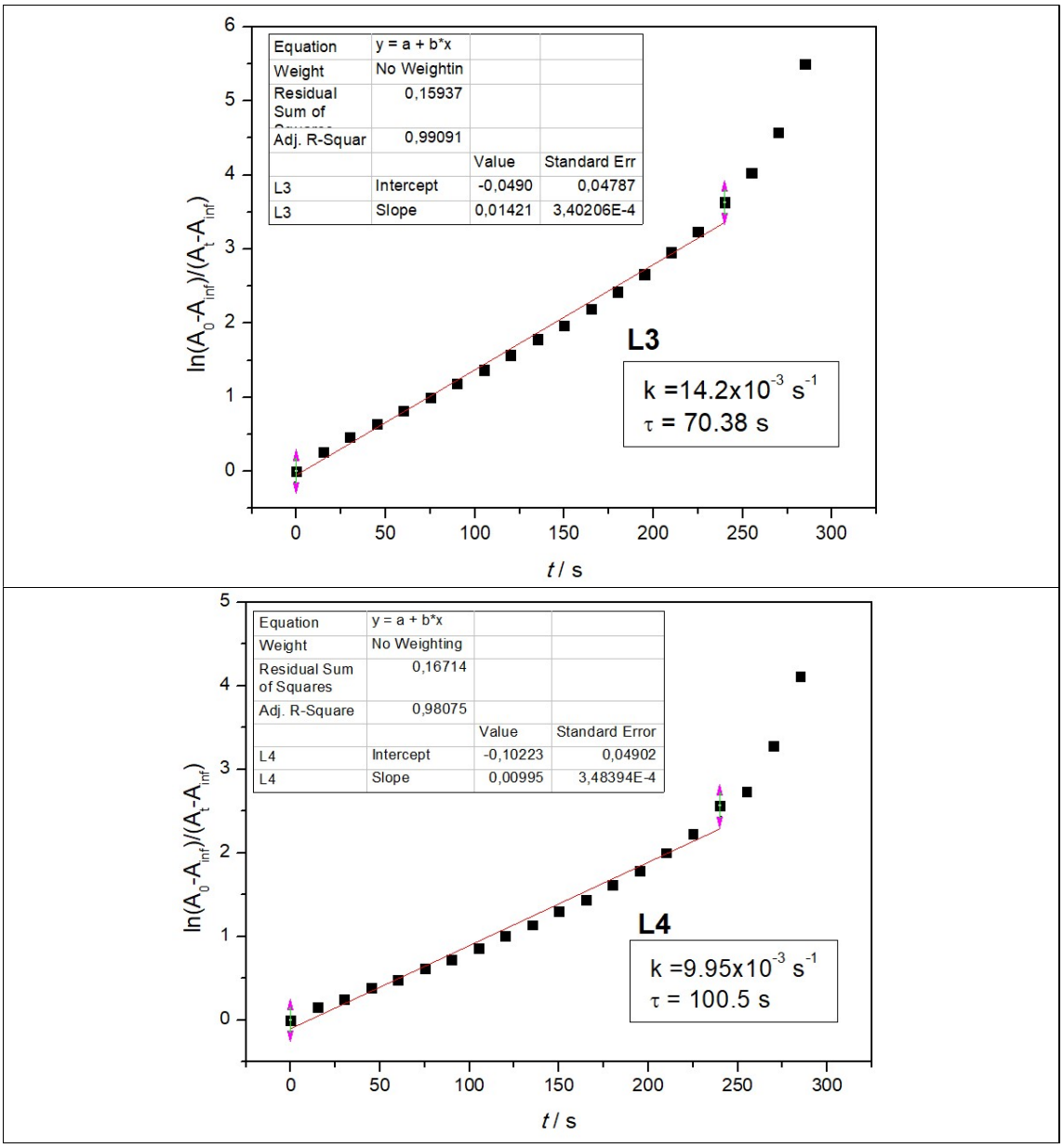
Equation y = a + b*x
Weight No Weightin
Residual Sum of 0,15937
Adj. R-Squar 0,99091
Value Standard Err
L3 Intercept -0,0490 0,04787
L3 Slope 0,01421 3,40206E-4
L3
k =14.2x10-3 s-1
τ = 70.38 s
ln(A0-Ainf)/(At-Ainf)
t / s
Equation y = a + b*x
Weight No Weighting
Residual Sum of Squares 0,16714
Adj. R-Square 0,98075
Value Standard Error
L4 Intercept -0,10223 0,04902
L4 Slope 0,00995 3,48394E-4
L4
k =9.95x10-3 s-1
τ = 100.5 s
ln(A0-Ainf)/(At-Ainf)
t / s

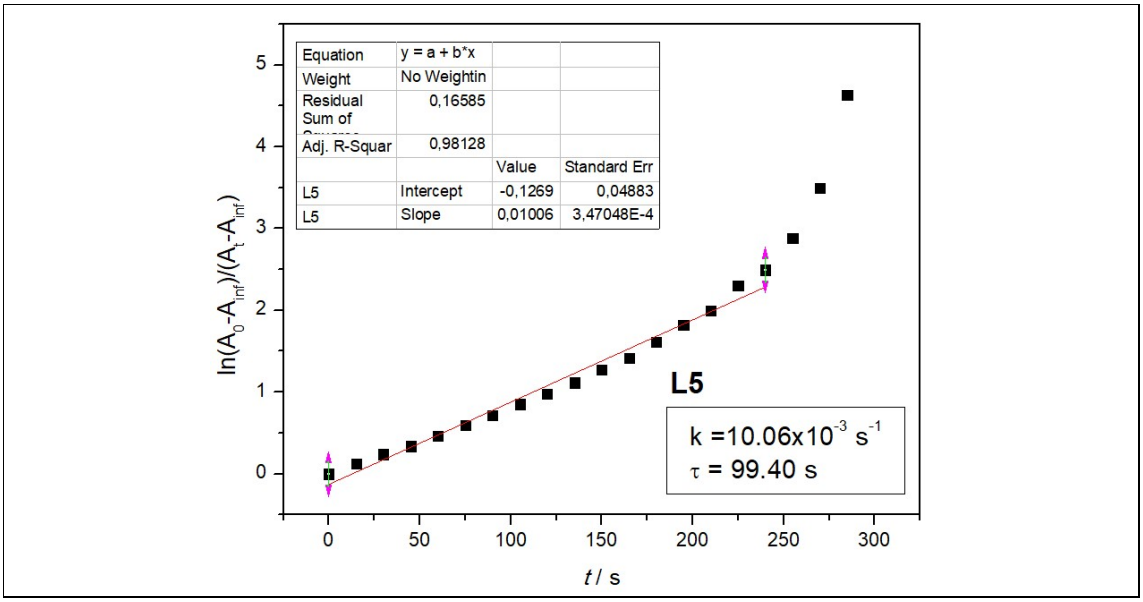

Figure S8. Calculated rate constants k for the $E \rightarrow Z$ isomerization of **L1-L5** in ethanol at room temperature. The linear fit corresponds to the first decrease of absorption at maximal wavelength of first 5 minutes upon UV light irradiation.

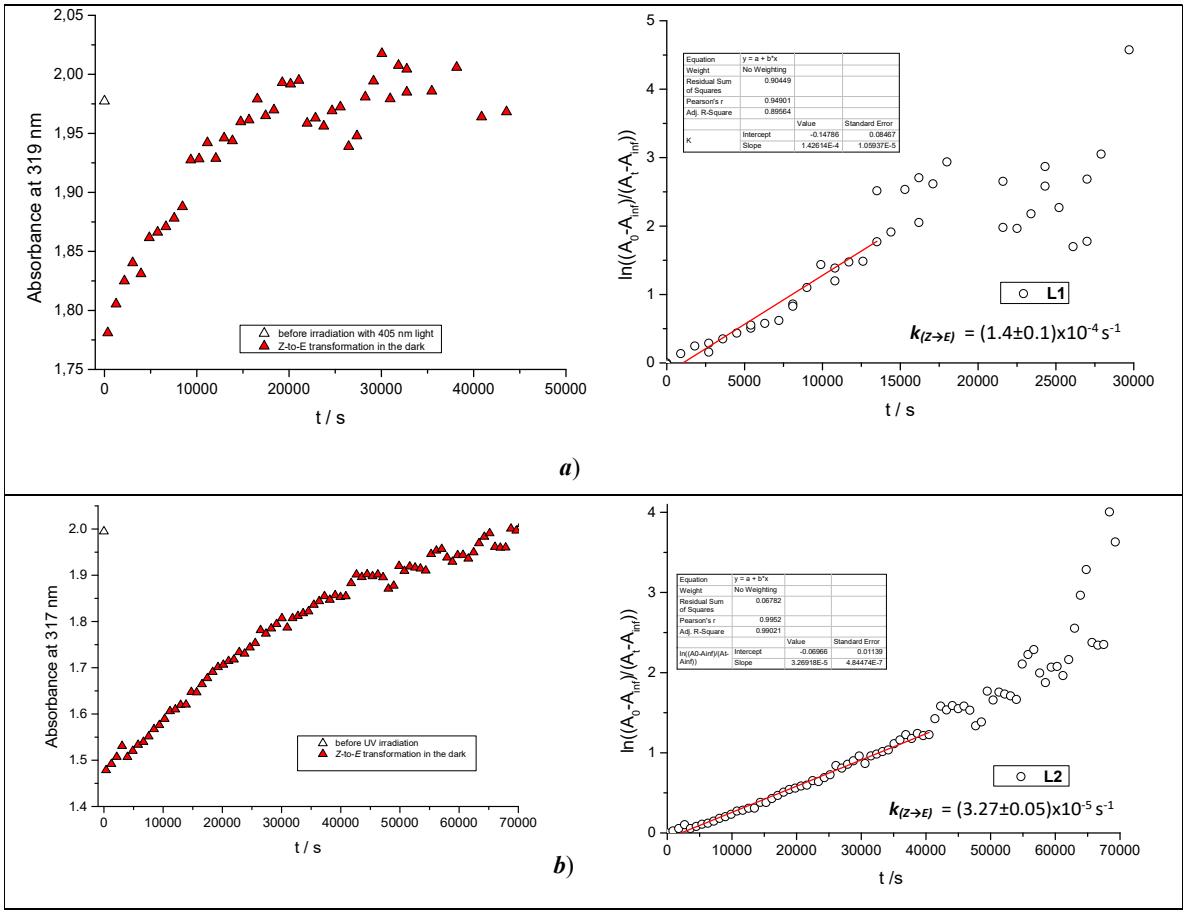

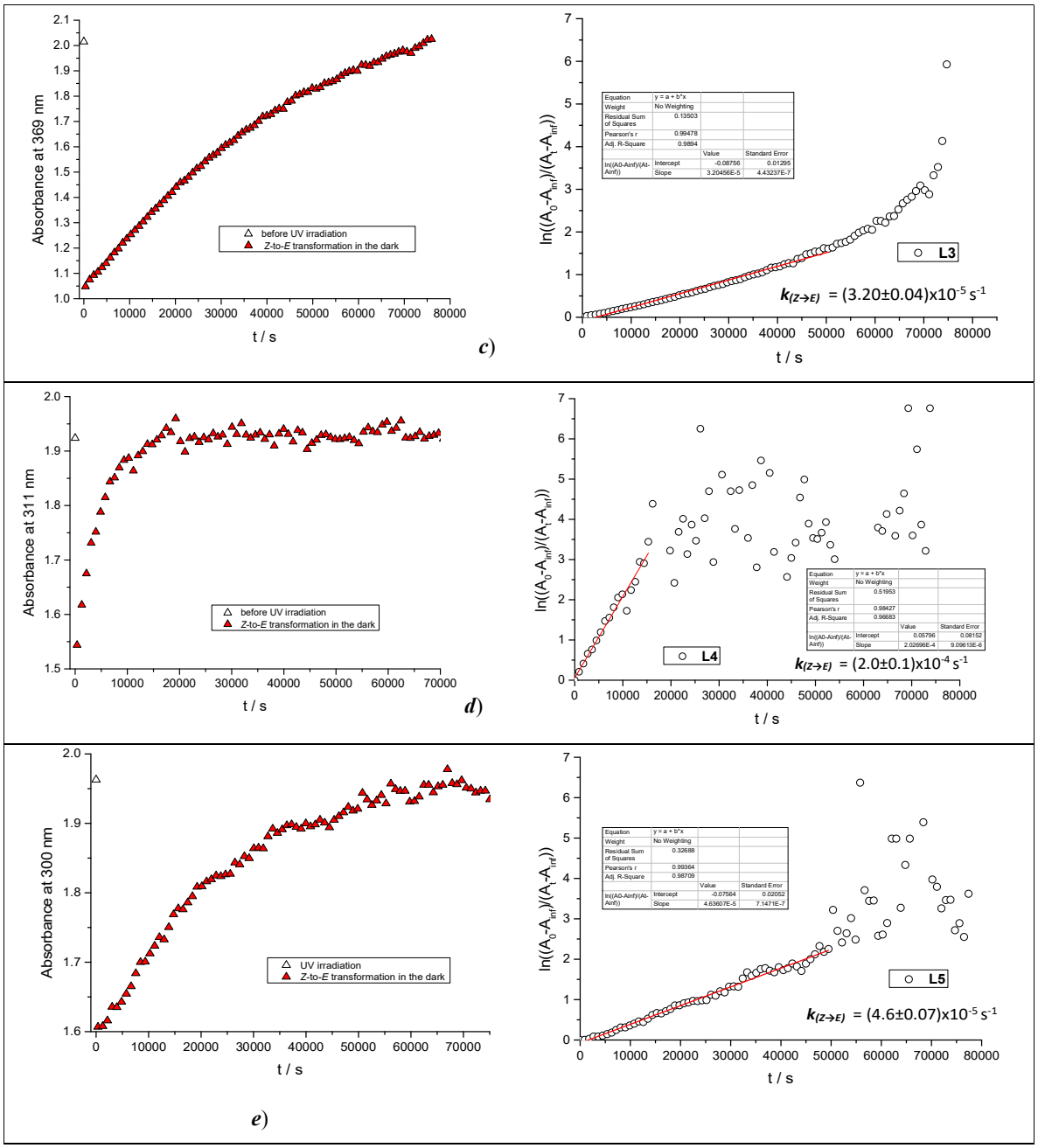

Figure S9. Time dependence of corresponding absorption maxima (*left*) and calculated rate constants (*right*) for ligands a) **L1**, b) **L2**, c) **L3**, d) **L4** and e) **L5** dissolved in ethanol. The corresponding solution was irradiated with blue or UV light for 5 minutes and then was kept in the dark. Data were collected every 5 minutes (**L1**) or 15 minutes (**L2-L5**). The blue light irradiation (405 nm) of **L1** solution afforded intense *E*-to-*Z* photoconversion comparing to UV light, therefore the blue laser light with 405 nm have been used for formation of photostationary state and for the kinetic studies.

SI 4. NMR spectroscopy and calculations

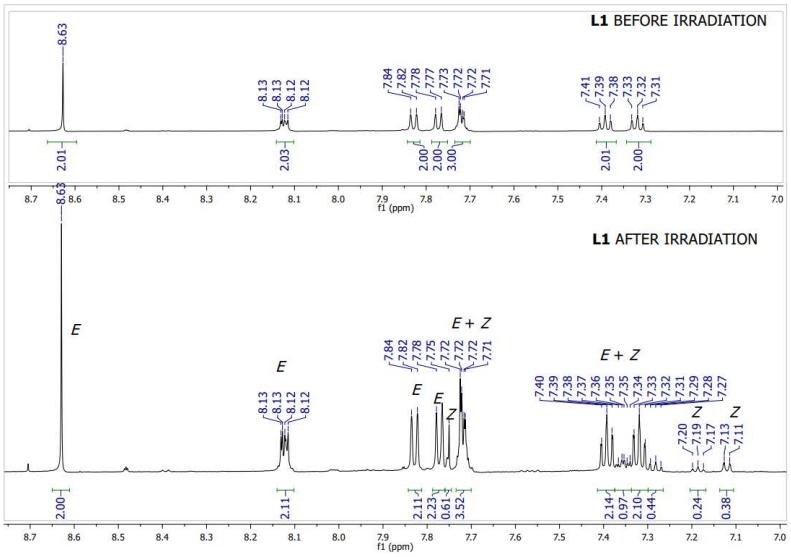

L1

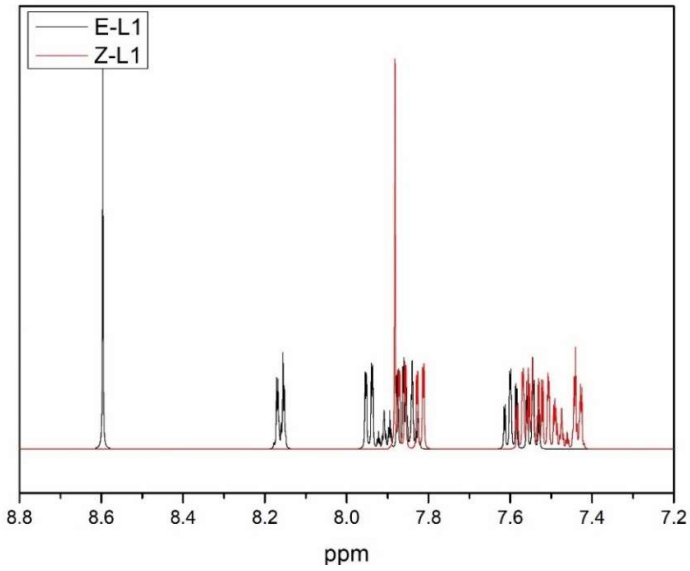

BEFORE IRRADIATION:

^{1}H NMR (600 MHz, DMSO-d_6) δ 8.63 (s, 2H), 8.14-8.11 (m, 2H), 7.83 (d, J=8.0 Hz, 2H), 7.77 (d, J=8.0 Hz, 2H), 7.74-7.70 (m, 3H), 7.41-7.37 (m, 2H), 7.34-7.30 (m, 2H).

L1 AFTER IRRADIATION:

^{1}H NMR (600 MHz, DMSO-d_6) δ 8.63 (s, 2H), 8.14-8.11(m, 2H), 7.83 (d, J=8.0 Hz, 2H), 7.77 (d, J=7.9 Hz, 2H), 7.77-7.75 (m, 2H), 7.75 (s, 2H), 7.73-7.70 (m, 5H), 7.41-7.38 (m, 2H), 7.37 – 7.34 (m, 4H), 7.34-7.30 (m, 2H), 7.30-7.27 (m, 2H), 7.20-7.17 (m, 1H), 7.14-7.11 (m, 2H).

CALCULATED SPECTRA in DMSO-d_6

***E*-L1**: 8.61-8.58 (s), 8.19-8.13(m), 7.98-7.93 (dd), 7.93-7.92 (t), 7.92-7.90 (t), 7.90-7.89 (t), 7.89-7.82 (m), 7.63-7.57 (m), 7.57-7.51 (m)

***Z*-L1**: 7.90-7.88 (s), 7.88-7.85 (dd), 7.85-7.80 (dd), 7.60-7.58 (d), 7.58-7.48 (m), 7.48-7.46 (t), 7.46-7.45 (t), 7.45-7.40 (m).

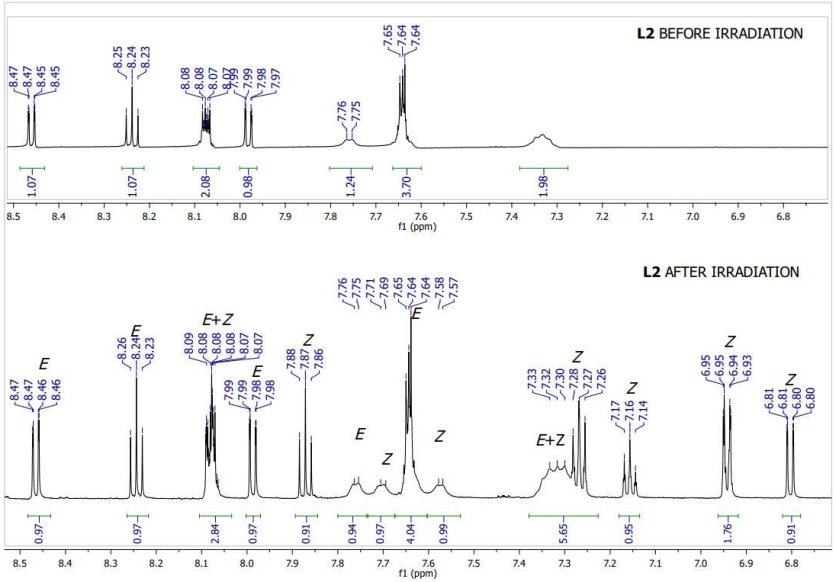

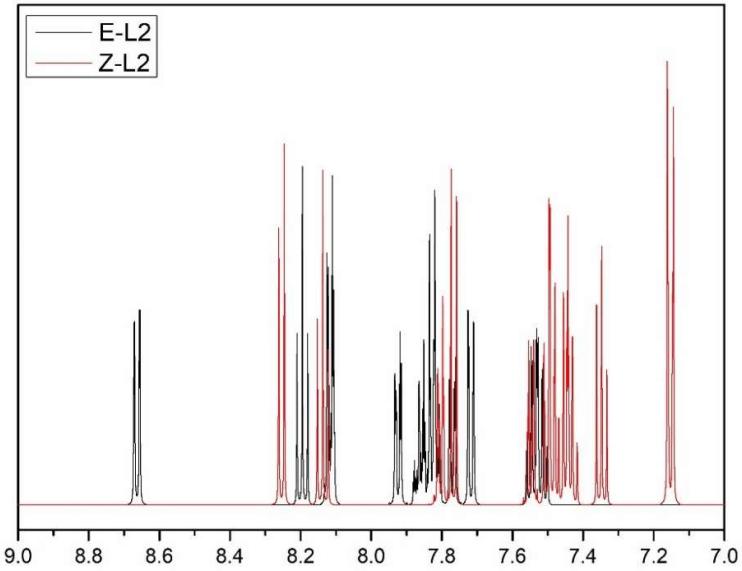

L2 BEFORE IRRADIATION

^{1}H NMR (600 MHz, CD_3OD) δ 8.46 (dd, *J* = 7.7, 0.9 Hz, 1H), 8.24 (t, *J* = 7.8 Hz, 1H), 8.10-8.05 (m, 2H), 7.98 (dd, *J* = 7.9, 0.9 Hz, 1H), 7.80-7.71 (m, 1H), 7.68 – 7.60 (m, 4H), 7.38-7.27 (m, 2H)

L2 AFTER IRRADIATION

^{1}H NMR (600 MHz, CD_3OD) δ 8.47 (dd, *J* = 7.7, 0.8 Hz, 1H), 8.24 (t, *J* = 7.8 Hz, 1H), 8.10 – 8.05 (m, 3H), 7.99 (dd, *J* = 2.8, 1.4 Hz, 1H), 7.87 (t, *J* = 7.9 Hz, 1H), 8.0-7.75 (m, 1H), 7.73-7.68 (m, 1H), 7.66– 7.60 (m, 4H), 7.59-7.53 (m, 1H), 7.38 – 7.24 (m, 6H), 7.18-7.14 (m, 1H), 6.96-6.92 (m, 2H), 6.80 (dd, *J* = 7.9, 0.8 Hz, 1H).

CALCULATED SPECTRA in CD_3OD

***E*-L2**: 8.69-8.63 (dd), 8.23-8.16 (t), 8.15-8.08 (m), 7.95-7.85 (dd), 7.95-7.79 (m), 7.79-7.75 (dd), 7.74-7.70 (dd),7.57-7.49 (m)

***Z*-L2**:8.28-8.23 (d), 8.17-8.10 (t), 7.83-7.78 (m), 7.78-7.76 (d), 7.56-7.52 (m),7.52-7.40 (m), 7.38-7.32 (t), 7.18-7.12 (dd)

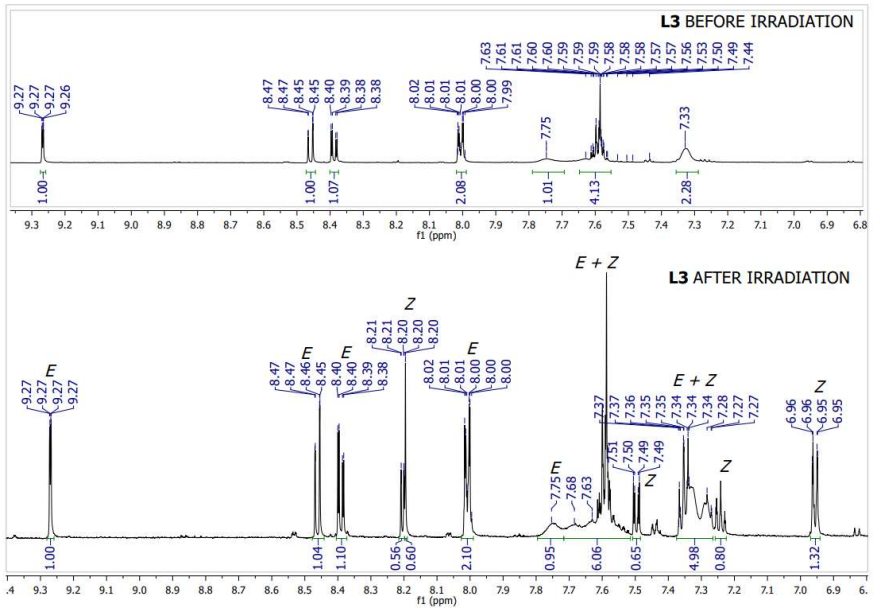

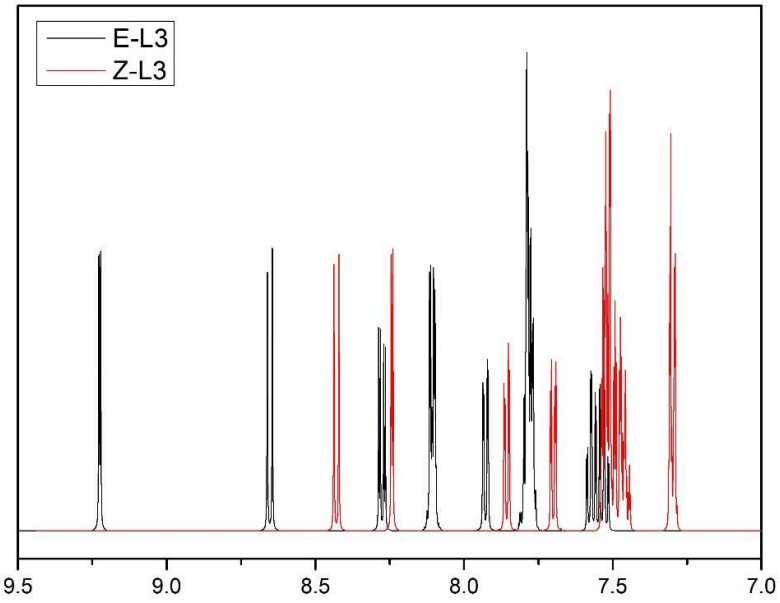

L3 BEFORE IRRADIATION:

^{1}H NMR (600 MHz, CD_3OD) δ 9.27 (dd, *J* = 2.3, 0.7 Hz, 1H), 8.46 (dd, *J* = 8.5, 0.7 Hz, 1H), 8.40 – 8.38 (dd, *J* = 8.5, 2.3 Hz, 1H), 8.00 (m, 2H), 7.75 (bs, 1H), 7.70-7.57 (m, 4H), 7.33 (bs, 2H).

L4 AFTER IRRADIATION:

^{1}H NMR (600 MHz, CD_3OD) δ 9.27 (dd, *J* = 2.3, 0.6 Hz, 1H), 8.46 (dd, *J* = 8.5, 0.7 Hz, 1H), 8.39 (dd, *J* = 8.5, 2.3 Hz, 1H), 8.20 (dd, *J* = 5.3, 0.6 Hz, 1H), 8.20 (s, 1H), 8.03-7.99 (m, 2H), 7.75 (bs, 1H), 7.71 – 7.51 (m, 6H), 7.51-7.48 (m, 1H), 7.38 – 7.26 (m, 6H), 7.26-7.23 (m, 1H), 6.97-6.94 (m, 2H).

CALCULATED SPECTRA in CD_3OD

***E*-L3**: 9.25-9.20 (d), 8.68-8.63 (d), 8.31-8.24 (dd), 8.14-8.07 (m), 7.95-7.90 (dd), 7.83-7.74 (m), 7.61-7.50 (m)

***Z*-L3:** 8.46-8.40 (d), 8.26-8.22 (d), 7.89-7.82 (dd), 7.73-7.67 (dd), 7.55-7.43 (m), 7.33-7.27 (m)

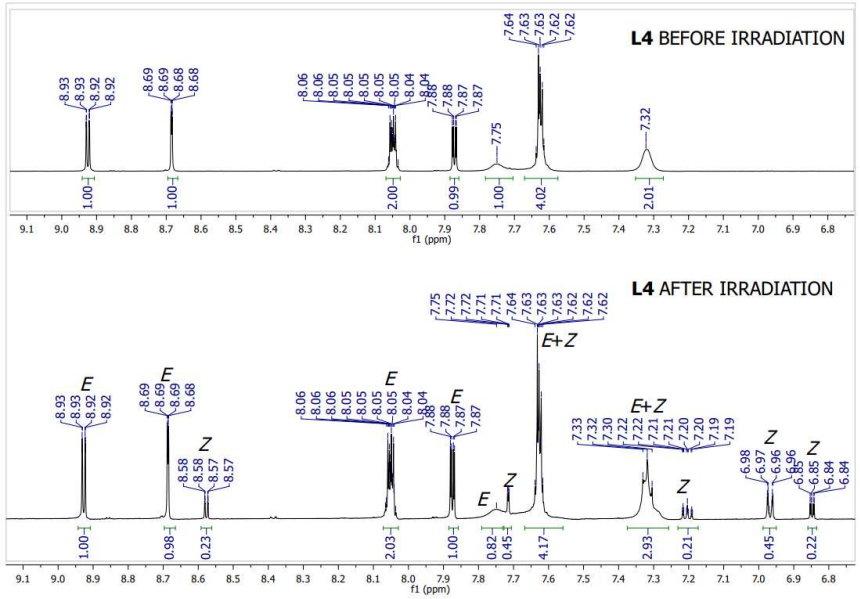

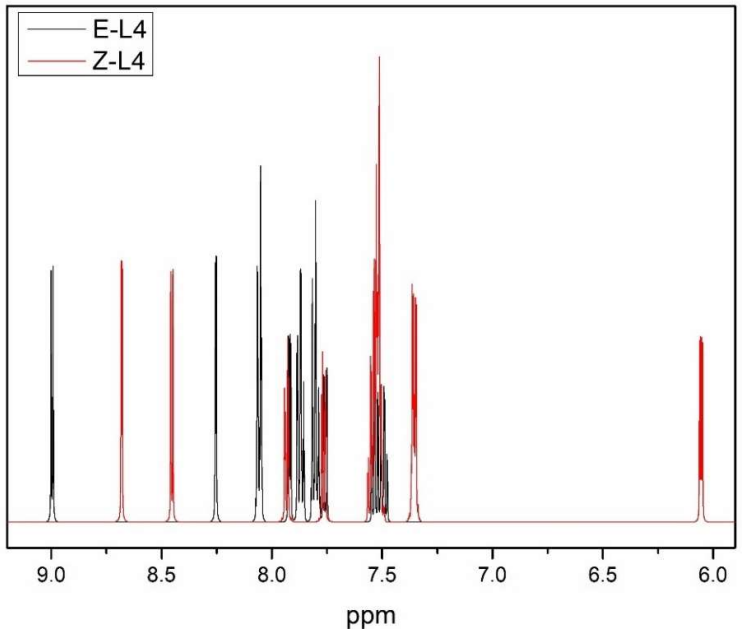

L4 BEFORE IRRADIATION:

^{1}H NMR (600 MHz, CD_3OD) δ 8.93 (dd, *J* = 5.1, 0.6 Hz, 1H), 8.68 (dd, *J* = 1.8, 0.7 Hz, 1H), 8.07 – 8.02 (m, 2H), 7.87 (dd, *J* = 5.1, 1.9 Hz, 1H), 7.75 (bs, 1H), 7.67 – 7.58 (m, 4H), 7.32 (bs, 2H).

L4 AFTER IRRADIATION:

^{1}H NMR (600 MHz, CD_3OD) δ 8.93 (dd, *J* = 5.1, 0.7 Hz, 1H), 8.69 (dd, *J* = 1.8, 0.7 Hz, 1H), 8.58 (dd, *J* = 5.2, 0.7 Hz, 1H), 8.07 – 8.03 (m, 2H), 7.87 (dd, *J* = 5.1, 1.9 Hz, 1H), 7.75 (bs, 1H), 7.71 (dd, *J* = 1.8, 0.7 Hz, 2H), 7.67 – 7.56 (m, 5H), 7.37 – 7.26 (m, 6H), 7.23 – 7.17 (m, 1H), 6.99 – 6.95 (m, 2H), 6.85 (dd, *J* = 5.2, 1.9 Hz, 1H).

CALCULATED SPECTRA in CD_3OD

***E*-L4**: 9.02-8.97 (d), 8.27-8.23 (d), 8.09-8.03 (m), 7.94-7.90 (q), 7.90-7.84 (m), 7.83-7.78 (m), 7.77-7.74 (dd), 7.57-7.46 (m),

***Z*-L4**: 8.71-8.65 (d), 8.48-8.42 (d), 7.97-7.89 (m), 7.80-7.73 (m), 7.58-7.48 (m), 7.42-7.32 (m), 7.09-7.02 (q)

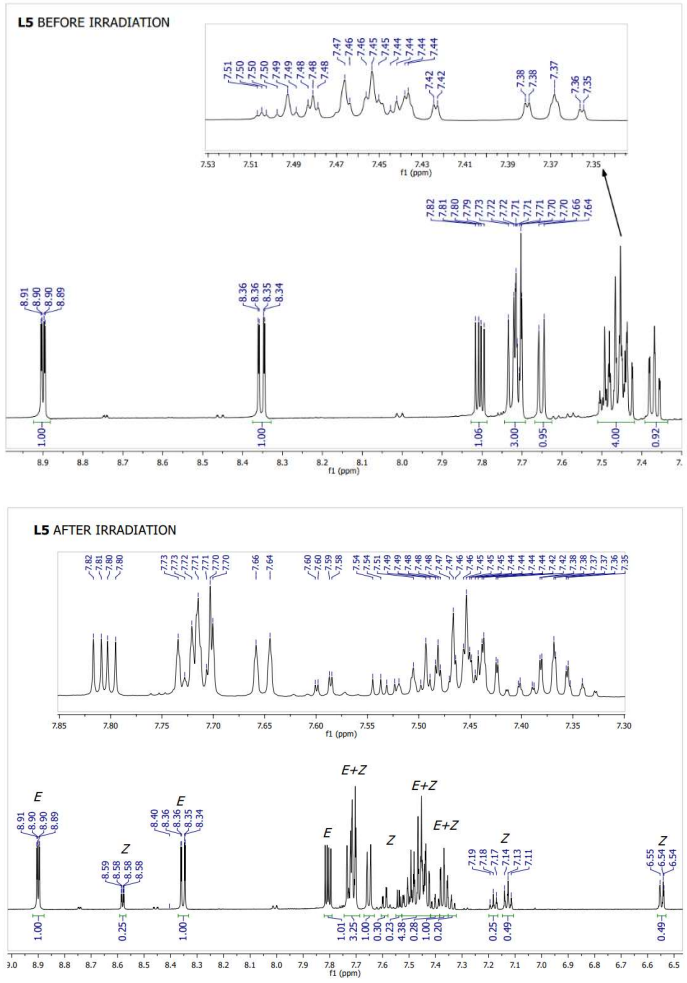

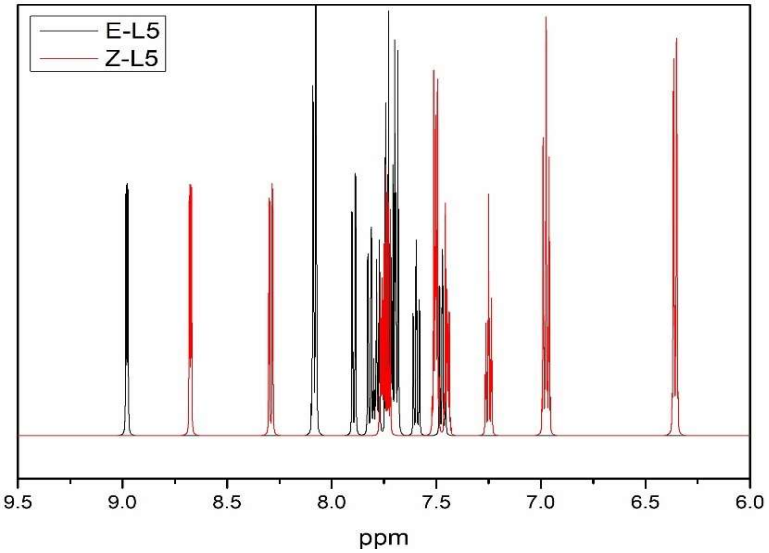

L5 BEFORE IRRADIATION

^{1}H NMR (600 MHz, CD_3OD) δ 8.90 (dd, *J* = 4.7, 1.5 Hz, 1H), 8.35 (dd, *J* = 8.3, 1.5 Hz, 1H), 7.81 (dd, *J* = 8.3, 4.7 Hz, 1H), 7.74 – 7.69 (m, 3H), 7.65 (d, *J* = 8.1 Hz, 1H), 7.51 – 7.42 (m, 4H), 7.39 – 7.34 (m, 1H).

L5 AFTER IRRADIATION

^{1}H NMR (600 MHz, CD_3OD) δ 8.90 (dd, *J* = 4.7, 1.5 Hz, 1H), 8.58 (dd, *J* = 4.7, 1.5 Hz, 1H), 8.35 (dd, *J* = 8.3, 1.5 Hz, 1H), 7.81 (dd, *J* = 8.3, 4.7 Hz, 1H), 7.72 (m, 4H), 7.65 (d, *J* = 8.1 Hz, 1H), 7.59 (dd, *J* = 8.2, 1.5 Hz, 1H), 7.54 (dd, *J* = 8.2, 1.5 Hz, 1H), 7.53 – 7.42 (m, 5H), 7.42 – 7.38 (m, 1H), 7.38 – 7.35 (m, 1H), 7.34 – 7.32 (m, 1H), 7.20 – 7.16 (m, 1H), 7.15 – 7.11 (m, 2H), 6.56 – 6.53 (m, 2H).

CALCULATED SPECTRA in CD_3OD

***E*-L5**: 8.98 (dd), 8.10-8.07 (m), 7.91-7.88 (dd), 7.84-7.81 (dd), 7.81-7.79 (t), 7.79-7.76 (m), 7.76-7.67 (m), 7.62-7.57 (dt),7.50-7.45 (dt)

***Z*-L5**: 8.70-8.65 (dd), 8.32-8.26 (dd), 7.80-7.70 (m), 7.54-7.47 (m), 7.47-7.42 (m), 7.28-7.22 (tt), 7.02-6.94 (m), 6.39-6.33 (m)

Figure S10. Left: Experimental NMR spectra before and after UV irradiation of **L1**-**L5** in corresponding solvents (c ≈ 10^{-3} mol.dm^{-3}), right: calculated NMR spectra for *E* and *Z* conformers in DMSO-d_6 (for **L1**) or methanol-d_4 (for **L2**-**L5**) at 293 K.

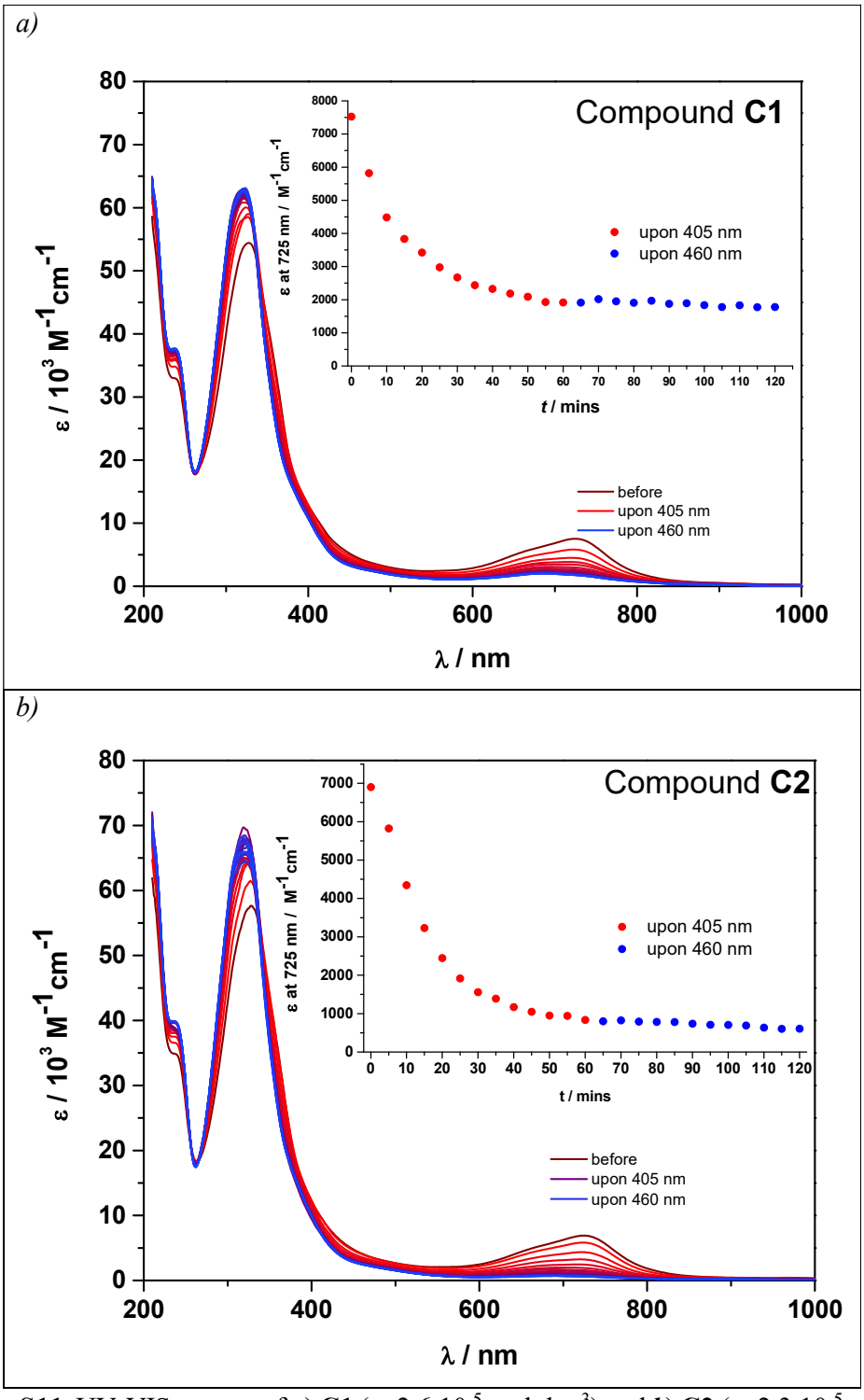

Figure S11. UV-VIS spectra of ***a***) **C1** (c≈2.6.10^{-5} mol.dm^{-3}) and ***b***) **C2** (c≈2.3.10^{-5} mol.dm^{-3}) in the dark ("before"), within the irradiation with 405 nm laser light and after consequential irradiation with 460 nm LEDs in four cycles. Inserted graphs: Time dependent change of absorbance at corresponding maximum $\boldsymbol{\lambda}_{max}$≈725 nm

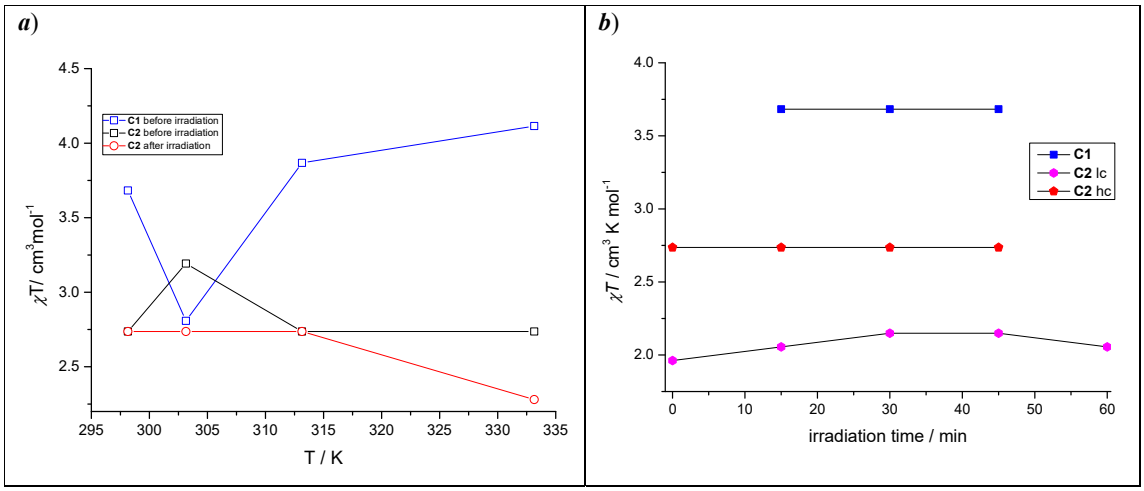

Figure S12. ***a***) χT vs T dependency of **C1** (c=1.54 mM) and **C2** (c=1.56 mM) measured in DMSO-d_6 by Evans method; ***b***) Time evolution of the product function χT of irradiated DMSO-d_6 solutions of **C1** and **C2** measured by Evans method at room temperature. Solutions of both compounds were irradiated with 405 nm laser light. Compound **C2** has been measured in high (HC) and low concentration (LC) solution (**C2** lc c=1.56 mM, **C2** hc c=15.23 mM)

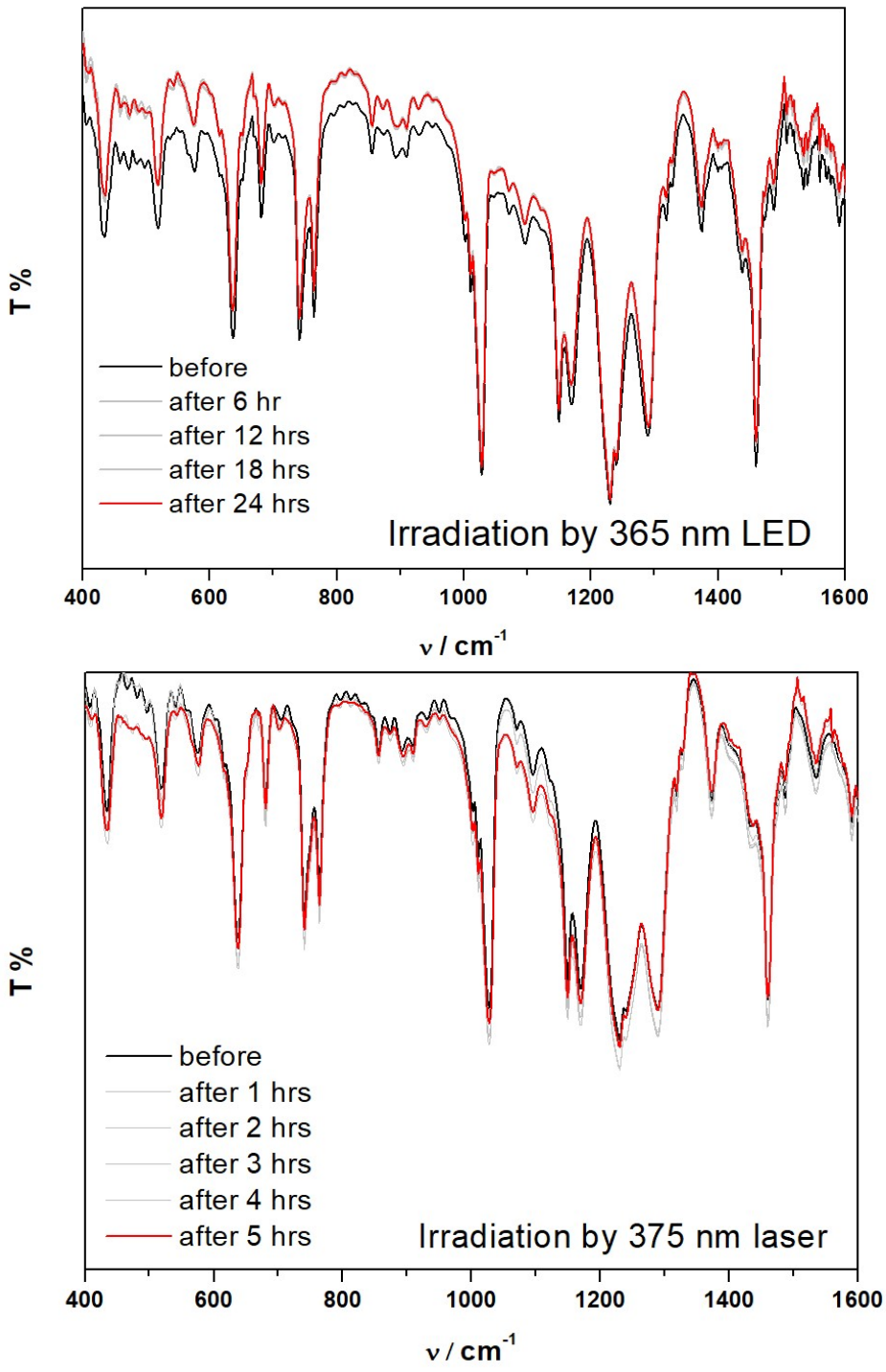

Figure S13. Evolution of FT-IR spectra of **C1** (KBr pellet) within the continuous irradiation by different laser sources at the room temperature.

SI 5. Computational study

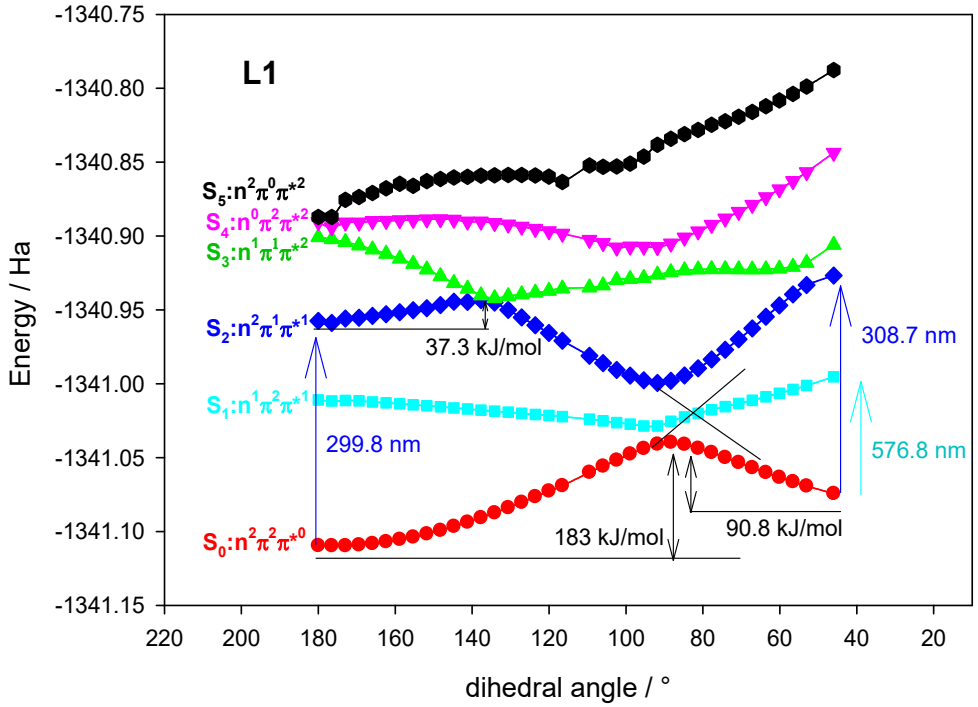

Figure S14. PES scan with respect to –CNNC– dihedral angle for **L1.**

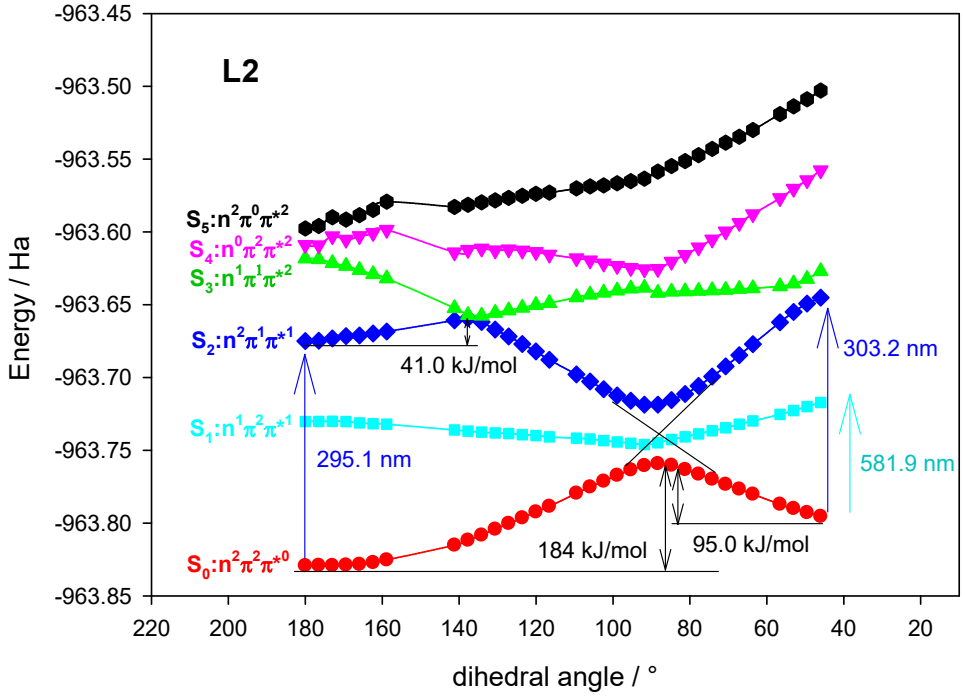

Figure S15. PES scan with respect to –CNNC– dihedral angle for **L2.**

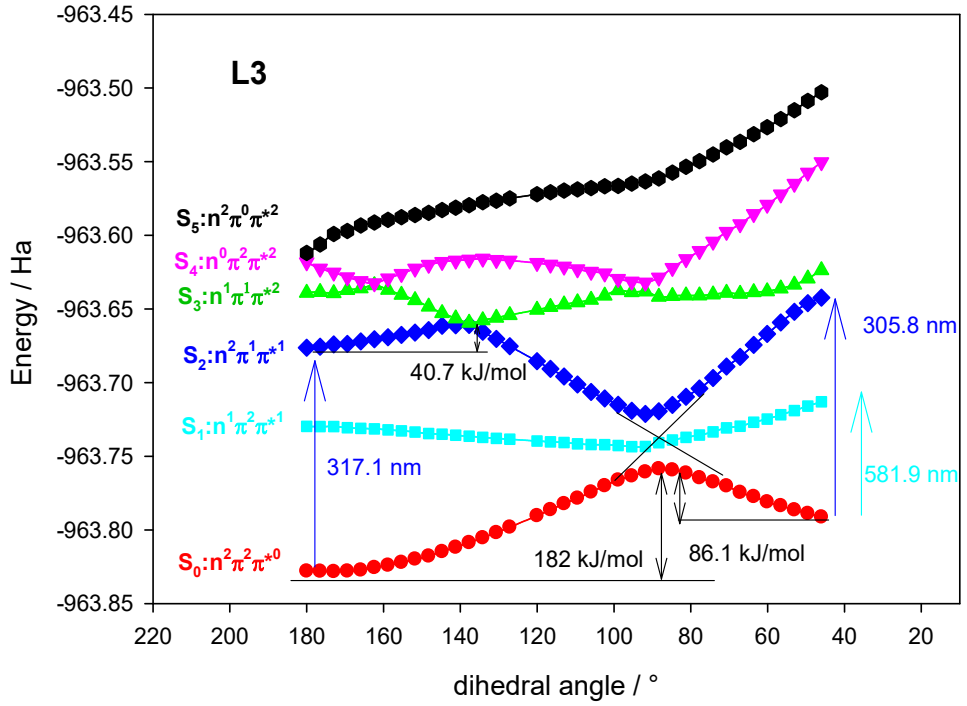

Figure S16. PES scan with respect to –CNNC– dihedral angle for **L3.**

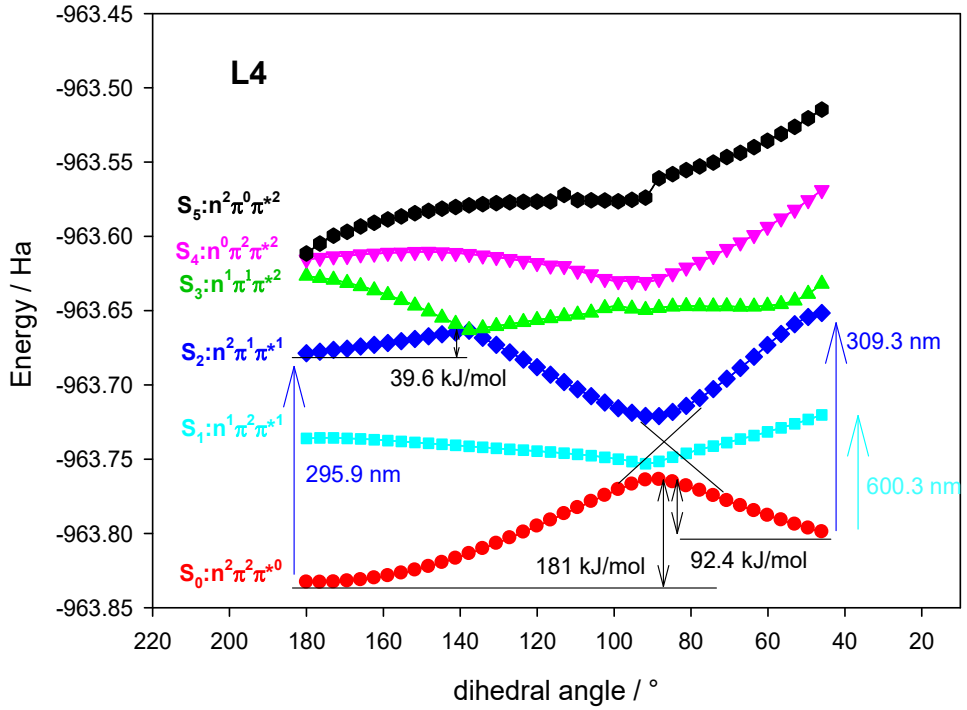

Figure S17. PES scan with respect to –CNNC– dihedral angle for **L4.**

***a*) L1**

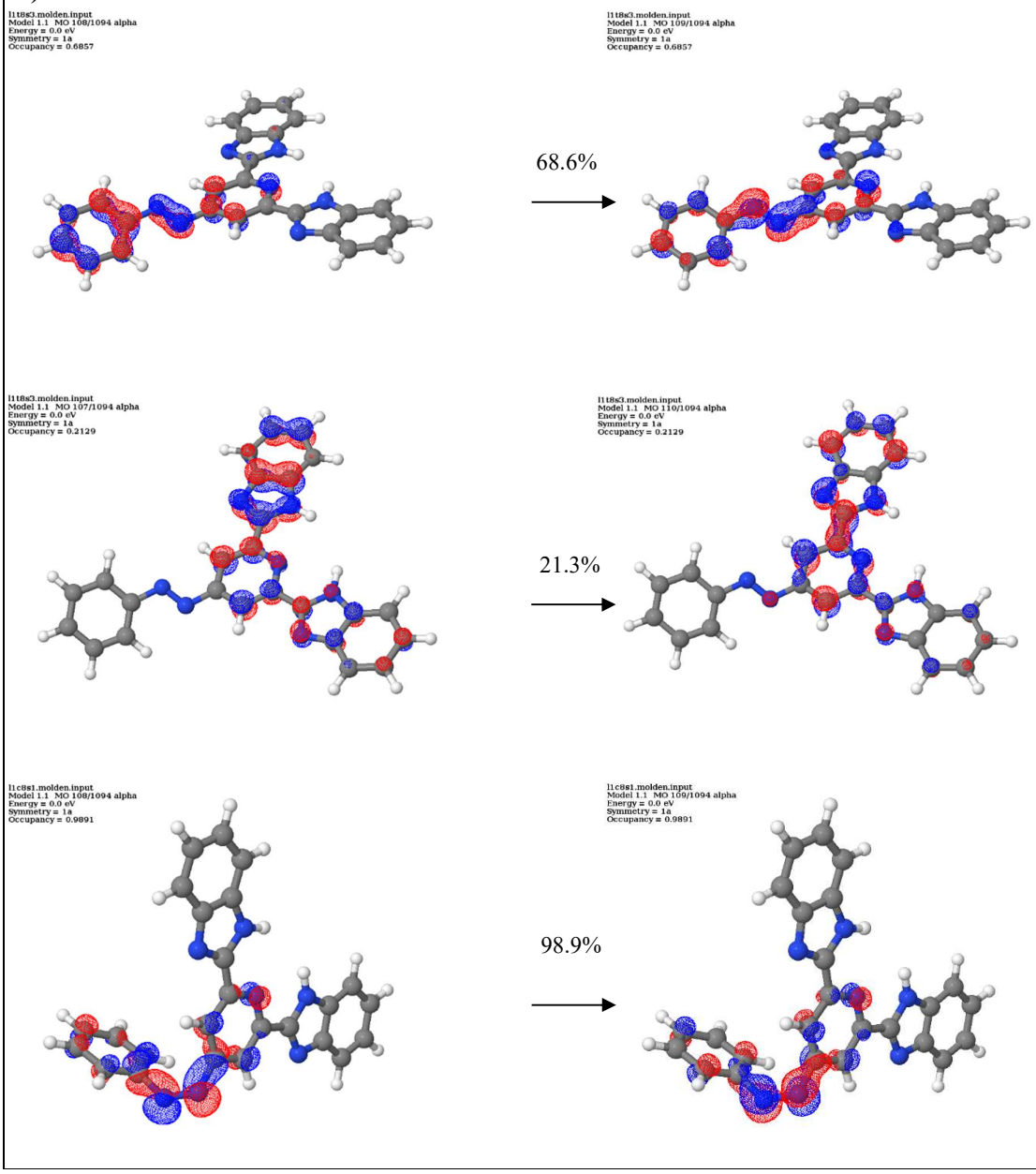
l1t8s3.molden.input
Model 1.1 MO 108/1094 alpha
Energy = 0.0 eV
Symmetry = 1a
Occupancy = 0.6857
l1t8s3.molden.input
Model 1.1 MO 109/1094 alpha
Energy = 0.0 eV
Symmetry = 1a
Occupancy = 0.6857
68.6%
l1t8s3.molden.input
Model 1.1 MO 107/1094 alpha
Energy = 0.0 eV
Symmetry = 1a
Occupancy = 0.2129
l1t8s3.molden.input
Model 1.1 MO 110/1094 alpha
Energy = 0.0 eV
Symmetry = 1a
Occupancy = 0.2129
21.3%
l1c8s1.molden.input
Model 1.1 MO 108/1094 alpha
Energy = 0.0 eV
Symmetry = 1a
Occupancy = 0.9891
l1c8s1.molden.input
Model 1.1 MO 109/1094 alpha
Energy = 0.0 eV
Symmetry = 1a
Occupancy = 0.9891
98.9%

***b*) L2**

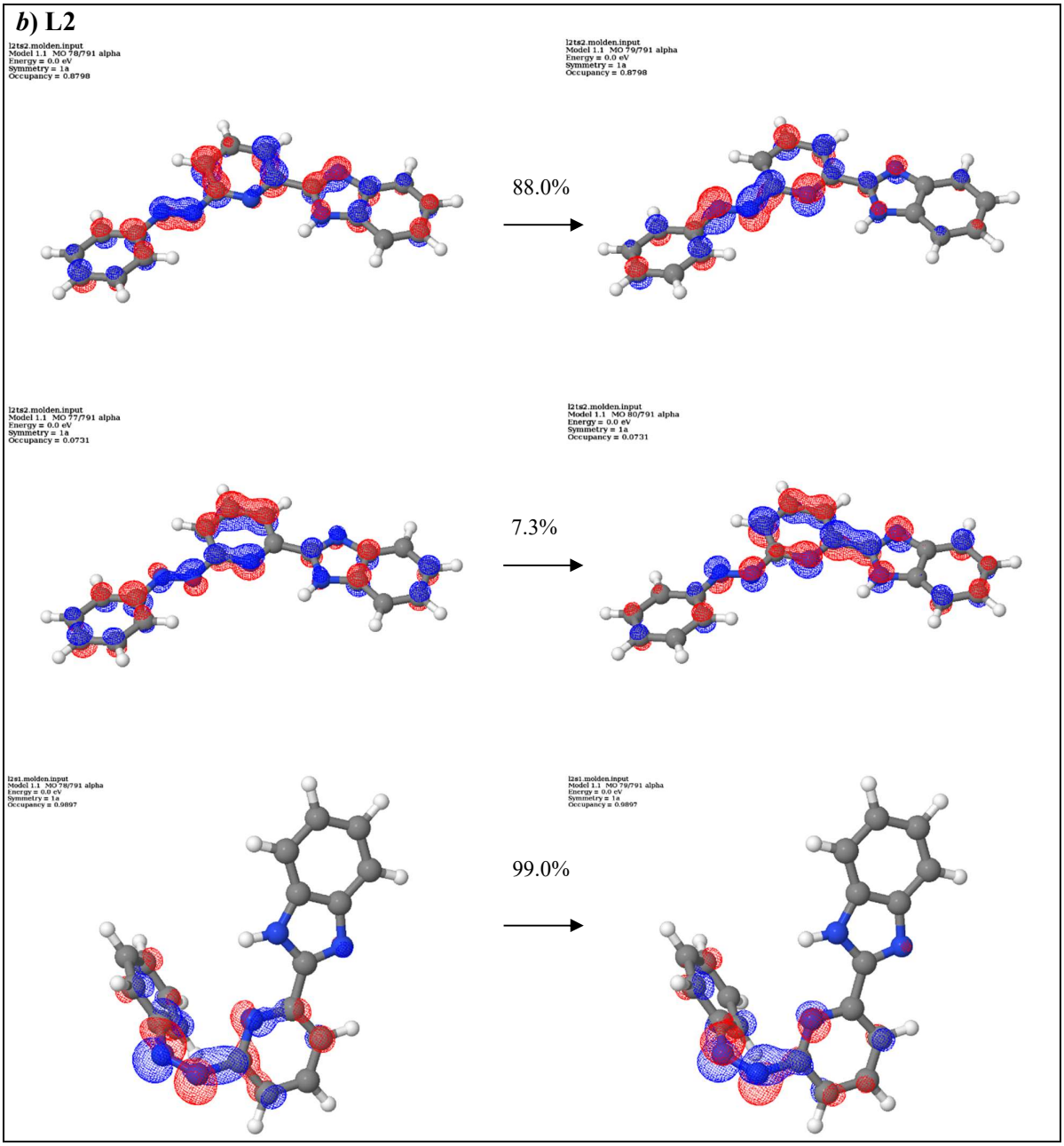
l2ts2.molden.input
Model 1.1 MO 78/791 alpha
Energy = 0.0 eV
Symmetry = 1a
Occupancy = 0.8798
88.0%
l2ts2.molden.input
Model 1.1 MO 79/791 alpha
Energy = 0.0 eV
Symmetry = 1a
Occupancy = 0.8798
l2ts2.molden.input
Model 1.1 MO 77/791 alpha
Energy = 0.0 eV
Symmetry = 1a
Occupancy = 0.0731
7.3%
l2ts2.molden.input
Model 1.1 MO 80/791 alpha
Energy = 0.0 eV
Symmetry = 1a
Occupancy = 0.0731
l2s1.molden.input
Model 1.1 MO 78/791 alpha
Energy = 0.0 eV
Symmetry = 1a
Occupancy = 0.9897
99.0%
l2s1.molden.input
Model 1.1 MO 79/791 alpha
Energy = 0.0 eV
Symmetry = 1a
Occupancy = 0.9897

c) L3

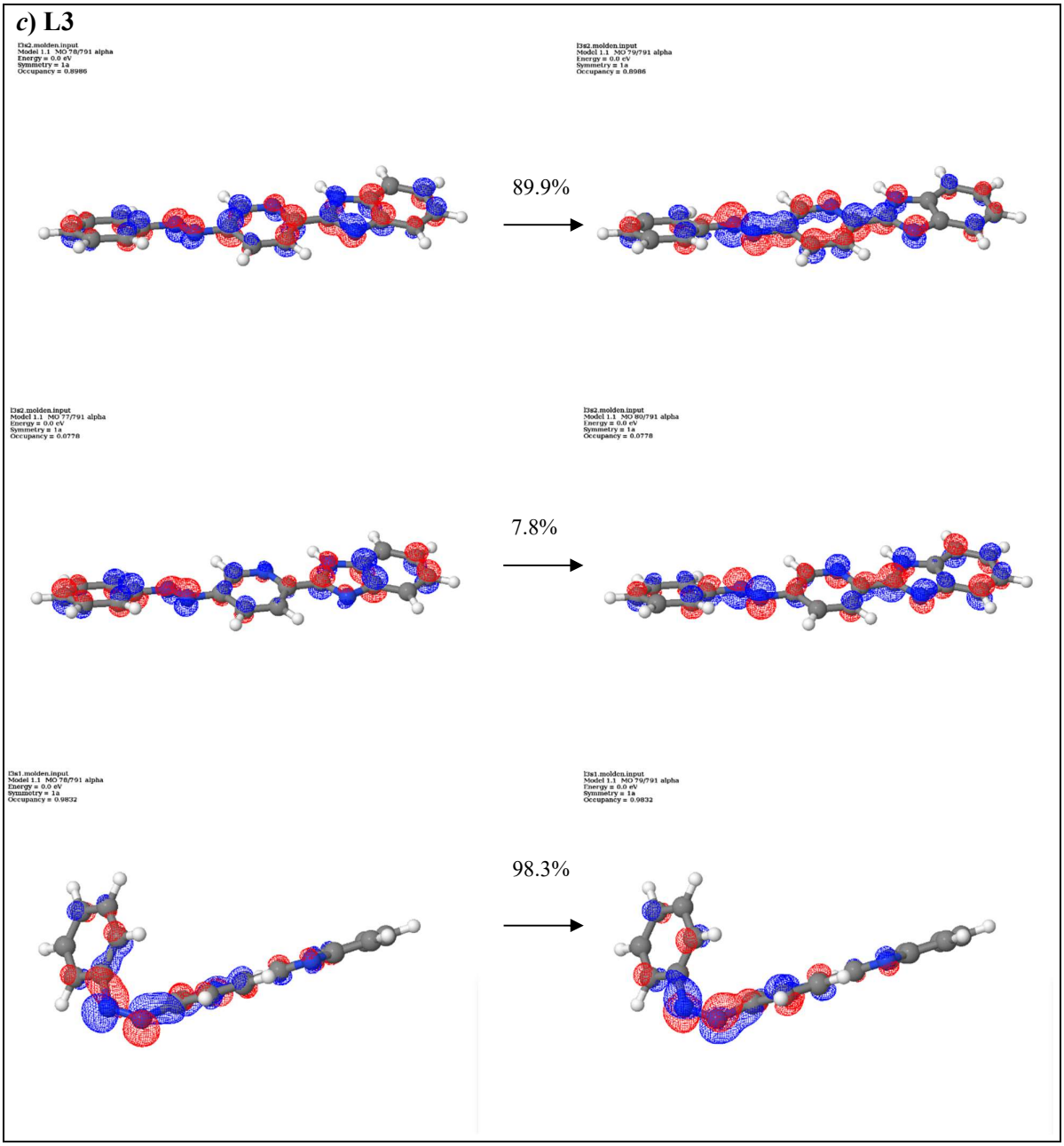
I3n2.molden.input
Model 1.1 MO 78/791 alpha
Energy = 0.0 eV
Symmetry = 1a
Occupancy = 0.8986
I3n2.molden.input
Model 1.1 MO 79/791 alpha
Energy = 0.0 eV
Symmetry = 1a
Occupancy = 0.8986
89.9%
I3n2.molden.input
Model 1.1 MO 77/791 alpha
Energy = 0.0 eV
Symmetry = 1a
Occupancy = 0.0778
I3n2.molden.input
Model 1.1 MO 80/791 alpha
Energy = 0.0 eV
Symmetry = 1a
Occupancy = 0.0778
7.8%
I3s1.molden.input
Model 1.1 MO 78/791 alpha
Energy = 0.0 eV
Symmetry = 1a
Occupancy = 0.9832
I3s1.molden.input
Model 1.1 MO 79/791 alpha
Energy = 0.0 eV
Symmetry = 1a
Occupancy = 0.9832
98.3%

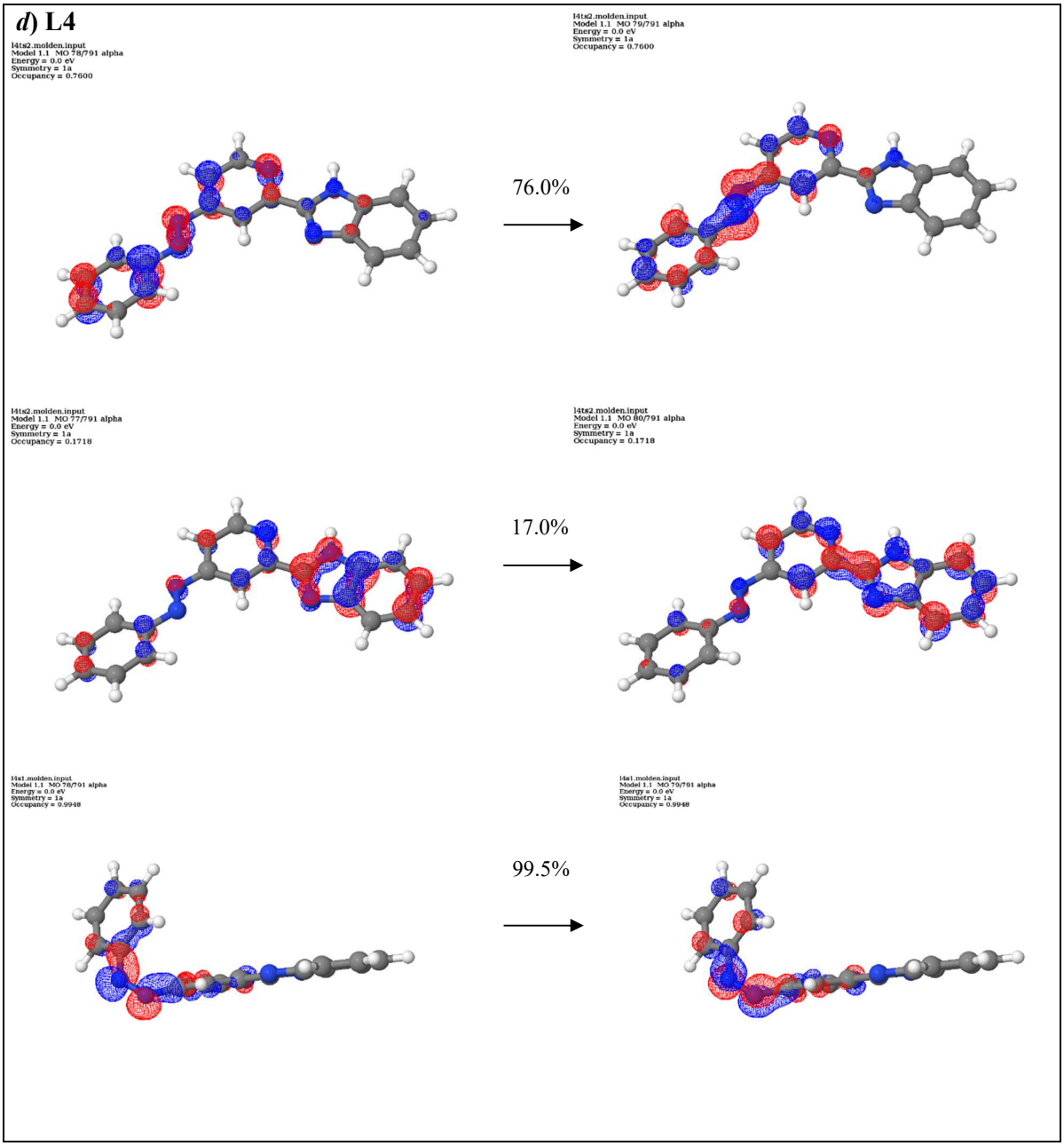
d) L4
l4ts2.molden.input
Model 1.1 MO 78/791 alpha
Energy = 0.0 eV
Symmetry = 1a
Occupancy = 0.7600
l4ts2.molden.input
Model 1.1 MO 79/791 alpha
Energy = 0.0 eV
Symmetry = 1a
Occupancy = 0.7600
76.0%
l4ts2.molden.input
Model 1.1 MO 77/791 alpha
Energy = 0.0 eV
Symmetry = 1a
Occupancy = 0.1718
l4ts2.molden.input
Model 1.1 MO 80/791 alpha
Energy = 0.0 eV
Symmetry = 1a
Occupancy = 0.1718
17.0%
l4s1.molden.input
Model 1.1 MO 78/791 alpha
Energy = 0.0 eV
Symmetry = 1a
Occupancy = 0.9948
l4s1.molden.input
Model 1.1 MO 79/791 alpha
Energy = 0.0 eV
Symmetry = 1a
Occupancy = 0.9948
99.5%

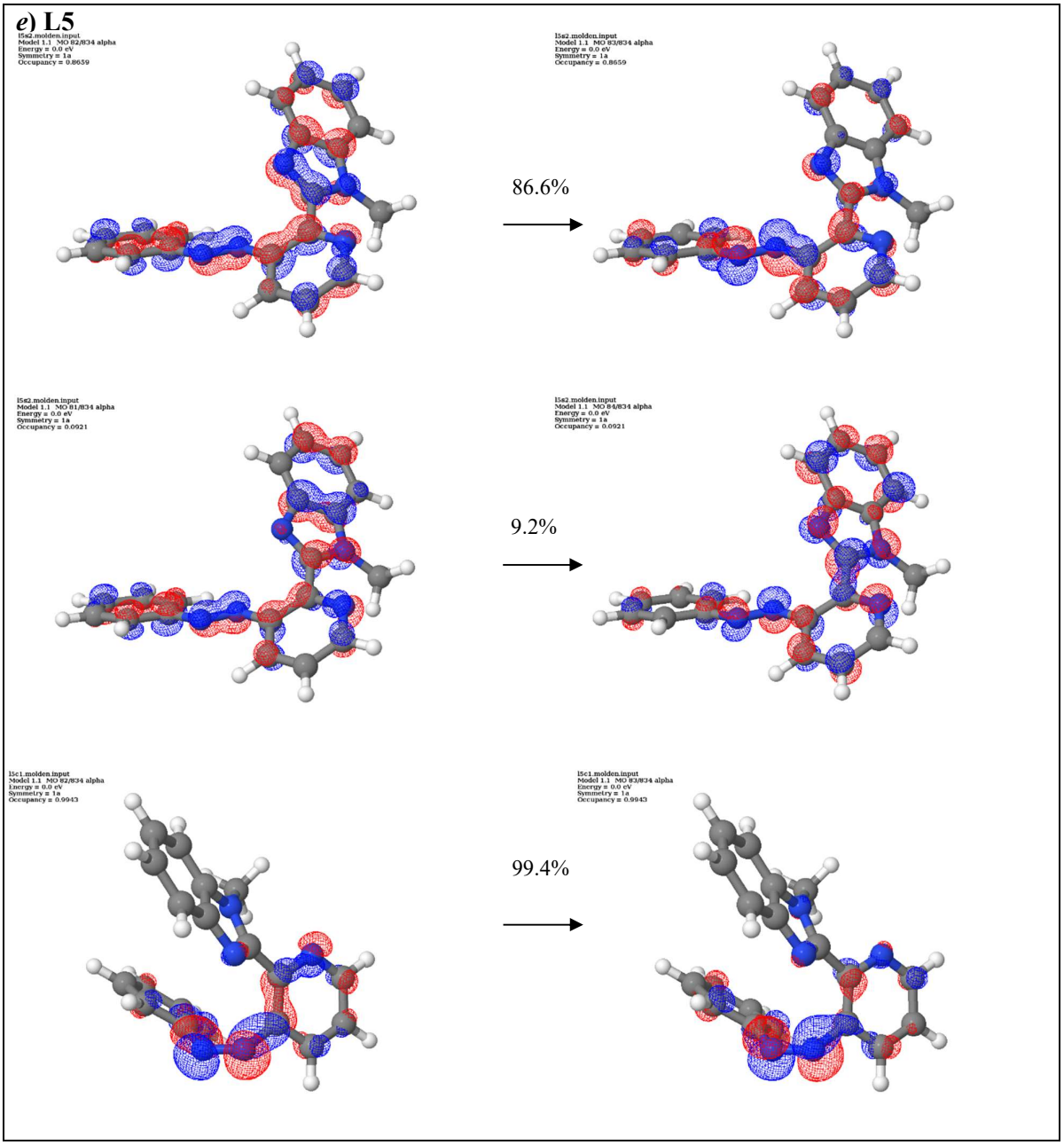

Figure S18. a)-e). Natural transition orbitals extracted from STEOM-DLPNO-CCSD calculation for the most intensive transition in the upper two pictures (*E* isomers) and for the highest wavelength transition in the lower picture (*Z* isomer) for **L1**-**L5**, respectively. In the case of *E* isomer, two orbital couples need to be considered to reach contribution higher than 90 %.

References

1 Z. E. A. Chamas, X. Guo, J.-L. Canet, A. Gautier, D. Boyer, R. Mathiou, *Dalton Trans.* **2010**, *39*, 7091–7097.

2 a) G. M. Sheldrick, *Acta Crystallogr. Sect. A*, **2015**, *A71*, 3–8; b) G. M. Sheldrick, *Acta Crystallogr. Sect. C*, **2015**, *C71*, 3–8; c) O. Dolomanov, L. J. Bourhis, R. J. Gildea, J. A. K. Howard, H. Puschmann, *J. Appl. Crystallogr.*, **2009**, *42*, 339–341; d) C. F. MacRae, I. Sovago, S. J. Cottrell, P. T. A. Galek, P. mcCabe, E. Pidcock, M. Platings, G. P. Shields, J. S. Stevens, M. Towler, P. A. Wood, *J. Appl. Crystallogr.*, **2020**, *53*, 226–235.

3 (a) F. Neese, *WIREs: Comput. Mol. Sci.* **2012**, *2*, 73-78. (b) F. Neese, *WIREs Comput. Mol. Sci.* **2018**, *8* (1), 1327.

4 P.A. Malmqvist, B.O. Roos, *Chem. Phys. Lett.* **1989**, *155* (2), 189−194.

5 (a) C. Angeli, R. Cimiraglia, J.-P. Malrieu, *Chem. Phys. Lett.* **2001**, *350* (3-4), 297−305. (b) C. Angeli, R. Cimiraglia, S. Evangelisti, T. Leininger, J.-P. Malrieu, *J. Chem. Phys.* **2001**, *114* (23), 10252−10264. (c) C. Angeli, R. Cimiraglia J.-P. Malrieu, *J. Chem. Phys.* **2002**, *117* (20), 9138−9153.

6 R. Izsak, F. Neese, *J. Chem. Phys.* **2011**, *135* (14), 144105

7 F. Weigend, R. Ahlrichs, *Phys. Chem. Chem. Phys.* **2005**, *7* (18), 3297-3305

8 F. Weigend, *Phys. Chem. Chem. Phys.* **2006**, *8*, 1057-1065.

9 C. Bannwarth, S. Ehlert, S. Grimme, *J. Chem. Theory Comput.* **2019**, *15*, 1652–1671.

10 C. Bannwarth, E. Caldeweyher, S. Ehlert, A. Hansen, P. Pracht, J. Seibert, S. Spicher, S. Grimme, *WIREs Comput. Mol. Sci.* **2020**, e01493.

11 P. Pracht, F. Bohle, S. Grimme, *Phys. Chem. Chem. Phys.* **2020**, *22*, 7169–7192.

12 S. Grimme, *J. Chem. Theory Comput.* **2019**, *15*, 2847–2862.

13 S. Grimme, F. Bohle, A. Hansen, P. Pracht, S. Spicher, M. Stahn, *J. Phys. Chem. A* **2021**, *125*, 4039-4054.

14 S. Grimme, C. Bannwarth, S. Dohm, A. Hansen, J. Pisarek, P. Pracht, J. Seibert, F. Neese, *Angew. Chem. Int. Ed.* **2017**, 56, 12485–12491.

15 J. Tomasi, B. Mennucci, R. Cammi, *Chem. Rev.* **2005**, *105*, 2999–3094.

16 J. G. Brandenburg, C. Bannwarth, A. Hansen, S. Grimme, *J. Chem. Phys.* **2018**, *148*, 064104.

17 S. Grimme, A. Hansen, S. Ehlert, J.-M. Mewes, *J. Chem. Phys.* **2021**, *154*, 064103.

18 Y. Zhao, D. G. Truhlar, *J. Phys. Chem. A* **2005**, *109*, 5656–5667.

19 S. Grimme, J. G. Brandenburg, C. Bannwarth, A. Hansen, *J. Chem. Phys.* **2015**, *143*, 054107.

20 J. M. Tao, J. P. Perdew, V. N. Staroverov, and G. E. Scuseria, *Phys. Rev. Lett.* **2003**, *91*, 146401.

21 E. Caldeweyher, S. Ehert, A. Hansen, H. Neugebauer, S. Spicher, C. Bannwarth, S. Grimme, *J. Chem. Phys.* **2019**, *150*, 154122.

22 F. Jensen *J. Chem. Theory Comput.* **2015**, *11*, 132–138.

23 F. Jensen *J. Chem. Theory Comput.* **2006**, *2*, 1360-1369.

24 a) R. Izsák *WIREs Comput Mol Sci.* **2020**; *10*:e1445; b) R. Berraud-Pache, F. Neese, G. Bistoni, R. Izsák *J. Chem. Theory Comput.* **2020**, *16*, 564-575 c) A. Sirohiwal, R.

Berraud-Pache, F. Neese, R. Izsák, D. A. Pantazis *J. Phys. Chem. B* **2020**, *124*, 8761-8771.

25 a) A. D. Becke, *J.Chem.Phys.* **1993**, *98*, 5648-5652; b) C. Lee, W. Yang, R. G. Parr, *Phys. Rev. B* 1998, *37*, 785-789; c) S. H. Vosko, L. Wilk, M. Nusair, *Can. J. Phys.* **1980**, *58*, 1200-1211; d) P. J. Stephens, F. J. Devlin, C. F. Chabalowski, M. J. Frisch, *J.Phys.Chem.* **1994**, *98*, 11623-11627.

26 a) S. Grimme, J. Antony, S. Ehrlich, H. Krieg, *J. Chem. Phys.* **2010**, *132*, 154104; b) S. Grimme, S. Ehrlich, L. Goerigk, *J. Comput. Chem.* **2011**, *32*, 1456.